Design and Development of a Device to Aid in Tissue Flap Monitoring

by
Kevin Mark Neaves

Thesis presented in partial fulfilment of the requirements for the degree of Master of Engineering (Mechatronic) in the Faculty of Engineering at Stellenbosch University

Supervisor: Dr. Jacobus Hendrik Muller
Co-supervisor: Dr. David Jacobus van den Heever

March 2016

DECLARATION

By submitting this thesis electronically, I declare that the entirety of the work contained therein is my own, original work, that I am the sole author thereof (save to the extent explicitly otherwise stated), that reproduction and publication thereof by Stellenbosch University will not infringe any third party rights and that I have not previously in its entirety or in part submitted it for obtaining any qualification.

Date: .....

Abstract

Tissue flaps form an important part of plastic and reconstructive surgery. They are transferred with their own blood supply and are typically applied to wounds where skin grafts are unsuitable. Monitoring of tissue flaps is an important practice as it can assist in determining flap condition and the detection of circulatory complications. Detecting complications timeously is beneficial if the flap is to be salvaged. In the case of pedicled groin flaps, a technique known as ischemic preconditioning (IP) has proven to be beneficial in promoting early flap separation. A literature survey revealed that IP has only been manually implemented and an automated procedure would benefit patient and staff, particularly in a South African public hospital setting.

A device was designed and developed which makes use of pulse oximetry to assist in tissue flap monitoring and analyses of current IP protocols. The device is capable of monitoring and recording information including the oxygen saturation (SpO_2) and photoplethysmogram (PPG) measured from three different sites. In addition to this, the device automated the IP process by controlling the inflation of a pneumatic tourniquet.

Several device tests were performed prior to clinical trials, including functionality tests which indicated that the device is capable of measurements on those areas of the body that are relevant to tissue flaps. Tests indicated that the device should not be limited to the monitoring of a single tissue flap type. The completed device was delivered to a plastic and reconstructive surgeon who carried out the clinical trials at Chris Hani Baragwanath Hospital.

Clinical testing was performed on four subjects who underwent pedicled groin flap surgery. Reasonable signal quality was obtained from the last three cases. Errors and shortcomings from the first case were addressed and corrected where possible. Analysis of the recorded data coincided with standard clinical observations, indicating that the device was able to assist determining flap condition. Two of the three patients undergoing IP benefited from early flap division.

Additional clinical tests could further prove the function and efficacy of the device, as well as improving post-testing data analysis methods.

Opsomming

Weefselflappe speel `n integrale rol in plastiese en rekonstruktiewe chirurgie. Weefselflappe beskik oor eie bloedtoevoer en geskik vir die behandeling van wonde waarvoor veloorplantings onmoontlik is. Die monitering van weefselflappe is ’n belangrike praktyk omdat dit ‘n bydrae kan lewer aan weefseltoestand metings en aan die vroegtydig waarneming van bloedsomloopkomplikasies. Om komplikasies vroegtydig waar te neem is voordelig wanneer die velweefsel gered moet word. ’n Tegniek genaamd isgemiese prekondisie (IP) is as voordelig bewys vir die aanmoediging van vroeë weefselonthegting in die geval van pedikel-liesflappe. Tot dusver is IP in literatuur slegs met die hand toegepas terwyl ’n geoutomatiseerde prosedure pasiënte en mediese personeel sal bevoordeel, spesifiek in die Suid-Afrikaanse staatshospitaal-omgewing.

’n Toestel wat van pols-oksimetrie gebruik maak is ontwerp en ontwikkel om behulpsaam te wees met weefselflap-monitering en die analise van huidige IP-protokolle. Die toestel kan inligting moniteer en opneem, insluitend suurstof-saturasie (SpO_2) en fotopletismogram (PPG), wat gemonitor is vanaf drie verskillende meetpunte. Die toestel is verder in staat om die IP-proses te outomatiseer deur die lugdruk in die knelverband te reguleer.

Voordat kliniese toetse uitgevoer is, is die toestel aan verskeie toetse onderwerp, insluitend funksionaliteitstoetse wat aangedui het dat die toestel geskik is vir metings op gedeeltes van die liggaam wat relevant tot weefselflappe is. Toetse het aangedui dat die toestel nie beperk behoort te word tot die monitering van ’n enkele weefselflaptipe nie. Die volledige toestel is oorhandig aan ’n plastiese-rekonstruktiewe chirurg wat dit by die Chris Hani Baragwanath-hospitaal aan kliniese toetsing onderwerp het.

Kliniese toetse is uitgevoer op vier pasiënte wat pedikel-liesflapchirurgie ondergaan het. ’n Redelike seinkwaliteit is verwerf in die laaste drie gevalle. Foute en tekortkominge tydens die eerste geval is aangespreek en reggestel waar moontlik. ’n Analise van aangetekende data het saamgeval met gestandaardiseerde kliniese waarnemings, wat aangedui het dat die toestel in staat is om te help met die monitering van weefselflaptoestande. Twee van die drie pasiënte wat IP ondergaan het, het by die monitering van vroeë weefselonthegting baat gevind.

Addisionele kliniese toetse kan die funksionaliteit en doeltreffendheid van die toestel, sowel as post-toetsing data-analise, verder verbeter.

Acknowledgements

I would like to extend my gratitude to all who assisted in making the completion of this report possible.

Firstly, I would like to thank my supervisors, Dr. Cobus Muller and the late Prof. Cornie Scheffer for their support, advice, understanding, reassurance and continued motivation. This thesis would not have been possible without their inputs. My gratitude also goes to my co-supervisor, Dr. Dawie van den Heever for his guidance and knowledgeable input.

This research would not have been possible without the assistance of Dr. Nebil Lahouel who willingly offered his medical expertise and countless medical explanations. I am particularly thankful for his time which was required to execute the clinical trials and the advice provided during and thereafter.

Furthermore I would like to thank all the personnel at the faculty of Mechanical and Mechatronic Engineering at Stellenbosch University for their cheerfulness, valued support and willingness to assist where possible. My sincere thanks goes to my office colleague and friend, Mr. Reynaldo Rodriguez for his encouragement and valuable advice.

Lastly, I am thankful to my family and friends, my close friend Melody van Rooyen for her motivation, valued input and support. I extend my thankfulness to my mother, Felicity, for her encouragement, support and always positive attitude.

Table of Contents

List of Figures

List of Tables

List of Equations

Glossary

Anastomosis – Surgical connection between two structures, for example blood vessels.

Angiogenesis – The development of new blood vessels.

Clamping – Process of interrupting the blood flow to the recipient site via a pedicle using a mechanical clamping mechanism.

CO-oximeter – A blood gas analyser that measures oxygen levels in a sample of blood.

Debridement – Removal of necrotic tissue to aid in wound healing.

Distal – Part which is furthest away from the source.

Electrocardiograph (ECG) – Instrument used to measure and record the heart's electrical activity.

Extinction coefficient (ε) – Measure of a substance's diminution at a specific wavelength of light.

Hypoxia – A deficiency or reduction of tissue oxygenation.

Ischemia – Restriction of blood supply.

Ischemic Preconditioning (IP) – For the purpose of this study, IP is defined as the technique of inducing alternating states of ischemia and reperfusion to a recipient site by clamping and unclamping the tube pedicle.

Necrosis – The death of body tissue.

Pedicle – A surgically formed tube or stem that connects one body part to another.

Perfusion – The flow of blood through arteries and capillaries.

Perfusion units (LDF related) – Relative measurement unit used by certain laser Doppler flowmetry machines for indicating flow.

Plethysmogram – Waveform produced by a plethysmograph for the measurement of volume changes in an organ or other areas of the body.

Photoplethysmogram (PPG) – Optically obtained waveform for the measurement of volume changes in an organ.

Proximal – Part which is closest to the source.

Occlusion – Blockage of a blood vessel.

Oedema – Fluid retention in the body. Usually causing swelling.

Sphygmomanometer – The instrument used to measure blood pressure.

Sutures – Stitches.

Tissue Flap – Tissue which is moved from a donor site to a recipient site with its own blood supply.

1. Introduction

Tissue flap surgery is a well-established technique used in plastic and reconstructive surgery. The technique involves raising tissue from a donor site and transferring it to a recipient site. A tissue flap consists of its own blood supply, a trait that distinguishes it from a graft which relies on the blood supply of the recipient site (Salama, 2012). Tissue flap failure is an unpleasant experience for both surgeon and patient (Keller, 2007). Tissue flap monitoring is an important tool used by surgeons during the treatment of a tissue defect as it provides an early warning to vascular complications which may threaten flap viability. A technique known as ischemic preconditioning (IP) has been found to facilitate the healing process of injuries treated with tissue flaps. This report concerns the design and development of a tissue flap monitoring and IP control device.

1.1. Background

Monitoring tissue flaps is an important technique in aiding in tissue flap survival. During this process doctors and nurses are able to detect possible complications with the flap, as regular monitoring provides a good indication of flap condition. The main focus of this study is the monitoring of the pedicled groin tissue flap by means of pulse oximetry, placing particular emphasis on the IP technique in facilitating the healing process for faster patient recovery times. Literature shows several preconditioning techniques have been applied to pedicled flaps with varying results. The IP method, on average, results in earlier flap division and therefore earlier recovery and discharge of the patient (Cheng *et al.*, 1999; Cheng *et al.*, 2000; Furnas *et al.*, 1985; Ha & Wilson, 2009).

1.1.1. Tissue Flaps

Tissue flaps are commonly used in breast reconstruction, hand injuries, facial, head and neck defects, as well as other areas with damaged tissue (Cheng *et al.*, 2000; Patel & Sykes, 2011; Salama, 2012;). Tissue flaps are classified in several ways, according to various factors including, proximity to recipient site, donor site or destination, vascular supply or types of tissue transferred (Salama, 2012). For example, pedicled groin flaps are created by forming a pedicle of tissue raised from the groin area. The distal part of the pedicle (tip) is then sutured to the injured recipient site, often the hand. This flap is the main focus of this thesis and will be explored in the literature review and device development.

Despite being developed almost a century ago, the pedicled flap technique remains popular in developing countries (Wallace, 1978). Unlike other tissue transfer techniques, such as free flaps, this technique is straightforward and does not require microsurgery, which is not always available in developing countries. Despite being simplistic the surgery is effective and has a high success rate (Goertz *et al.*, 2012).

1.1.2. Ischemic Preconditioning

A post-surgery technique known as clamping or ischemic preconditioning (IP) has been applied to pedicled flaps and was found to promote early flap separation (Cheng *et al.*, 1999; Cheng *et al.*, 2000). The IP procedure involves timed periods of clamping and unclamping of the pedicle. The alternating periods of ischemia and reperfusion primarily promote healing by the process of angiogenesis. Angiogenesis is the development of new blood vessels from existing vessels (Akhavani *et al.*, 2008). Current literature, however, does not provide indications of optimal preconditioning times (Cheng *et al.*, 1999; Cheng *et al.*, 2000; Furnas *et al.*, 1985). IP also requires regular monitoring on behalf of hospital staff and this is not always possible within the South African context.

Automating the IP process could save working-hours, hospitalisation costs and reduce the possibility of human error, as well as provide a platform for research into optimal IP timings for more effective and timeous recovery.

1.1.3. Pulse Oximetry

Pulse oximetry has become widely used in emergency medicine and is more reliable than clinical indicators at detecting hypoxia (Sinex, 1999). The method allows for non-invasive estimation of arterial oxygen saturation (SaO_2) provided there is a pulsatile flow.

The majority of pulse oximeters make use of two wavelengths of light which illuminate the tissue concerned. The light is either measured adjacent to the emitters by reflectance or on the opposing side by transmittance. The measured light contains a low amplitude alternating signal. By making use of the signal from each wavelength, oxygen saturation can be calculated (Moyle, 2002: 17-23).

Pulse oximetry has been used successfully to monitor the condition of tissue flaps and to provide an early warning of flap failure (Hallock & Rice, 2003; Pickett *et al.*, 1997; Zaman *et al.*, 2013). This technique and the use of photoplethysmography is employed in the monitoring of pedicled groin flaps in this study.

1.2. Objectives

The aim of this study was to devise a technique to assist medical staff in the monitoring of a pedicled groin flap. Additionally the study aimed to explore the implementation of automated IP according to clamping times as specified in literature.

In order to achieve this aim, the following primary objectives had to be met:

- Design and construct a device within the budget of R 30 000 which is safe to use for patient and staff and is capable of monitoring tissue flaps including pedicled groin flaps.

- Using the developed device, monitor and record pulse oximetry measurements including SpO_2 and photoplethysmogram to aid in early flap division and detection of vascular complications.
- Design and incorporate an automated clamping system into the monitoring device to perform automated IP on pedicled flaps and aid in improving current IP protocols.

Once these objectives had been met the device was used post-surgery for monitoring and the implementation of automated IP. Recorded patient data was then analysed for device effectiveness in monitoring and automating IP procedures.

1.3. Motivation

Tissue flaps play an important role in plastic and reconstructive surgery. They offer improved coverage and function which skin grafts cannot always achieve on their own. The disadvantage is that flaps require close and regular monitoring, in order to reduce the chance of flap loss, which is traumatic for both patient and surgeon. If flap complications are not timeously detected it can result in increased expenses, extended hospitalisation as well as complete flap loss (Steele, 2011). Literature shows that flap monitoring can provide early warning (prior to standard clinical tests) of flap complications, thereby allowing appropriate action to be taken sooner. Although various monitoring techniques have been developed, few of these have focused on monitoring of tissue flaps (Zaman *et al.*, 2011).

In the case of a pedicled groin flap tissue is raised from the groin area and shaped into a pedicle. The distal part of the pedicle is then attached to the recipient site (often the hand). The pedicle remains attached for 24 to 28 days before it is separated. This is where the benefits of the aforementioned technique of ischemic preconditioning (IP) can be seen. When applied to pedicled flaps, IP makes a significant difference in patient recovery time. One study shows that following IP, the separation of the pedicle from the donor site occurred after only five days (Furnas *et al.*, 1985). Earlier pedicle separation reduces hospitalisation costs, patient discomfort and disruption to the patient's life, and also enables the patient to begin physical therapy earlier, further improving on recovery time.

Despite its proven success the IP technique is not practiced at Chris Hani Baragwanath Hospital (Lahouel, 2013), and has thus far only been manually implemented in literature. Manual clamping does have its benefits, however, it is not practical at Chris Hani Baragwanath Hospital mainly due to a lack of staff and discontinuity between shifts. Manual clamping is time-consuming and requires staff to adhere to a strict schedule. An automatic or semi-automatic IP system would be beneficial to hospital staff, and by extension to the patient. The system can provide consistent IP times that will not be affected by lack of staff or human error.

While the timing of the clamping plays a significant role in the patient's recovery time, optimal timing is yet to be established. Real-time viewing of sensor data

during on and off clamping intervals promises to assist medical staff in detecting complications and maintaining wound condition. Analysis of sensor data will aid in determining the effectiveness of current and future IP protocols.

1.4. Scope

A device using pulse oximetry was developed and used to monitor flaps, assisted in implementing automated IP and aided in detecting vascular complications. In the case of monitoring pedicled flaps, the device was used for clamping the pedicle at intervals initially determined by data obtained from available literature. These intervals were analysed using pulse oximetry and comparing the data to standard clinical tests. The main outcome of these measurements would be to prove the device concept and in future to test and optimise IP protocols.

A commercially available pulse oximetry system was purchased. The design of the probe and signal processing circuitry falls beyond the scope of this thesis however a section of the literature review is dedicated to explaining the principles of pulse oximetry.

Existing IP and monitoring devices do not fulfil all the requirements for this thesis therefore a device was designed incorporating the necessary components.

Dr. Nebil Lahouel, a plastic and reconstructive surgeon at Chris Hani Baragwanath Hospital served as the clinical consultant for this study. He provided medical input on the device and its functionality and assisted by carrying out the clinical testing. Only ethically approved procedures were followed during clinical testing. Ethical approval was obtained from the Human Research Ethics Committee (medical) of the University of Witwatersrand (application number M141165).

2. Literature Review

A literature review was conducted, reviewing monitoring options, tissue flap monitoring and pedicled flap IP techniques. For the purpose of this thesis emphasis is placed on the condition monitoring of pedicled tissue flaps through pulse oximetry measurements that employ photoplethysmography.

2.1. Monitoring Options

In this section a review of common monitoring techniques employed in clinical settings is provided. Focus is placed on the basic operating principles and the advantages and disadvantages of each system.

2.1.1. Pulse Oximetry

Pulse oximetry is a non-invasive method of measuring blood oxygen saturation. At the time of its invention in 1972, pulse oximetry represented an important advancement in clinical patient monitoring (Aoyagi, 2003; Sahni, 2012). Shortly after it became commercially available in 1975, the pulse oximeter found popularity as a monitoring tool in anaesthesia practices and its use has since extended to modern ICUs and general monitoring situations (Aoyagi, 2003; Cloete, 2012; Ortega *et al.*, 2011; Tremper *et al.*, 1993).

2.1.1.1. Principles

Pulse oximeters work on the principle that when light of a specific wavelength and intensity is transmitted through tissue, part of it is absorbed and the rest is transmitted through the tissue. The transmitted light can be measured using a photodetector and then used to calculate how much of the light was absorbed (Sinex, 1999).

Most modern pulse oximeters use two wavelengths of light, i.e. approximately 660 nm (red) and 940 nm (near-infrared), which are typically emitted by LEDs. Light emitted at these two wavelengths have the benefit of easily penetrating human tissue. The 660 nm light has the additional property that de-oxygenated Hb (haemoglobin) absorbs more light than that of oxygenated Hb (HbO_2). The opposite is true for the near-infrared wavelength, which is more readily absorbed by HbO_2 than by Hb (Sinex, 1999). Figure 1 shows the extinction coefficients, which is a measure of light absorption, of Hb and HbO_2 for wavelengths 600 to 1000 nm.

By converting the changing current from the photodetector to a voltage, a photoplethysmogram (PPG) can be obtained for the red and near-infrared light. The PPG consists of an AC component, which indicates the pulsatile component of arterial blood and a DC component representing the venous blood, tissue and non-pulsatile arterial blood (Sinex, 1999; Tremper *et al.*, 1993). These values are substituted into equation (1) (Sahni, 2012). This ratio can be directly linked to the oxygen saturation value.

$$R = \frac{f(AC_{red}/DC_{red})}{(AC_{infrared}/DC_{infrared})} \quad (1)$$

where f is a calibration constant.

Most commercially-available pulse oximeters are calibrated using a group of healthy individuals. The individual's blood oxygen concentration is gradually lowered and multiple blood samples are taken. The samples are then tested for oxyhaemoglobin saturation using a CO-oximeter. This information is subsequently programmed into a lookup table for cross-reference with the pulse oximeter in order to obtain the calibration constant f in equation (1). Most oximeters are designed for reliable measurement of SpO_2 above 85 % due to the possibility of brain damage at lower concentrations. Values of SpO_2 below 85 % have usually been extrapolated (Moyle, 2002: 41).

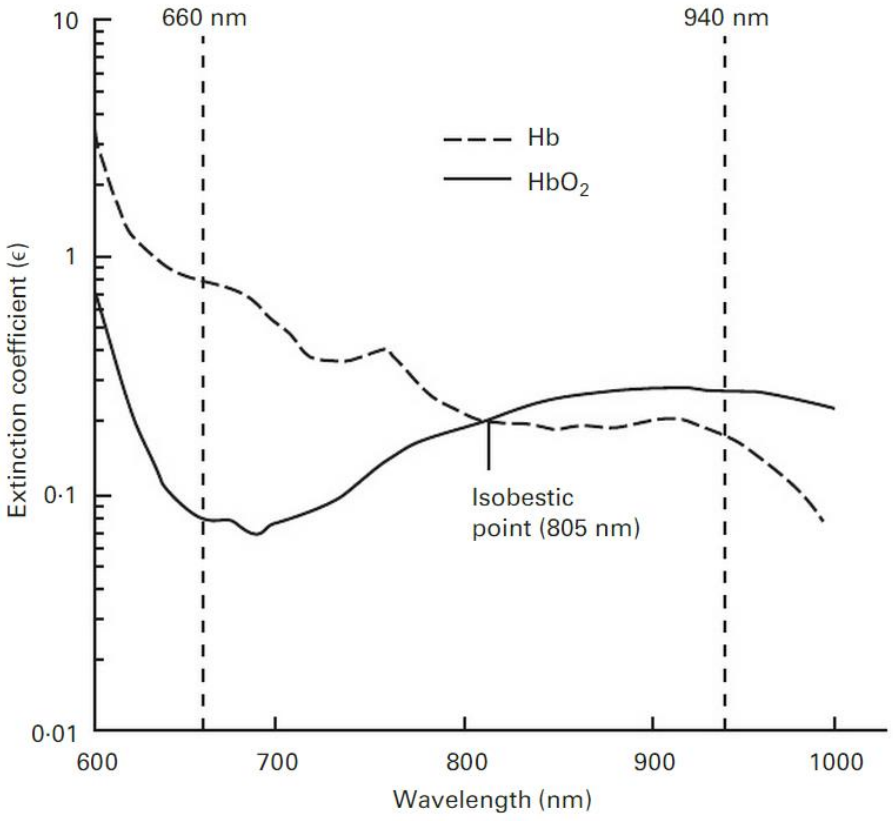

Figure 1: Extinction coefficients of oxygenated haemoglobin (HbO_2) and deoxygenated haemoglobin (Hb) as a function of wavelength (Moyle, 2002: 16)

2.1.1.2. Common Sensor Types

There are two types of sensors which are typically used: a transmittance sensor and a reflectance sensor. The most common sensor found in medical practice is the transmittance sensor. These are typically placed on the finger, toe or earlobe (Wax *et al.*, 2009). The sensor relies on the transmittance of light through the tissue. Figure 2 illustrates the positioning of a transmittance sensor. Due to the construction and operation of the transmittance sensor it has limited placement areas.

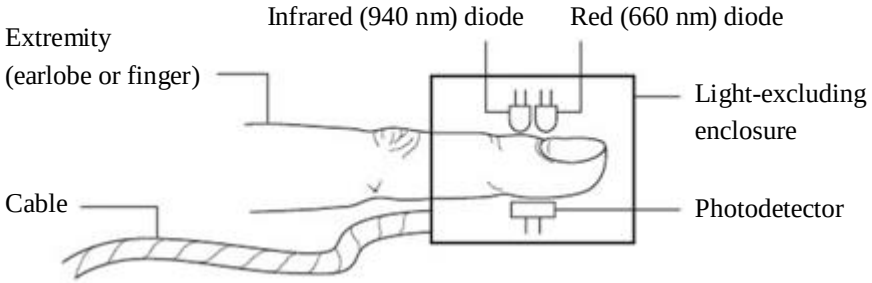

Figure 2: Transmittance sensor. Adapted from Moyle (2002: 18)

The reflectance sensor, although not as common as the transmittance sensor, has several advantages over its transmittance counterpart - the sensor design is simpler, has more placement options and can be used on patients whose perfusion may be low due to hypothermia and other conditions (Moyle, 2002; Wax *et al.*, 2009). Figure 3 illustrates the mechanism of the reflectance type sensor. In this study the reflectance sensor will be used. The reflectance sensor is better suited to the physical characteristics of most tissue flaps and the areas which must be measured.

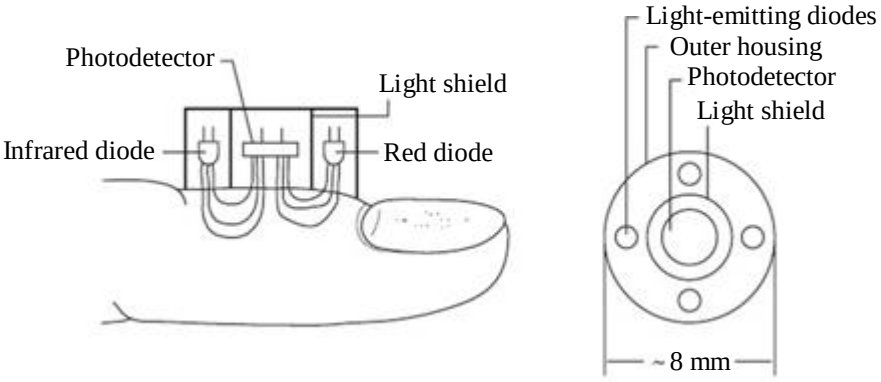

Figure 3: Reflectance sensor. Adapted from Moyle (2002: 31)

2.1.1.3. Data Obtained from Sensors

Aside from providing the SpO_2 reading sensors are also capable of providing a wide variety of important measurements. Some oximeter systems provide a heart rate reading as well as a PPG output. There are particular benefits to having access to a PPG. This type of waveform not only provides an indication of the suitability of sensor placement, but also signals the quality of perfusion within the tissue. Motion artefacts that result from patient interference can be clearly inferred from the signal. Furthermore accurate SpO_2 readings can be obtained from a clear signal with sufficient amplitude when measured on a patient with normal haemoglobin. Should signal quality compromise the indication of SpO_2, the waveform can be inspected for a pulsatile component.

For the purpose of this study the PPG was required. It was therefore necessary to select a commercially-available sensor system that provided all the necessary outputs as the probe and signal processing design of a new oximetry system is beyond the scope of this study.

2.1.1.4. Future and Limitations

The pulse oximeter is widely used throughout the medical world as it provides an accurate, non-invasive way to measure oxygen saturation. Medical companies and researchers are actively exploring ways to improve on this technique and it is in this author's opinion that pulse oximeters will become even more versatile and accurate in the future (Jubran, 2015). With advances in existing technology, pulse oximeters will become less susceptible to motion artefacts and light interference as well as more sensitive to low perfusion and low arterial pulses.

The aforementioned advances in pulse oximetry represent the common limitations of many current pulse oximeters. The presence of motion artefacts and light interference compromises the signal quality. These effects are especially prominent when the signal is measured in low perfusion states or on a weak arterial pulse. Reduced accuracy is also observed for lower oxygen saturation levels owing to the calibration techniques (Aoyagi, 2003; Mardirossian & Schneider, 1992; Nitzan *et al.*, 2014).

It is important that members of medical staff are aware of these limitations as well as the basic operating principles of pulse oximeters. Failure to recognise these restrictions may result in inaccurate measurements or no measurements at all.

2.1.2. Near-infrared Spectroscopy

The operating principles and hardware of medical near-infrared spectroscopy (NIRS) devices are very similar to that of pulse oximetry. The primary hardware similarities are the use of light detectors and light emitters (mainly laser diodes although LEDs are also used). The technology is non-invasive and operates using light sources of wavelengths between 700 and 1000 nm. NIRS also relies on the principle that near-infrared light is absorbed differently for de-oxygenated and oxygenated Hb. Certain NIRS devices are capable of producing continuous

measurements, including tissue oxygenation levels (Pellicer & Bravo, 2011; Scheeren *et al.*, 2012).

The primary advantages of NIRS in relation to this study are the cost, non-invasiveness and that device measurements are not reliant on the pulsatile component of the signal. Unlike pulse oximetry, NIRS devices possess higher measurement sensitivity in poor perfusion situations (Mittnacht, 2010; Moerman & Wouters, 2010). NIRS, however, shares some of the disadvantages of pulse oximetry, namely, motion artefacts and light interference.

2.1.3. Laser Doppler Flowmetry

Experimentation measuring blood flow using Laser Doppler Flowmetry (LDF) technology began in the early 1970's. Since then LDF devices have developed into a reliable method for continuously and non-invasively measuring blood perfusion by observing differences in blood flow. Typically the devices make use of a low-power monochromatic laser of approximately 1 to 2 mW that generates wavelengths of light within the red and near-infrared spectrum similar to the spectral range of pulse oximetry.

The laser probe is placed on the area of interest, lighting the tissue. The light is scattered by bone, tissue and flowing blood cells. The motion of the red blood cells causes a frequency broadening as a result of the Doppler Effect. The frequency distribution of the backscattered light is then measured and analysed to provide an estimation of perfusion (BIOPAC Systems, [S.a.]; Fredriksson *et al.*, 2007; Hallock & Rice, 2003).

As with pulse oximetry, LDF is also extremely sensitive to movement. Probe motion relative to the measurement site will result in a Doppler shift of the light frequency, skewing the desired frequency shift measurement caused by flowing blood cells.

The primary disadvantage of using LDF for this thesis is the cost. A commercial unit can cost in excess of $ 10 000 (Hallock & Rice, 2003; Hu *et al.*, 2013).

2.1.4. Transcutaneous Electrode

Transcutaneous partial oxygen pressure ($TcPO_2$) measurement can be achieved using a modified Clark electrode. The electrode contains a platinum cathode and a silver anode and is separated from the skin by a permeable membrane. This electrode is heated to ensure adequate perfusion and is placed on the skin (Agarwal & Jindal, 2008). Oxygen from the skin is reduced at the cathode according to equation (2) (Kanwisher, 1959):

$$4e^- + O_2 + 2H_20 \rightarrow 4OH^- \quad (2)$$

This reduction results in an electrical signal which is converted to a partial oxygen pressure (PO_2) and is used for display and measurement purposes (Agarwal & Jindal, 2008).

Primary advantages of transcutaneous oxygen monitoring are continuous and non-invasive monitoring with low sensitivity to motion artefacts. Disadvantages include a slow measurement response (10 to 20 seconds), the relocation of the probe due to a possibility of burns, the inaccuracy at low perfusion and a long setup time (Barnette, Criner & D'Alonzo, 2010). Furthermore, this technology has largely been replaced by pulse oximetry (Kenner & Lott, 2013).

2.1.5. CO-oximeter

The CO-oximeter is considered the "gold standard" for measuring arterial oxygen saturation (SaO_2) (McGovern *et al.*, 1996; Mengelkoch *et al.*, 1994). CO-oximeters typically analyse a blood sample using four wavelengths of light. Multiple measurements can be determined using a CO-oximeter including oxygen saturation (SO_2), oxyhaemoglobin (HbO_2), deoxyhemoglobin (Hb), total haemoglobin (tHb) and carboxyhemoglobin (COHb) (Thomason, Batki & Nayyar, 2010:3).

Advantages of CO-oximetry technology include accurate measurement in low perfusion conditions as well as providing a standard for in vitro calibration of pulse oximeters (Nitzan *et al.*, 2014; Roberts, 2013). Disadvantages include the high relative cost, the invasiveness of the blood extraction, longer processing times per sample and non-continuous nature of measurements (Haessler *et al.*, 1992; Wyka, Mathews & Rutkowski, 2011: 437).

2.2. Tissue Flaps

Tissue flaps are used in cosmetic and reconstructive surgery. While there are several types of tissue flaps, this thesis focuses on the pedicled flap. The pedicle tube was initially developed by the clinician Vladimir Petrovich Filatov who employed the flap for treating a reoccurring malignant tumour. Independently, in 1917, Harold Gillies invented the tube pedicle for the treatment of a severe facial burn and shared the technique with surgeons around the world (Wallace, 1978).

2.2.1. Pedicled Groin Flap

The pedicled groin flap was first developed by McGregor and Jackson (1972) in 1972 when they made use of the superficial circumflex iliac arterio-venous (SCIA) system (illustrated in Figure 4). This arterio-venous system was chosen as it was regarded as a self-contained vascular territory, making it similar to the robust delto-pectoral flap. McGregor and Jackson (1972) successfully made use of the pedicled groin flap on 35 patients with few complications (McGregor & Jackson, 1972).

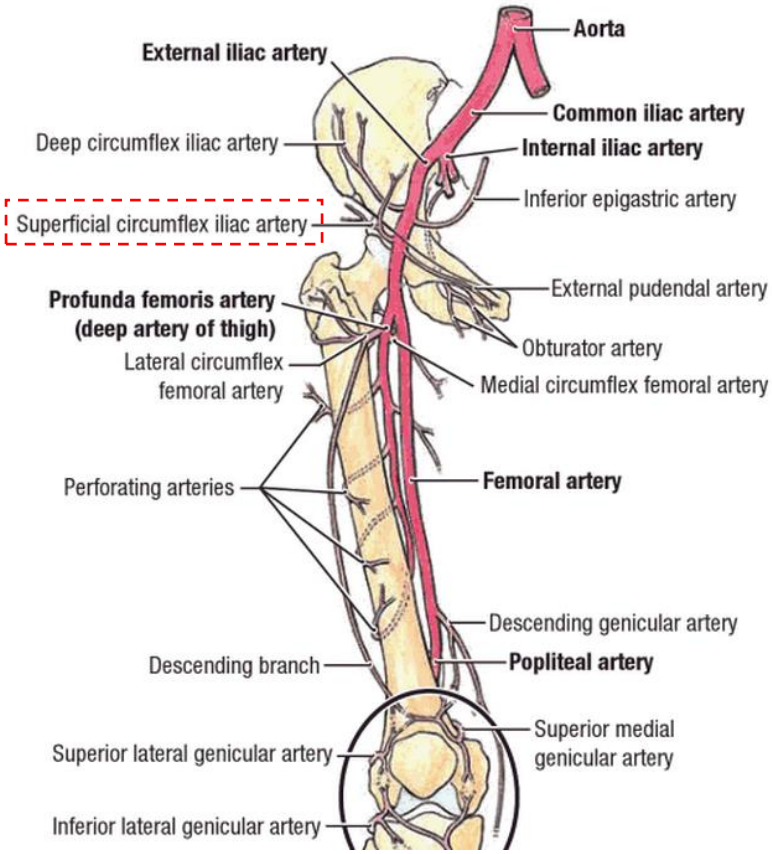

Figure 4: Arteries of the thigh. Image adapted from Agur, Dalley & Grant (2013: 370)

Despite having its origins in the early twentieth century, the pedicled groin flap remains a common practice today and still has several advantages for modern use. The flap surgery does not require elaborate planning and is less intricate than free flap operations. Operating theatre time is significantly less when compared to free flaps (approximately one hour as opposed to six hours). This is an important factor in a public hospital as surgeons are pressed for time and resources (Lahouel, 2013). In addition to this the tissue can be quickly harvested and there are more favourable possibilities for hair distribution (Goertz *et al.*, 2012; McGregor & Jackson, 1972).

Figure 5 shows an example of a pedicled groin flap. The flap is being used to cover a wound which was obtained in a motor vehicle accident. Pedicled groin flaps are frequently used for the treatment of hand and arm injuries. The pedicle is post-operatively typically divided between 24 to 28 days following attachment (Cheng *et al.*, 1999; Goertz *et al.*, 2012).

Figure 5: A pedicled groin flap on the left forearm. Covering an injury obtained in a motor vehicle accident (Buchman *et al.*, 2002)

2.2.2. Tissue Flap Monitoring

The benchmark for flap monitoring is clinical observation of skin colour, dermal bleeding and capillary refill (Keller, 2007; Keller, 2009). Thrombosis and other circulatory complications can threaten flap success. If complications are discovered early the chance of successful flap re-exploration and other corrective methods is improved. Various methods have been employed to monitor flaps in order to detect complications over and above observation methods. Non-invasive methods include photoplethysmography, near infra-red spectroscopy (NIRS) and laser Doppler flowmetry (Irwin *et al.*, 1995).

The literature reviewed in this section relates the history of flap monitoring techniques and has been arranged in chronological order in order to highlight the latest monitoring options and techniques.

1991

Lindsey *et al.* (1991) used an Ohmeda Biox 3700e (Ohmeda, Hatfield, Herts, UK) pulse oximeter to monitor four free muscle flaps. A reflectance type probe was not available and it was necessary to raise a section of the flap for the probe to clamp onto. In two of the cases the signal strength rose post-operatively and the flap survived with no complications.

In another instance it was decided that the flap was not viable after there was no readable signal from the oximeter for 20 hours. Re-exploration of the flap revealed a blocked artery. After the blockage was corrected a signal was obtained but it dropped in amplitude once again and an extensive debridement had to be performed. The lack of signal was not given adequate attention in the operating theatre as it indicated a lack of initial anastomosis. Based on their findings a weak or absent plethysmogram signal or a SpO_2 value under 80 % indicated a possible complication with the surgery.

1997

Hirigoyen *et al.* (1997) performed preliminary animal experiments followed by a clinical study. A Clark type electrode was used to monitor oxygen tension during free-tissue transfers. These results were correlated with that of standard flap observations as well as clinical parameters. They concluded that monitoring oxygen tension provided an appropriate method for determining flap viability but was unreliable for revascularised cutaneous flaps.

1997

Pickett *et al.* (1997) realised the need for a flap monitoring device. They developed their own system as the commercially-available pulse oximeters at the time had difficulty obtaining reliable readings from flaps. This system consisted of a probe using two wavelengths of light. The LED current was adjustable to a higher range than that of a commercial pulse oximeter therefore allowing optimal adjustment for PPG signals.

Their device was tested on normal subjects and a breast flap model. It was found that PPG amplitudes were at least five times smaller for the flap model than normal measurement sites. Additionally, it was found that the optimal LED drive currents were within range of the commercial device, indicating that the commercial device was failing elsewhere.

1997

Edwards & Chapman (1997) monitored two pedicled flap patients using an Ohmeda Biox 3700 pulse oximeter with a standard ear probe. After the operation, the probe was applied to the pedicle and oxygen saturation was measured between 85 % and 90 %. The plethysmogram waveform was displayed to provide the patient with feedback of suitable positions to rest the pedicle.

The flap was clamped daily and it was noted that oxygen saturation fell to 50 % in the first week. After 9 days the saturation was at 85 % while the pedicle was clamped, showing that the flap was obtaining sufficient supply from the recipient site.

Both flaps were divided one week earlier than the standard three week period. Edwards & Chapman (1997) believed that the technique of monitoring pedicled flaps would not only allow for earlier division, but also reduced flap morbidity and failure.

2003

Hallock & Rice (2003) compared the use of pulse oximetry and LDF for monitoring occlusive events generated on a rabbit ear model. Their primary reason for the comparison was to observe whether pulse oximetry was a suitable

substitute to LDF. The LDF system and probes are costly, whereas pulse oximetry is cheap in comparison and readily available in most settings. The LDF probes were also found to be difficult to handle and easily broken.

Both probes were affixed to one of the rabbit's ears and the following was noted during tests:

- An arterial occlusion resulted in a steep and immediate drop on the LDF machine as well as a drop in SpO_2 to zero a few seconds later (likely due to the lack of arterial pulsations)
- A venous occlusion caused a rapid drop in LDF measured blood flow to below 50 % of the nominal flow. The pulse oximeter showed a much slower drop in SpO_2 reaching 89 % after 30 minutes.

Hallock & Rice (2003) discussed that the gradual drop in SpO_2 observed by the oximeter is not ideal and that the threshold of 90 % to 93 % SpO_2 may be too low to indicate venous occlusion. Neither device was found to be ideal, but pulse oximetry offers a promising option provided that thresholds for venous occlusion are obtained.

2007

In a previous study, Keller (2007) used an ODISsey™ (ViOptix Inc., Fremont, CA, USA) tissue oximeter to monitor 30 free flap patients. There were no flap failures, despite three returns to the operating room. A drop in oxygen saturation was measured when the flap was being transferred and equally saturation increased when the flap was revascularised.

In one case the standard methods of capillary refill and dermal bleeding were normal yet the flap developed light blue specks with a pink background. Soon after these clinical observations the oxygen saturation fell. Despite the fall in oxygen saturation the flap appearance did not change. After a few hours the flap's physical appearance improved as did oxygen saturation. The oxygen saturation readings coincided with what was physically happening to the patient, however further investigation was required to fully interpret the readings.

2008

Repež *et al.* (2008) made use of a NIRS tissue spectrometer (InSpectra™ Model 325, Hutchinson Technology Inc., Hutchinson, MN, USA) to continuously monitor 48 patients for the first three post-operative days. This monitoring period was used as typically only a few thrombosis cases develop after this period. All monitored flaps were performed as breast reconstruction with three flap types: deep inferior epigastric perforator (DIEP) flap, superficial inferior epigastric artery (SIEA) flap and superior gluteal artery perforator (s-GAP) flap.

The probe was attached by a protective shield, as shown in Figure 6, which allowed for consistent probe mounting and minimal ambient light interference.

Monitoring was commenced immediately after the completion of the surgical procedure.

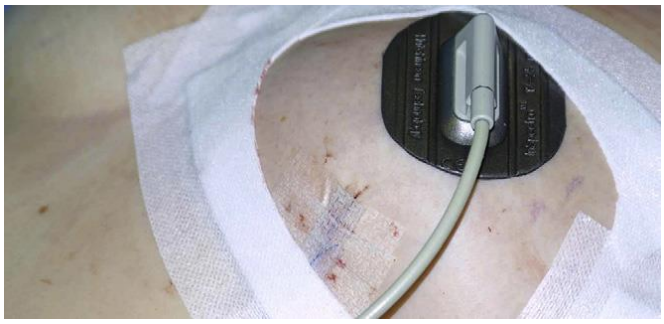

Figure 6: Probe attachment using of an adhesive shield (Repež *et al.*, 2008)

Out of the 48 patients, 13 cases of microvascular thrombosis occurred. It was found that circulatory failure resulted in a sudden change in all measured parameters from their steady-state (baseline) values. All cases were first detected by NIRS monitoring and then verified by clinical assessment. Both venous and arterial thrombosis resulted in a decrease in tissue oxygen saturation (S_tO_2). Changes occurred gradually with S_tO_2 dropping to zero after 46 minutes (mean) for venous thrombosis and 37 minutes (mean) for arterial thrombosis.

It should be noted that steady-state S_tO_2 values differed by a notable amount between patients, preventing the standardisation of threshold values and alarms. Additionally, the NIRS monitoring technique produced no false negatives or positives.

2009

Keller (2009) monitored 208 breast flaps using oxygen saturation measurements from a ViOptix T.Ox tissue oximeter (ViOptix Inc., Fremont, CA, USA). None of the flaps being monitored were lost despite several complications. Keller (2009) was able to predict a complication within one hour of an occlusive event. This was done using an algorithm which tracks the change of tissue oxygen saturation (StO_2) over time as indicated in equation (3):

$$Drop\ rate = \frac{\Delta StO_2}{\Delta t} \tag{3}$$

If a drop rate of greater or equal to 20 % was maintained for longer than 30 minutes, it indicated vascular complications.

2013

Kyriacou *et al.* (2013) developed a purpose built free flap monitoring device using reflectance photoplethysmography. They designed and built two identical reflectance sensors consisting of LEDs of commonly used wavelengths (660 nm and 940 nm) and a suitable photodiode for placement at a finger and a flap measurement site (Figure 7). The two sensors were then used in conjunction with a National Instruments (National Instruments, TX, USA) data acquisition card, where signal processing, storing and displaying of data was done in Labview (National Instruments, TX, USA).

The sensor was inserted into a black housing to block out ambient light and then placed onto the flap. The physical size of the sensor was kept small as to not interfere with other clinical tests and observations which had to be performed on the flap. The new reflectance sensor was positioned within a modified finger clip from which the original sensor was removed.

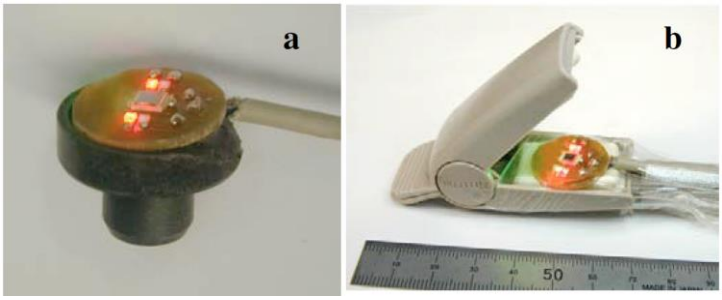

Figure 7: (a) Flap sensor, (b) finger sensor (Kyriacou & Zaman, 2013)

The system was used on five patients undergoing breast reconstruction using the DIEP flap technique. PPG signals were obtained from both the finger and flap sensors. It was noted that the signal amplitude from the finger was significantly higher than that of the flap (due to good blood supply and perfusion relative to the flap). The signal to noise ratio (SNR) for the flap PPG was still high enough to make an acceptable estimation of SpO_2. The mean infrared PPG amplitude from all patients was $277{,}1 \pm 200{,}9$ mV for the flap and $2964 \pm 972{,}5$ mV for the finger. The large standard deviation was caused by differences in flap design, such as thickness and weight. It was also found that the flap PPG amplitudes typically increased with time and suddenly dropped at approximately seven hours after the operation. Additionally, the flap SpO_2 values were lower than that of the finger due to poor perfusion immediately after surgery.

Their system performed adequately as a non-invasive free flap monitor and the measured SpO_2 values were in agreement with those taken by a commercial pulse oximeter. It should be noted that this paper was published well after the

commencement of this thesis. However, it reinforces the use of reflectance photoplethysmography with tissue flaps and the use of Labview as a suitable display and recording interface.

2.2.3. Ischemic Preconditioning

Ischemic preconditioning (IP) is a technique which can be applied to pedicled flaps by mechanically clamping the pedicle thereby stopping circulation to the recipient site via the pedicle. Doing so at timed intervals stimulates angiogenesis (Akhavani *et al.*, 2008). This IP-induced stimulation allows the pedicle to be divided significantly earlier, saving time and costs for both the patient and medical staff. To the knowledge of the clinical consultant and the author, this technique is not currently practiced at the Chris Hani Baragwanath Hospital. The method will, however, be applied as part of the performance testing for the device developed in this thesis.

As with the Tissue Flap Monitoring section, this literature section has also been arranged in chronological order to emphasise current research.

1985

Furnas *et al.* (1985) applied cross clamping to achieve alternating ischemia and reperfusion periods to a groin flap and a cross-leg flap. Clamping was accomplished by using rubber shod bowel clamps. Flap monitoring was performed by using transcutaneous oxygen measurements and standard clinical observation techniques. The efficacy of the clamping was evident by a decrease in transcutaneous oxygen levels. Table 1 shows the cross-clamping protocol for each patient. In both cases the pedicles were divided after five post-operative days.

Table 1: Cross-clamping protocol

Patient 1			**Patient 2**		
Post-operative time	**Ischemia**	**Reperfusion**	**Post-operative time**	**Ischemia**	**Reperfusion**
Day (hours)	Minutes	Minutes	Day (hours)	Minutes	Minutes
1-2 (30)	15	45	1 (30)	15	105
2-3 (56)	30	30	1-2 (40)	30	90
3 (68)	60	60	2-3 (64)	60	60
3-4 (80)	90	60	3-4 (88)	120	60
4 (104)	120	60	4-5 (110)	180	60
4 (116)	150	60	5 (114)	300	Divided
5 (128)	180	60			
5 (134)	330	Divided			

1996

George *et al.* (1996) experimented with a simple occlusion clamp which they applied to the pedicle on the fifth post-operative day. The clamp, shown in Figure 8, was tightened every 12 hours by one to two millimetres, progressively reducing the blood flow through the pedicle. By the tenth post-operative day the clamp was fully tightened. The occlusion clamp was tested on 20 patients and it was found that the mean period until division was ten days. By using this technique patients were discharged earlier than the standard three week period.

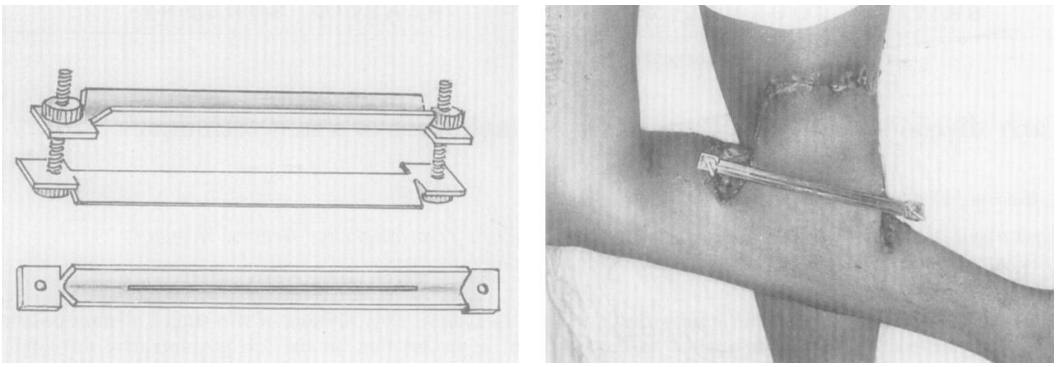

Figure 8: Left, sketch of the occlusion clamp construction. Right, the clamp applied to a cross leg flap (George *et al.*, 1996)

2000

In 1998, Cheng *et al.* (2000) tested rubber bands, custom-made Orthoplast (North Coast Medical, Gilroy, CA, USA) sheets, long-nose locking pliers, intestinal clamps, and a pneumatic tourniquet for suitability as devices for IP of pedicled groin flaps. Figure 9 shows a pneumatic tourniquet which has been applied to a pedicle. Their clamping technique was as follows:

Post-operative day 1: 0,5 hours of ischemia, 7.5 hours of reperfusion. Executed three times.

Post-operative day 2: 1 hour of ischemia, 7 hours of reperfusion.

Post-operative day 3 until day of division: 2 hours of ischemia, 6 hours of reperfusion.

Figure 9: A pneumatic tourniquet applied to a pedicle (Cheng *et al.*, 2000)

A total of thirteen flaps were monitored using a PeriFlux 5000 (Perimed, Stockholm, Sweden) LDF meter. One flap suffered partial flap necrosis, however the remaining flaps were successful. The mean period until division of the twelve flaps was 8,3 days. It was found that the pneumatic tourniquet was the best option to use for the following reasons: it provided the most comfort for the patient, had a strong adjustable ischemic effect, was reusable and reliable and was easily applied to the pedicle.

2009

Ha & Wilson (2009) made use of a modified bowel clamp in order to perform IP on a pedicled flap. The modification involved using DueDERM Extra Thin (ConvaTec, Flintshire, UK) strips which were placed on the clamping surface of the clamp. The clamp was held in place and tightened using an elastic band.

This modification of the standard bowel clamp design enhanced patient comfort. Ha & Wilson (2009) believed that the clamp would apply even pressure across the pedicle which can be set using the elastic band, making the clamp a useful tool for assessment of early flap division and IP methods.

3. System Design

This chapter explains the initial concept for the device and the development of an initial prototype. This prototype was then tested and approved by the clinical consultant before proceeding with the design process. A second prototype was developed to fulfil all the requirements and recommendations provided by the clinical consultant.

3.1. Concept

In this section, the concept development for the monitoring device is outlined with emphasis placed on the required device specifications.

3.1.1. Concept Specifications

In order to successfully generate device concepts a list of preliminary specifications were noted from discussions with the clinical consultant and from the literature review. Concept generation was then guided by these initial specifications, which are summarised in Table 2.

Table 2: Guideline specifications

Requirement	Unit	Value
Cost	ZAR	< 30 000
Oxygenation measurement		Yes
Comfort (clamping and sensors)	Scale 1 to 10	6
Heart rate measurement	BPM	Yes, but optional
Running time	Hours	> 72
Data logging		Yes
Automated clamping		Yes
Size	W x H x D (mm)	Less than 400 x 400 x 400
Non-invasive		Yes
Number of sensors		≥ 3

Cost

As a prototype device was required, it was essential to keep costs to a minimum. The device is aimed at South African public hospitals and therefore future iterations of the device should also be made as cost effectively as possible.

Oxygenation Measurement

In order for the device to successfully monitor a tissue flap, some form of oxygenation measurement or circulatory feedback is required. This could be done using monitoring options such as NIRS, photoplethysmography and pulse oximetry.

Comfort

The chosen clamping method should not add any additional discomfort when deactivated and not further limit the patient's range of motion.

Heart Rate Measurement

Heart rate measurement is an additional feature which is convenient to hospital staff for general patient monitoring. However, it is not a requirement for the monitoring of tissue flaps.

Running Time

The running (monitoring) time of the device should be at least 72 hours for the successful detection of any flap complications. Monitoring can be continued or restarted for pedicle division. The clamping system of the device is required to remain active until flap division or until deemed unnecessary by hospital staff.

Data Logging

Data logging is required for the analysis of data and for recording monitoring data for each patient.

Automated Clamping

In order to achieve reliable and accurate IP, the clamping system must be automated. The clamping can either be determined by preset timers or based on current and/or previous measurements. Regardless of the method used, the patient and system must be frequently checked as part of the patient recovery routine.

Size

The device size should be optimised in order to allow for flexible use. By limiting its dimensions, the device should easily mount onto a table or trolley for convenient transportation through hospital halls.

Non-invasive

The measurement system should be non-invasive. Invasive methods are generally more time consuming to apply and pose a higher risk of complications. The monitoring setup should not interfere with routine clinical checks or cause harm to the measured area.

Number of Sensors

A minimum of three sensors is required in order to measure the groin/abdomen/flank, proximal portion of the flap and distal portion of the flap. While having more than three sensors is not necessary, it would be beneficial. Additional sensor placement sites should also be considered.

3.1.2. Concept Generation

A basic device layout, illustrated in Figure 10, was created based on the specifications mentioned in Table 2. Several continuous monitoring options and IP concepts were compared by means of a decision matrix. The matrices can be seen in Table 3 and Table 4, respectively. The monitoring technology options listed in Table 3 (labelled 1 to 4) and the IP design concepts in Table 4 (labelled 1 to 3) are individually described prior to their respective tables.

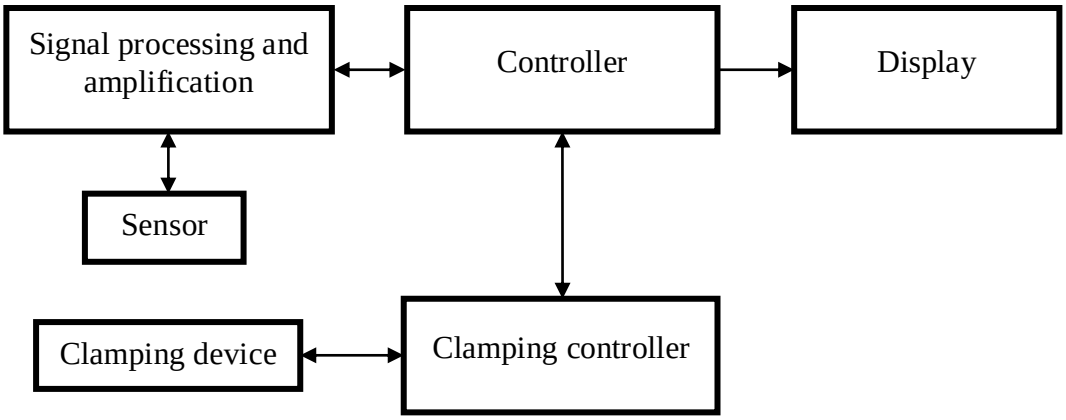

Figure 10: Basic device layout

An initial concept was created for the device on the basis that it should fulfil the following criteria:

- Measure and display the oxygen parameter.
- Measure and display the heart rate (if available).
- Display the photoplethysmogram (if available).
- Automatically operate a blood pressure cuff.

Technology 1: Pulse Oximetry (PO)

This technology makes use of reflectance pulse oximetry technology which typically incorporates a photodetector and two LEDs of different wavelengths. The oxygen saturation (SpO_2) can be calculated based on the change in absorbance of the two light sources. However, the signal must have a detectable pulsatile component.

The reflectance type sensor would be preferred as the transmittance sensor has limited mounting positions. Monitored information will be displayed on a computer screen or on a suitably sized LCD panel. As with all the listed technologies, it is important that the unit sourced can be manipulated to the user's needs.

Technology 2: NIRS Monitoring

The NIRS technology operates in a similar fashion to pulse oximetry and can also provide continuous oxygen saturation measurements. These measurements could then be used for control and displayed either on a computer screen or on the device screen itself (if a development unit is not available).

Technology 3: $TcPO_2$ Monitoring

This system would make use of modified transcutaneous Clark electrodes coupled to a monitoring system. The measurement information will be displayed on a computer screen or on the device screen itself.

Technology 4: Laser Doppler Flowmetry (LDF)

The laser Doppler flowmetry technology would make use of a laser Doppler probe and relevant system to continuously monitor blood flow and provide a relative measurement of perfusion units (PU).

Monitoring Technology Conclusion

Pulse oximetry technology scored the highest in the decision matrix (Table 3). It is the most affordable option and readily available in instrument and kit form.

Table 3: Monitoring technology decision matrix that aided in the selection of a sensor system

Specification Set (Score 1-5, where 5 is excellent)	Weight (%)	Monitoring Technology			
		PO	NIRS	$TcPO_2$	LDF
Cost	20	5	3,5	3	2
Non-invasive	15	5	5	5	5
Accuracy	10	3,5	4	3,5	3,5
Size	10	5	4	4	3,5
Number of sensors	10	3	4,5	4,5	2
Comfort	10	4	4	1	4
Patient safety	10	4,5	4,5	2	4,5
Running time	5	4	4	1	4
Heart rate measurement	5	5	4	1	1
User friendliness	5	3,5	4	2,5	4
Score (maximum of 5)		4,4	4,2	3,1	3,4

Concept 1: Padded Bowel Clamp

This concept would make use of an adapted version of Ha & Wilson's (2009) modified padded bowel clamp. The primary modification of the clamp would be to automate the clamp adjustment by making use of a stepper motor and lead screw which would be coupled to the clamp handles. Alternatively, a geared motor with rotation feedback could be attached to the pivot of the clamp.

Concept 2: Blood Pressure Cuff

Cheng *et al.* (2000) compared several clamping techniques including a pneumatic tourniquet. They found that the tourniquet had several advantages including good patient comfort. In order to automate the tourniquet an inflation system would be required. The system could consist of an electric pump or be implemented using compressed air.

Concept 3: Wedges

George *et al.* (1996) made use of two opposing v-shaped bars (as shown in Figure 8) which could be tightened by turning a screw on either side of the clamp. As with the previous methods, this system would require automation. This could be achieved through the use of one or two stepper motors controlling the screw. Alternatively, a linear actuator could apply pressure to the plates. For this modification, the screws could be replaced by linear guides.

Clamping Concept Conclusion

The blood pressure cuff scored the highest in the decision matrix (Table 4). As Cheng *et al.* (2000) discussed, it was found to be the most comfortable. The cuffs are inexpensive and readily available in a variety of sizes at hospitals.

Table 4: Decision matrix for clamping concepts that aided in the selection of a clamping system

Specification Set (Score 1-5, where 5 is excellent)	Weight (%)	Concept		
		Padded Bowel Clamp	Blood Pressure Cuff	V-Shaped Wedges
Cost	20	4	3,5	4
Accuracy	10	3	4,5	3
Size	10	3,5	4	3,5
Controllability	20	3	5	4,5
Comfort	10	3,5	4,5	3
Patient safety	10	3	4	2
Adjustability	10	3	4,5	3
User friendliness	10	3,5	4	3
Score (maximum 5)		3,4	4,3	3,5

3.2. Proof of Concept (First Prototype)

In order to test the concept, a prototype device was built making use of a single sensor. This device was demonstrated to and its function verified by the clinical consultant, before progressing to a second prototype.

3.2.1. Specifications

The initial prototype followed the basic component layout as specified in Figure 10 and provided the required functionality. Aside from the inclusion of base criteria mentioned in Table 2, alterations were made to the original guideline specifications based on feedback from the clinical consultant. The modified specifications are shown in Table 5, with the changes made to the original specifications shown in italics.

Table 5: First prototype specifications

Requirement	Unit	Value
Cost	*ZAR*	*< 10000*
O_2 saturation measurement		Yes
Comfort (clamping and sensors)	Scale 1 to 10	6
Heart rate measurement	BPM	Yes
Running time	Hours	> 72
Data logging		*Optional*
Automated clamping		Yes
Size	*W* x *H* x *D* (mm)	*Less than 400* x *280* x *280*
Non-invasive		Yes
Number of sensors		*1*
Reusable for future iterations		*Yes, if possible*

3.2.2. Component Selection

Component selection was conducted based on the guideline specifications (Table 2), first prototype specifications (Table 5) and the two decision matrices (Table 3 and Table 4). The primary factors for sourcing the majority of the components were functionality, availability and cost.

The core hardware components were identified as the sensor, relevant amplifier and signal processing system. Section 3.1.2 revealed that pulse oximetry using photoplethysmography was the most suitable measurement system. Designing such a system was out of the scope of this thesis due to the availability of well-developed, commercially available systems. Accomplishing similar levels of accuracy, filtering, build quality and signal processing quality to that of commercial devices would require expertise in multiple fields and a large amount of development time beyond the time frame available for the research required for this thesis.

The selection of an appropriate sensor system was evaluated based on the availability and compatibility of the reflectance versions, as well as their ability to provide plethysmogram, heart rate and SpO_2 output. In order to meet the above criteria, several options from different manufacturers were compared. Table 6 shows a comparison of the key specifications between different brands.

Table 6: Sensor comparison

	Nonin OEM III + reflectance sensor [1]	Masimo MS-2040 + Radical 7 [2]	Smiths Medical Digital Micro Oximeter Board [3]	Nellcor Multi-functional Respiratory PCB Assembly [4]	APM Korea OEM SpO2 kit [5]
Power consumption & supply	29 mW @ 3,3 V DC 3,3 or 5 V DC	< 45 mW @ 3,3 V DC 3,3 V DC	46 mW @ 3,3 V DC 3,3 V DC	232 mW @ 5 V DC 5 V DC	100 mW @ 3,3 V DC 3,3 or 5 V DC
Size	34,3 x 24,1 x 6,2 mm	50,8 x 35,05 x 9,14 mm	39 x 20 x 6,1 mm	51,05 x 38,35 x 21,34 mm	43 x 23 x 5,5 mm
Accuracy SpO_2	± 3 digits	± 2 digits	± 2 digits	NA	± 2 digits
Accuracy SpO_2 Low Perfusion	± 2 digits	± 3 digits	± 2 digits	NA	NA
Accuracy from	70 %	NA	70 %	60 %	NA
Reflectance Sensor Compatibility	Yes	Yes	No	Yes	Yes
Plethysmogram	Yes, 16 bit	NA	Yes	Yes, 8 bit	Yes, analogue
Cost [6] (1 to 10)	7	4	8	NA	7

[1] Nonin Medical, North Plymouth, MN, USA. [2] Masimo Corporation, Irvine, CA, USA. [3] Smiths Medical, St Paul, MN, USA. [4] Medtronics, Minneapolis, MN, USA. [5] APM Korea, Daejeon, Korea. [6] Actual cost has been omitted due to confidentiality.

From Table 6 it is clear that the Nonin OEM III board and 8000R reflectance sensor are suitable for this project due to their lower relative costs, higher resolution plethysmogram output, as well as fulfilling all the requirements for the prototype.

At the time of choosing an appropriate oximeter the author was already in possession of an APM Korea BME PPG Kit and DCM01 sensor. These were tested and the following results were found:

- The on-board sensor worked well in displaying a plethysmogram and pulse output.
- When an external sensor was used, in this case the DCM01, the pulse was still detected but the amplitude of the plethysmogram was very low. The gains of the amplifiers were modified for improved results but the signal remained unsatisfactory.
- The kit itself only has an analogue output for the plethysmogram and pulse, limiting the number of recordable signals.
- Only the infra-red plethysmogram was available.
- The kit was designed around the on-board sensor and modifications would be needed to use the DCM01.

Based on these grounds, the kit was deemed unsuitable for this project as it would require several modifications and additions in order to achieve the project specifications. Instead, the Nonin OEM III module and 8000R reflectance sensor were chosen for the prototype setup. Other key components and features are shown below:

Nonin OEM III Signal Processing Module

The Nonin OEM III uses Nonin Medical's PureSAT® oximetry technology. This technology has intelligent filtering and advanced algorithms which help eliminate artefacts caused by low perfusion, motion and other interference (Nonin Medical Inc., 2008).

The module has an asynchronous serial output allowing it to be directly interfaced with most microcontrollers and computers. All information, including heart rate, SpO_2, and 16 bit PPG waveform can be obtained from this output. This makes it relatively simple to interface with a microcontroller that has serial communication (Nonin Medical Inc., 2007).

Nonin Medical claims a power draw of 45 mW when running the module at 5 V DC. This is a small amount of power and will assist in maintaining energy efficiency.

Various Nonin Medical sensors are compatible with the module, including a finger clip and reflectance sensor.

One disadvantage of using the OEM III is that a board is required per sensor.

Nonin 8000R Reflectance Sensor

This reusable sensor is compatible with the OEM III module and can be mounted in an area which does not necessarily allow for light transmittance, therefore making it suitable for monitoring different flap types. The Nonin 8000R sensor's dependence on light reflectance rather than transmittance makes it more versatile than a finger clamp, allowing it to be placed on more areas of the body. Although the preferred mounting location is the forehead, the sensor also operates on other areas of the body (Nonin Medical Inc., [S.a.]). The primary disadvantage of using the sensor on areas other than the forehead is the lack of clinical validation by the manufacturer for these areas, possibly resulting in inaccurate readings.

Other components that were required for the design included a microcontroller, power supply, blood pressure cuff and cuff control. The following components were selected based on the highlighted reasons:

Arduino Duemilanove Microcontroller (Arduino, Ivrea, Italy)

- The author already owned this device.
- It supports the use of C type programming language with a rich source of examples and online support.
- The PCB contains a built in programming interface (RS232) which can be used for general communication once the Atmel chip has been programmed.
- Suitable I/O ports for project interfacing.
- The functionality of being able to programme and then remove microcontroller without the need of the baseboard.

Neonatal Blood Pressure Cuff

- Cuff is supplied in suitable sizes for pedicled flaps.
- High relative patient comfort and already tested on pedicled flaps (Cheng *et al.*, 2000).
- It is readily available in hospitals.

Festo MHE3-MS1H-3/2G-1/8 Solenoid Valve (Festo, Esslingen, Germany)

- Uses standard Festo fittings which were readily available to the author.
- Allows for zero bar switching pressure. This valve was specifically chosen with low minimum switching pressure and direct pilot in order for it to function under the low pressure required to operate the cuff.
- Includes an exhaust port for deflating the cuff.
- Boasts a compact design.

Schneider Electric ABL7 RE2403 24 V DC Power Supply (Schneider Electric, Rueil-Malmaison, France)

- The author already owned this device.
- Boasts a compact design.
- Supplies 24 V DC which was suitable for the solenoid valve.

3.2.3. Interfacing

The interfacing of the OEM III module with the Arduino was done using the Arduino's programming port. This had the disadvantage that the OEM III must be disconnected to gain access to the USB interface on the Arduino for programming.

A Nokia 5110 LCD (Nokia, Espoo, Finland) was used to display the necessary information. The display is low cost and simple to interface with an Arduino. This interface was done using a software implemented UART (universal asynchronous receiver/transmitter) port on the Arduino Duemilanove. The software implemented port makes use of the NewSoftSerial library (Hart, 2013) and was required to overcome the single UART port limitation. This port proved reliable for the LCD display; however, not for reading the OEM III data. The NewSoftSerial library is interrupt driven making it processor intensive and not completely reliable. The library has received several speed and reliability updates after it was implemented in the first prototype. If re-implemented, the author believes either port would be suitable for the OEM III.

The solenoid valve operates off a 24 V DC signal whereas the Arduino only has 5 V DC outputs with low current delivery. To overcome this, a 5 V DC reed relay was used to switch a larger 24 V DC 2 A relay. All of the programming of the Arduino was done using the native and freely available software provided by Arduino.

The components were mounted on a piece of plywood and electrical circuitry was developed on a sheet of strip board. The unit is compact, measuring 150 mm x 160 mm x 70 mm (excluding cabling). A top view of the complete prototype is shown in Figure 11.

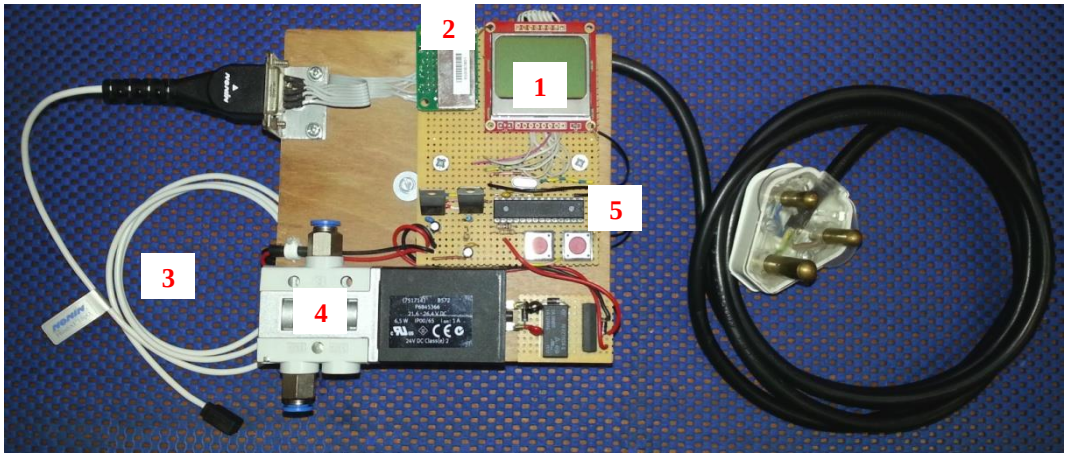

Figure 11: Complete assembly of the first prototype. 1, Nokia 5110 LCD. 2, Nonin OEM III module. 3, Nonin 8000R sensor. 4, Festo solenoid valve. 5, Atmel ATMega328P microcontroller

3.2.4. Testing

Once all components had been implemented and programming was completed, basic testing was conducted. The reflectance sensor was attached to the index finger. Once an acceptable signal was acquired by the OEM III board the heart rate and SpO_2 reading was displayed on the LCD (Figure 12).

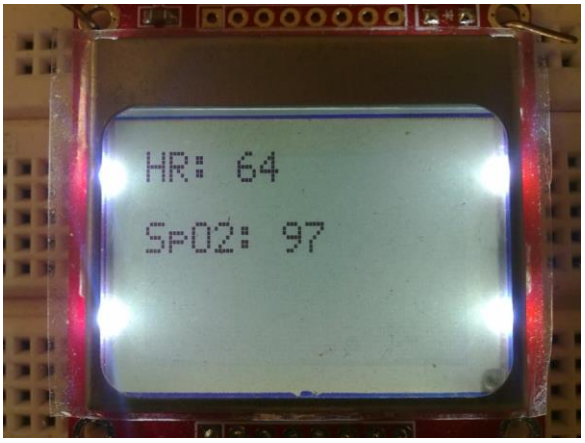

Figure 12: Nokia 5110 LCD display of heart rate and SpO_2

Two separate screens were programmed, one for the heart rate and SpO_2, the other for the photoplethysmogram which were alternately selected by a push button switch. Figure 13 shows the LCD display of the plethysmogram.

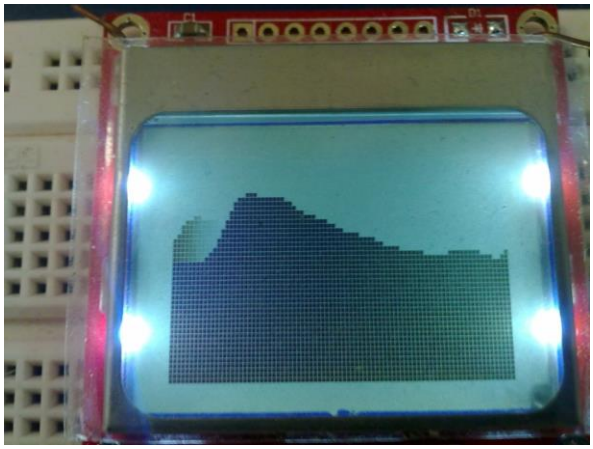

Figure 13: Nokia 5110 LCD display of the plethysmogram

It was found that the display of the plethysmogram (on a fixed scale) on the LCD was useful but offered limited information due to the small screen size. The LCD was then more appropriately used for displaying the heart rate, SpO_2 and valve duty cycle (DC %) and timing of the valve as seen in Figure 14. This setup was subsequently demonstrated to the clinical consultant using compressed air to inflate the blood pressure cuff. It was also explained that the plethysmogram was displayed but proved ineffective on the LCD.

Figure 14: Final display design

Several alterations and improvements were adopted while developing this prototype and were incorporated together with suggestions from the clinical consultant in the final prototype design. The most important adjustments were:

- Incorporate two more sensors with relevant signal processing modules.
- Increase timer lengths for the cuff control.
- Include a computer interface with logging capability.
- Find a substitute for shop supplied compressed air.
- Display the plethysmogram for each sensor.
- Ensure the availability of adequate UART communication resources.

The modifications determined the final component selection and design and are outlined in Section 3.3.

3.3. Second Prototype

The first prototype received the clinical consultant's approval and final specifications were set for the device. The system was developed in sections which were individually tested as they were integrated with the final product. Once the final prototype was developed, it was delivered to the clinical consultant for clinical testing.

3.3.1. Specifications

Several additional specifications were added which differed from the first prototype. These were implemented in a second and final prototype. The additions and changes to the specifications of Table 5 are listed:

- Incorporate three reflectance sensors that operate simultaneously.
- Provide a graphical user interface (GUI) which displays heart rate, SpO_2 and plethysmogram. In addition to this, controls for the pneumatic cuff, sensor control and logging must also be present on the interface.
- Incorporate a data logging functionality.
- Eliminate the use of shop compressed air for mobility and practicality purposes.
- Add a simple electrocardiograph (ECG) to the system for future tests. The ECG was included for future tests which will attempt to detect arterial congestion by observing a change in time delay between the ECG pulse and photoplethysmogram.

3.3.2. Component Selection

Component selection was done in a similar fashion to the first prototype, again making use of the guideline specifications in Table 2 and the noted improvements and suggestions from the first prototype. In order to fulfil the system's measurement and control objectives, the following hardware was required:

- Oximetry sensor amplifier and signal processing module
- Three reflectance pulse oximetry sensors
- Programmable controller
- Air supply
- Motor driver
- Clamping device
- Pressure transducer
- Valve
- ECG

Components which were reused from the first prototype were the Nonin OEM III module, Nonin 8000R sensor and neonatal blood pressure cuff. New components required were a microcontroller, pump, motor driver, pressure transducer and ECG. The components that were selected are mentioned below.

Nonin OEM III Signal Processing Module

It was decided that the Nonin OEM III used in the first prototype was to be reused as the author obtained satisfactory results from this module. Two identical modules were additionally purchased.

Nonin 8000R Reflectance Sensor

As with the Nonin OEM III, the 8000R sensor was reused and an additional two were purchased.

Arduino Mega ADK Microcontroller

Despite the satisfactory performance of the Arduino Duemilanove for the first prototype, there were several limitations which would disqualify its incorporation in the second prototype. The main limitation was that it only has one UART port, which hampered its ability to receive data from the OEM III board and communicate with a PC simultaneously. Three or more UART ports were necessary for the second prototype due to the increase in OEM III boards.

It was decided to purchase an Arduino with improved capacity and capabilities. Using this Arduino has the benefits of similar interfacing to that of the previous device, allowing programmes from the Duemilanove to be easily adapted.

The Arduino Mega ADK is ideally suited for use with the Nonin OEM III modules as it has four UART ports, one of which is connected to a USB to TTL (transistor-transistor logic) converter. The USB to TTL converter allows for direct programme downloads and communication with a computer (Arduino, [S.a.]). Native PWM outputs and analogue inputs will be needed for pressure measurement and pump control. Table 7 shows a summary of the microcontroller's features.

Table 7: Main microcontroller features

Feature	**Specification**
Microcontroller	ATmega2560
Operating Voltage	5 V
Digital I/O Pins	54 (of which 15 provide 8 bit PWM output)
Analogue Input Pins	16 (10 bit)
DC Current per I/O Pin	40 mA
DC Current for 3.3 V Pin	50 mA
Flash Memory	256 KB of which 8 KB used by bootloader
SRAM	8 KB
EEPROM	4 KB
Clock Speed	16 MHz
UART Ports	4

Verderflex EZ Peristaltic Pump (Verderflex, Vleuten, Netherlands)

The pump is capable of producing 750 mmHg of pressure and a maximum flow of 1,26 l/min (Verder International B.V., [S.a.]), which is adequate for overcoming systolic pressure. Being fairly compact it contributes towards system mobility. A pressure vessel was considered, however the clamping system only requires a small volume and reduced flow rate. The direction of the pump can be switched in order to deflate the blood pressure cuff which eliminates the need for a separate valve to release the cuff pressure. Another benefit of using this peristaltic pump is that the system is sealed when the pump is off due to the three roller design of the pump head, thereby improving power consumption and pump duty cycle.

Pololu 18v15 Motor Driver (Pololu, NV, USA)

A motor driver was required to control the direction and speed of the peristaltic pump. A Pololu 18v15 was available to the author and sufficient for use in this project. This driver can handle 15 A continuous current while having a very compact footprint of 33 mm x 20 mm (Pololu Corporation, [S.a.]). Using a PWM output and a digital output of the microcontroller, it was possible to control motor speed and direction, allowing variable flow rate in and out of the blood pressure cuff to be achieved.

CRITIKON SOFT-CUF, Neonatal Blood Pressure Cuff (GE Healthcare, Little Chalfont, UK)

A method for reducing or restricting blood supply in a pedicled flap was required. The neonatal blood pressure cuff was used, as it is a suitable size and is readily available in hospitals.

Honeywell 15psi Gauge Pressure Sensor (Honeywell, NJ, USA)

A transducer was required in order to measure the pressure in the neonatal blood pressure cuff. The pressure needed to overcome systolic pressure should not be more than 300 mmHg. This sensor was suitable as it measures from 0 mmHg to 775 mmHg, where 775 mmHg is marginally higher than the maximum pump pressure. Its output is amplified internally, therefore simplifying interface circuitry with the microcontroller.

ECG

Only basic electronic components were needed to build a simple ECG. Components used were, resistors, capacitors and three operational amplifiers (op-amps). The ECG would not function as a diagnostic tool for heart problems but only for timing related measurements with the PPG obtained from the Nonin OEM modules.

3.3.3. Software Selection

Several options were considered for the GUI and more than one programme was tested for this purpose. A GUI was needed to enable surgeons and other medical staff to observe parameters and make system adjustments. The interface must include all necessary displays and controls for air pressure, clamping timers, logging, PPGs and sensor control. A user interface was also useful to the patient as they will be able to observe the measurements and pump timers, as well as the effects of their body movement on the sensor signals, thus allowing them to find rest positions which favour the system.

The Arduino programming was done using its native software as the software is user friendly and is supported by a wealth of libraries and support on the internet.

MATLAB (Mathworks, MA, USA)

The first software package that was tested was MATLAB (The MathWorks Inc., [S.a.]), which is a useful tool for computation and visualisation with built-in toolboxes and functions that allow users to create programmes with relative ease. The ease of array manipulation was advantageous for this project, as the sensor data is best read in an array style. A programme was created and tested, however it was found that when reading data from all three sensors, data acquisition was not fast enough and eventually the serial port buffer would overflow, causing the programme to lose synchronisation with the Arduino. Unfortunately, due to the asynchronous data transmission design of the OEM III boards, any loss of synchronisation requires that the current packet be scrapped and that a new start byte is acquired. Plotting a real time plot of the PPG required the most processing time. Once this shortfall was noticed it was decided to move to a different software package which was better suited for data capturing and live display.

National Instruments Labview

Labview has proven to be a strong candidate for displaying and recording real-time data. It is easy to create a user-friendly GUI in a small amount of time owing to a programming style which is more visual than MATLAB styles. However, it contains many of the same functions, as well as many additional functions that make certain tasks simpler for the programmer.

A Labview programme was created that performed the following:

- Read data from the Arduino.
- Send data to the Arduino, primarily for pump control and synchronisation check.
- Process and display data from the Arduino, including heart rate, SpO_2 and PPG values.
- Provide the user with controls for the inflation and deflation of the blood pressure cuff.
- Log the data to file.

The display panel is shown in Figure 15.

Figure 15: Labview display panel

All three PPG signals were displayed on one chart, which could be activated or deactivated via a push button. This was implemented so that sensors could be disabled if they were unused or faulty. Despite the usefulness of the auto-scale chart, a large difference in PPG signal amplitudes could result in a larger signal that may overshadow the smaller one. Therefore, a manually adjustable scale was implemented such that the smaller signal may be viewed properly.

A chart for the ECG and pressure were included for observation. If there is a slow leak or a pressure change due to movement or muscle contractions, it is easily detected on the chart.

Given the possibility of a leak developing in the cuff or pipe system, a leak detection alarm was included. The alarm will flash and also generate an audio tone if the pump has been running for 10 seconds without reaching its set point.

Labview's performance was deemed satisfactory after testing the software with all necessary features. The programme was compiled into an 'exe' allowing it to be

used without an installation of Labview. This programme was later tested on a dated entry level laptop that had a 2 GHz dual core CPU and 2 GB of memory. The programme ran acceptably, consuming approximately 20 % of the CPU and 35 MB of memory. Review of the recorded data files indicated an acquisition rate of 75 Hz which matched the transmission rate from the Nonin OEM III modules. This laptop, along with device, was delivered to the clinical consultant for clinical testing.

3.3.4. Programming

The programming required for this thesis was divided into two primary sections, namely, microcontroller programming and computer-side software programming. Each one of these sections was broken down into smaller subsections, which are listed in Table 8.

Table 8: Programming subsections

Microcontroller	**Computer-side**
Initialisation (variables, I/O assignment, etc.)	Initialisation (variables, communication, etc.)
Communication	Communication
Processing	Processing
Control	Display
	Storage
	Control

After initial experimentation, it was decided to conduct the majority of the data processing and control on the computer-side. This was done due to the nature of the asynchronous serial communication with the Nonin OEM III modules. It was found that synchronisation could easily be lost if too much processing was done by the microcontroller.

The Labview and microcontroller programming was an iterative and ongoing process in the early stages of clinical testing. This was mostly due to continuous improvements, observations and recommendations from hospital staff. A basic software flow diagram for the Arduino is shown in Figure 16 followed by a brief explanation.

Arduino Programming

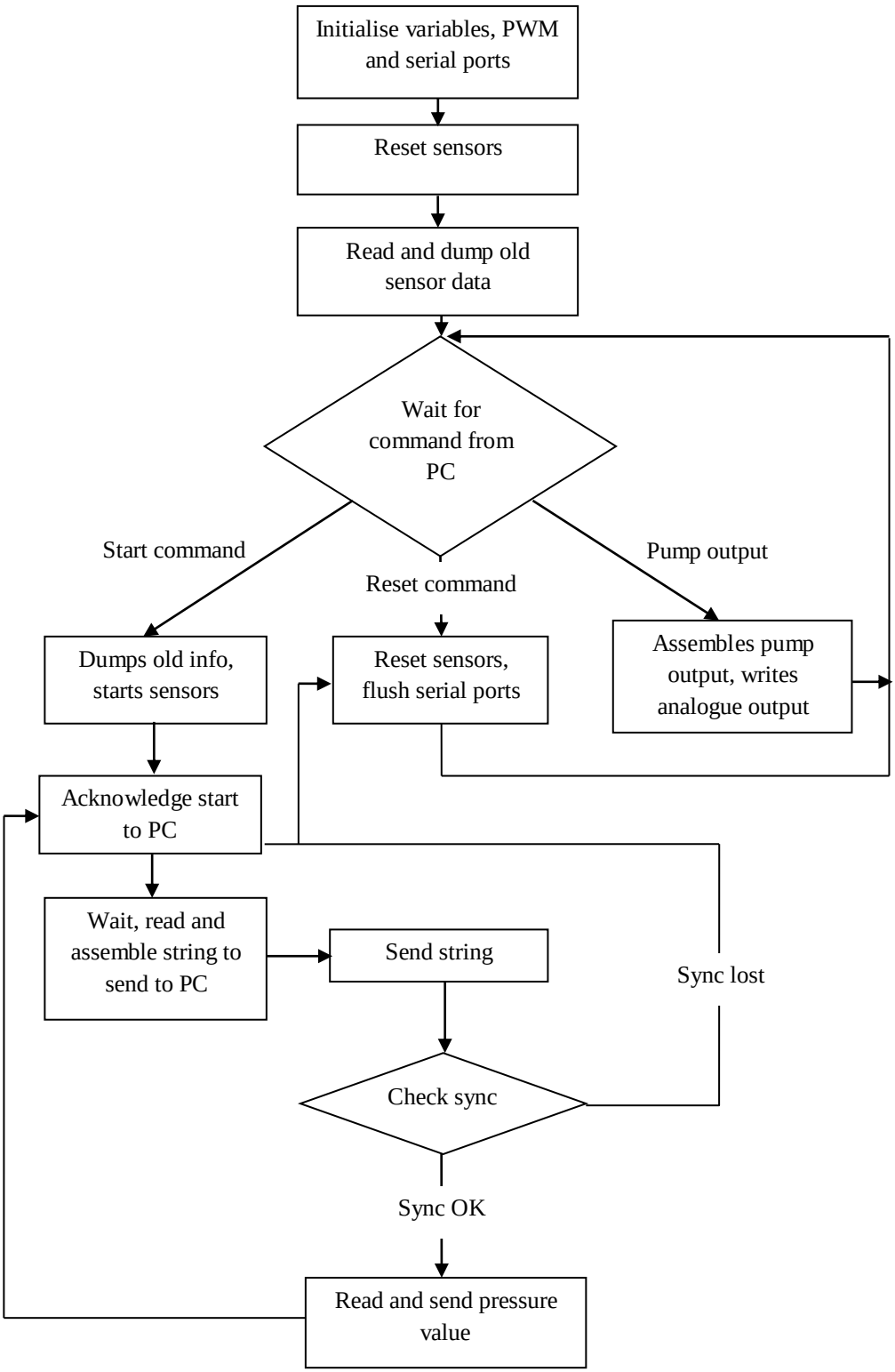

Figure 16: Software flow diagram for the Arduino microcontroller

The Arduino programme sequence is briefly described as follows:

- When the Arduino is powered up it initialises all the variables, inputs, outputs and serial communication ports.
- It then resets all three sensors by creating a “HIGH” signal on the OEM III reset pin. The reset line is a dedicated pin provided on the OEM III boards.
- Following this, it reads and dumps any information found on the serial port such as residual data within the buffer.
- Once this has been done, the Arduino waits for a command from the computer (sent via USB).
- There are three possible commands which the computer may send, namely, start, reset and pump output commands. For start-up, the “start” command is the most likely. If the “start” command is received the Arduino will once again dump any old serial port data and then change the sensor reset line to “LOW” beginning the transmission of data from the OEM III modules.
- The Arduino then acknowledges that it has received the start command and assembles strings of data from the sensors to send to the computer. Once the entire packet is sent (125 strings) a synchronisation check is done. If the check is successful, the pressure reading is sent to the computer. If the check fails, the sensors are reset and the serial ports flushed.
- The last possible command that can be received from the computer is the “pump output” command. This command is used to control the speed and direction of the pump. The command sends an integer which contains the speed and direction information. This integer value is calculated by the PID loop running in the Labview programme.

Figure 17 shows a simplified Labview flow diagram for the Labview programme running on the computer. This programme handles the displaying and logging of information, amongst other tasks. The full Labview code can be found in Appendix A.

Labview Programming

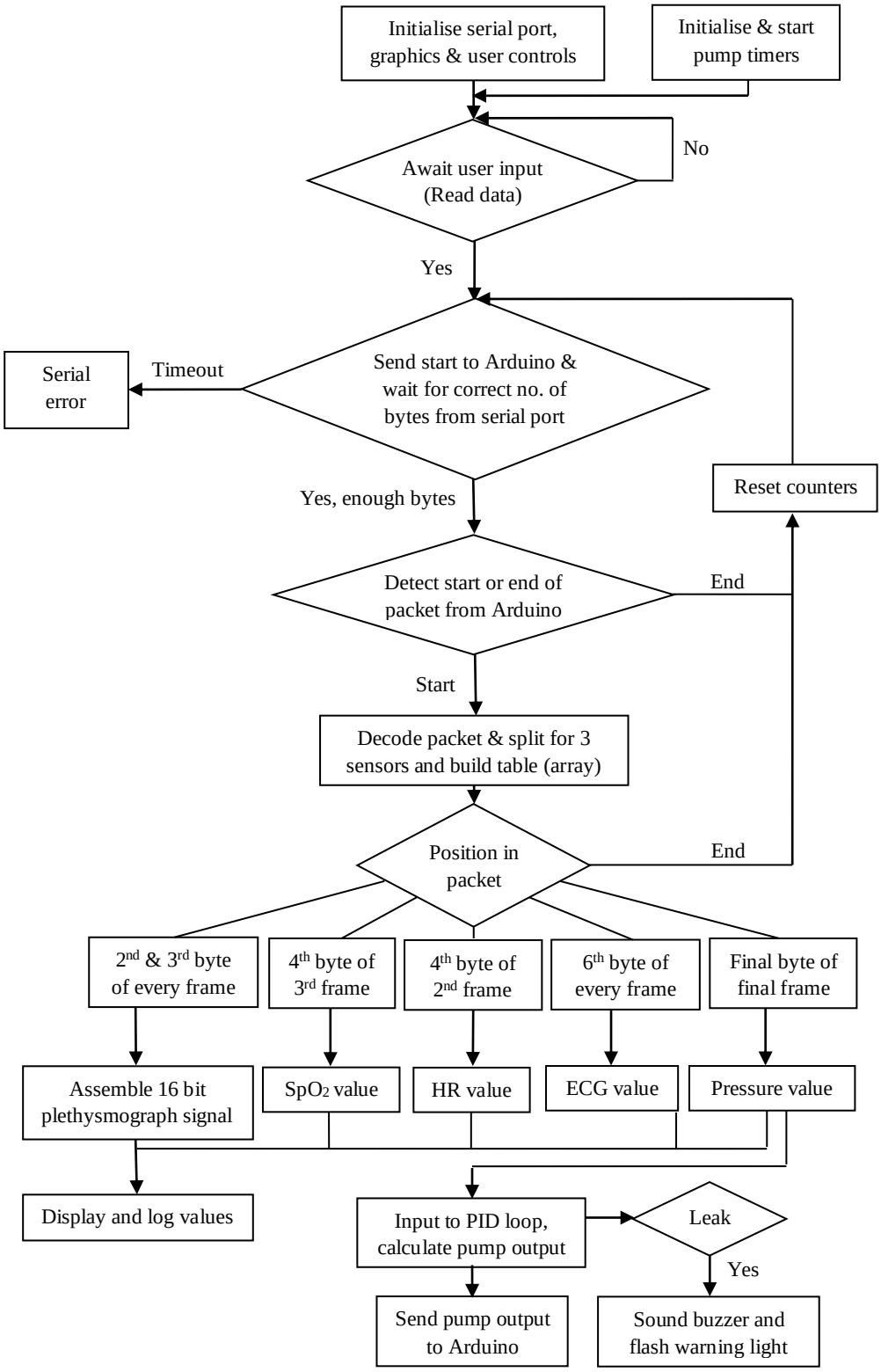

Figure 17: Software flow diagram for the Labview programme

The Nonin OEM III modules have several serial data format options. Serial data format #7 was chosen as it provides the highest resolution for the PPG signal (16 bit). The OEM III modules make use of asynchronous serial communication and transmit data in a packet format. Each packet consists of 25 frames. Table 9 shows an example of a frame from the serial data format #7 packet. See Appendix C for additional information and the complete packet structure.

Table 9: Example of Nonin OEM III frame format

Byte 1	**Byte 2**	**Byte 3**	**Byte 4**	**Byte 5**
STATUS	PLETH (MSB)	PLETH (LSB)	SpO2	CHK

The programme sequence is briefly described as follows:

Once the Labview programme is run, it initialises the serial port, graphics, user controls and pump timers.

The programme then waits for the user's command to begin reading data from the Arduino. If no command is given, the programme will wait until the "Read data" button is pressed.

- If the "Read data" button is pressed, Labview will instruct the Arduino to begin transmitting data. The Labview programme will only proceed if the user selected number of bytes (typically 18 bytes) has been received. If not, the programme will wait. While waiting, the read serial data loop will be exited every 4000 iterations to process any other program changes. Under normal circumstances the loop will be exited in under 4000 iterations. In the case of a serial port communication failure a timeout error will be generated after three seconds.
- The computer then waits to receive the "start" command from the Arduino. This indicates the beginning of a packet. If the computer receives an end of packet marker, the Labview programme resets the counters used to re-assemble the packet.
- Once the start command is received from the Arduino, the computer begins to decode the received information (split information per sensor) and build an array.
- Depending on the position in the packet, certain variables will be extracted. The most critical variables include:

  16 bit plethysmogram signal – This signal is assembled from 2 bytes per a sensor and is received 25 times per packet.

  SpO_2 value – The SpO_2 value is received once per packet per sensor.

Heart rate value – The heart rate value is received once per packet per sensor.

ECG value – The ECG value is received 25 times per packet.

Pressure value – The pressure value is received once per packet.

- All of the critical values mentioned in the previous step are displayed on various charts and indicators. The user can choose if they wish to log the values.
- The pressure value received from the Arduino is further used for the control of the pump. This value is used as feedback for the PID controller. The Labview PID controller determines the appropriate pump output required to reach the desired set point. Labview sends this pump output value to the Arduino. The Arduino interprets this information and generates a PWM signal for controlling the pump.
- Based on the pump output and pressure value the Labview programme determines whether there is a leak in the air system. If a leak is detected, the programme sounds an alarm.

Control System

A control system was required in order to maintain a set pressure in the clamping system. A PID algorithm was chosen for its ability to actively control the pressure at a given set point. It is a pre-existing Labview function and allows for parameter adjustment to tune the algorithm for the pump system. Figure 18 shows a simplified diagram of the PID algorithm which Labview employs.

The P, I and D parameters can be adjusted to tune the system for optimal transient response, overshoot and oscillation.

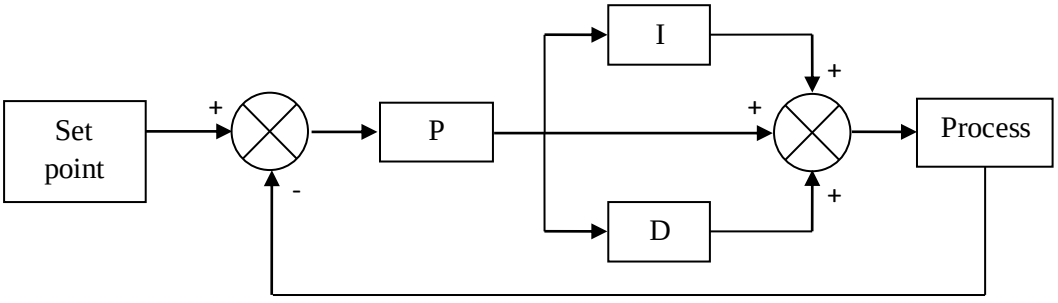

Figure 18: Simplified PID diagram for the peristaltic pump

Figure 19 shows a simplified connection diagram of the hardware setup that controls the pump. After the Labview PID algorithm has calculated the necessary pump output, this value is then sent to the Arduino via the serial port. The Arduino reads this value and writes a PWM output as well as a direction output. Both of these outputs are fed to a PWM motor driver (coupled to the pump motor) which amplifies the PWM signal. Feedback for the control loop is obtained for a pressure transducer that has been placed on the output side of the pump.

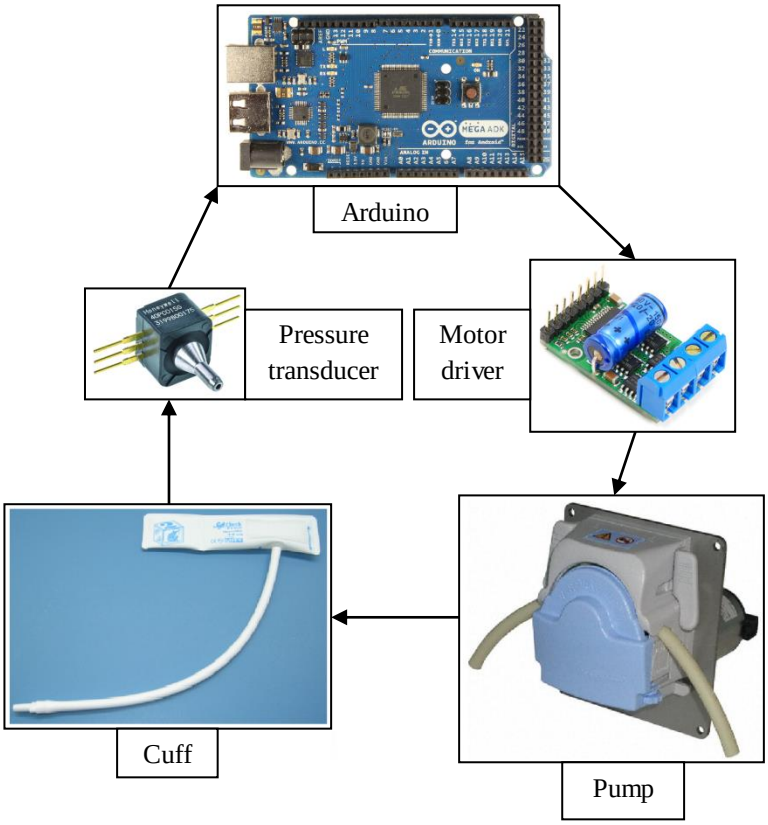

Figure 19: Hardware layout of the pump control system

Tuning of the PID loop was initially done using the Ziegler–Nichols method (Bequette, 2003: 198) followed by fine adjustments made by trial and error. It was not necessary for the controller to have a rapid response as the clamping process is slow, with inflation to a maximum pressure of 300 mmHg taking approximately 15 seconds and remaining inflated for 15 minutes or more. Pressure overshoots were within the range of 10 mmHg which had negligible effect due to the inflation pressure chosen well above systolic pressure. Additionally, a slow response also prevents unnecessary strain on the pump.

3.3.5. Construction

Device construction was carried out once a majority of the components had been sourced and preliminary testing had been conducted.

Printed Circuit Board

A PCB (printed circuit board) was designed in order to cater for the three Nonin OEM III signal processing boards and to provide a simple interface between the Arduino and Nonin products, pressure sensor and motor driver. The design was created using RS Component's Design Spark (RS Components, Corby, UK). This software is free and has all the required functionality. A local PCB manufacturing company printed the final design which was a double sided PCB with through-hole plating.

The PCB was designed in the form of an Arduino shield, as shown in Figure 20, which contains sockets for the three signal processing boards as well as D-sub 9 sockets for the three 8000R reflectance sensors. Additional Arduino inputs and outputs were made accessible via a female header. This was added as a precautionary measure should the system need slight modification or expansion. OEM III serial data types are easily selectable via a jumper provided near each signal processing board. The PCB schematic can be found in Appendix B.

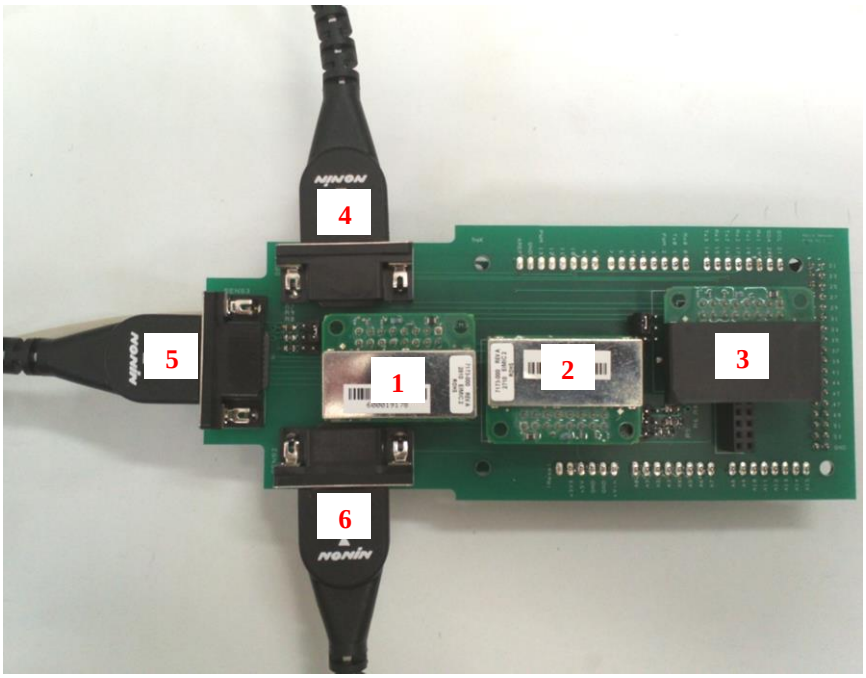

Figure 20: Populated Arduino PCB shield showing Nonin OEM III boards (1 to 3) and the Nonin 8000R reflectance sensor ports (4 to 6)

ECG Circuitry

A very simplistic ECG circuit was adapted and built based on an online schematic (Raul, 2013). The circuit makes use of three op-amps. An INA121 instrumentation amplifier was used for the initial amplification from the ECG electrodes. It has a large common mode rejection ratio (CMMR) and is suitable for this application as per the datasheet application notes (Appendix C). Two LM324 op-amps were used: one to create a virtual ground and the other as a final amplification and filtering stage. The schematic diagram can be found in Appendix B.

Device Housing and Final Assembly

High device mobility was required so that it could be transferred from patient to patient and between hospital wards. Therefore its overall size was limited (as per the specifications set out in section 3.1.1). Commercially available components were used as far as possible in order to reduce development costs and to allow for ease of repair.

All components (excluding sensors) are housed in a plastic enclosure (Figure 21). The enclosure is inexpensive, lightweight and durable. It measures 320 mm x 220 mm x 180 mm. The components were mounted in place on a piece of plywood. The wood is lightweight, sturdy, easy to manipulate and readily available.

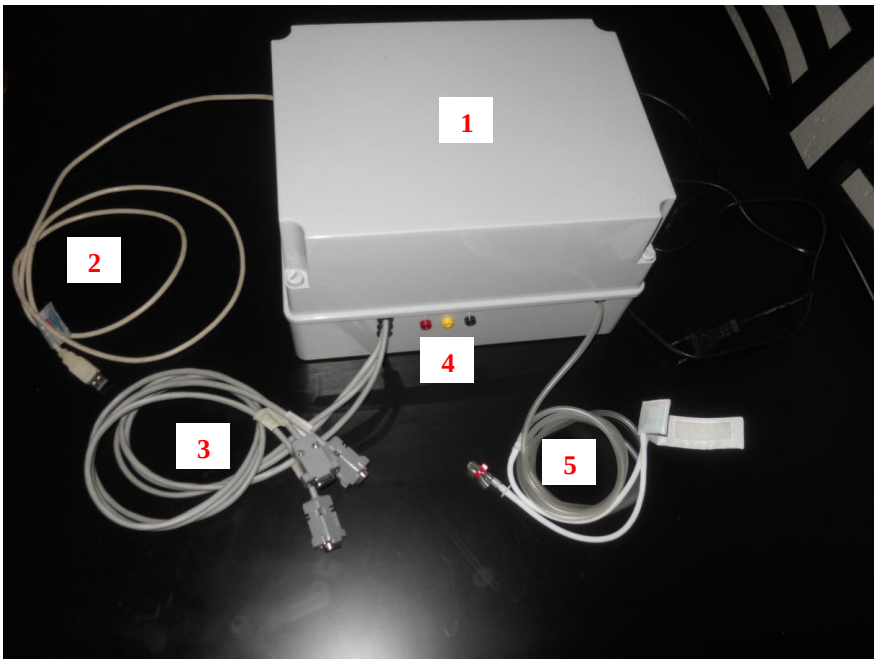

Figure 21: Second prototype with closed device housing (1), USB interface (2), reflectance sensor extensions (3), ECG ports (4) and pneumatic cuff output (5)

Figure 22 shows the open enclosure which houses all of the device components. The peristaltic pump occupies a majority of the enclosure. Device dimensions can therefore be reduced by simply sourcing a smaller pump and enclosure. Two pine handles were attached to the base board to keep the board in place (should the device be placed upside down) as well as for simplifying the removal process for repair or servicing.

The component layout was chosen based on electrical noise considerations and the available space within the enclosure. Conductors passing high current were separated from signal wires in order to reduce noise. It was found that the cable of the Nonin 8000R reflectance sensor was too short for the sensor to be placed on areas other than the finger. Three shielded extensions were made in order to overcome this.

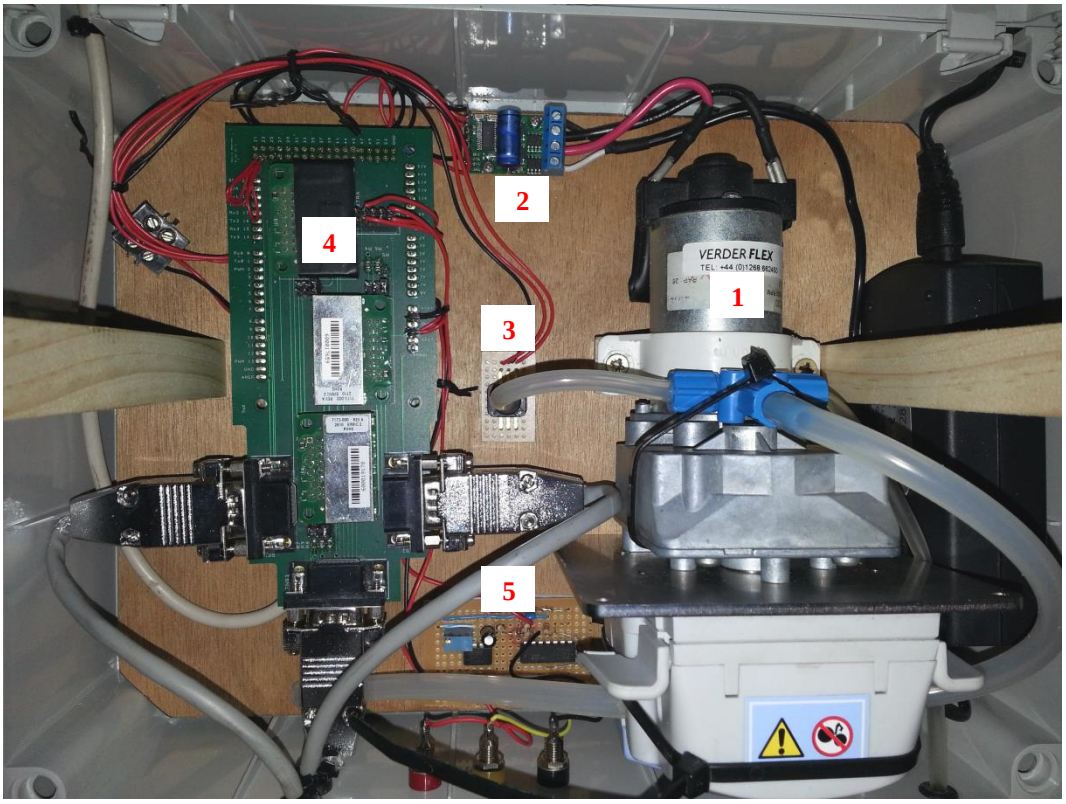

Figure 22: Second prototype with open view of device housing showing peristaltic pump (1), motor driver (2), pressure sensor (3), Arduino microcontroller with shield (4) and ECG circuitry (5)

Sensor Housings

Although the Nonin 8000R reflectance sensors were supplied with 8000H sensor holders (Figure 23), it was found that the mounting of the sensor using the provided double sided tape was not sturdy enough. In addition, the clear plastic does not block ambient light. The 8000H does feature a small piece of foam placed behind the sensor. The foam applies pressure on the sensor so that it mounts rigidly on the skin. Doing this reduces the chance of ambient light interference and insufficient mounting pressure.

Figure 23: Nonin 8000H adhesive sensor holder

Through testing it was found that mounting pressure and location can affect measurement quality, therefore a reliable mounting method was required. There are many mounting options available, including tapes and plasters. However, these are more susceptible to sensor movement.

Two sensor housings were development in a CAD (computer-aided design) package. This was then printed, using an Objet 3D printer (Stratasys, MN, USA). Figure 24 shows one of the designs with slots for elastic or bandage material, foam insert (similar to the 8000H) and small tolerance between sensor and housing to reduce sensor movement.

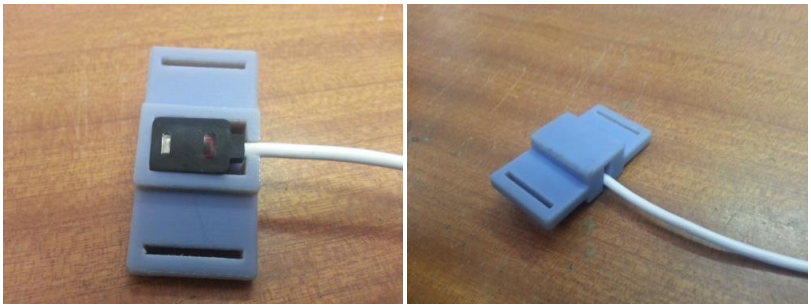

Figure 24: A 3D printed sensor housing, bottom view (left), top view (right)

The second housing design is shown in Figure 25. It features a small footprint (compared with the slotted design), with premade holes for sutures and retaining ribs to assist with suture fastening.

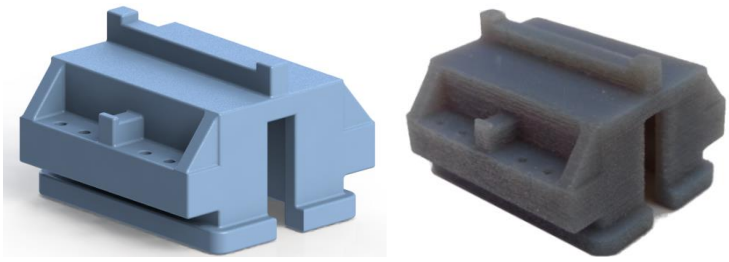

Figure 25: Render of the sensor housing to be used with sutures (left) and finished 3D printed part (right)

3.3.6. Budget

The overall cost of the device was important to the project. Every effort was made to keep costs as low as possible, from using components which were already available to the author, reusing components from earlier prototypes to opting to make use of pulse oximetry. Should future iterations of the device be developed, the overall cost should not differ significantly. An estimate of the project costs is shown in Table 10 with items 6 to 8 used for the independent safety system. Although the independent safety device was not originally part of the design it was included and despite its inclusion, the device remained within budget.

Table 10: Second prototype budget (prices as of 2012)

Item	Description	Cost
1	Three Nonin OEM III and 8000R oximetry sensors	R 10 000
2	Arduino MEGA ADK microcontroller	R 800
3	Verderflex 12V OEM pump	R 3 300
4	Pololu 18v15 motor driver	R 400
5	Honeywell pressure transducer	R 700
6	GIC 1CMDT0 Timer	R 450
7	Festo MHE3-MS1H-3/2G-1/8 solenoid valve	R 1 200
8	Schneider Electric ABL7 RE2403 power supply	R 800
9	General hardware, wire, enclosure etc.	R 1 500
	Total Cost	R 19 150

3.4. Pre-clinical Testing

Pre-clinical testing of the second prototype was performed to test overall system functionality and reliability before it was approved for operation in a formal clinical setting under the observation of the clinical consultant. Additionally, the reflectance sensors were tested on multiple body sites with the intention of providing the clinical consultant and the author with some guideline of what signal shape and amplitude to expect. Reliability tests were performed on the device to ensure reliable functionality over long test periods. Safety measures were programmed into the device to reset and resynchronise it in the case of a synchronisation loss. The resynchronisation would result in the loss of a few seconds of data. This was of minimal concern, as post-operative measurements would span several hours.

3.4.1. Procedure

The testing procedure was split into several sections with each section testing a specific aspect or event. Some tests overlap, for example the sensor functionality would be tested in both sensor response tests. A single sensor version of the device was built as the author did not have access to the second prototype once it was delivered. This device was used for the sensor response and pulse transit time (PTT) tests. The single sensor device is based on the PCB layout of the second prototype and makes use of an Arduino Due microcontroller (same footprint as the Arduino Mega ADK), Sparkfun AD8262 ECG monitor (Sparkfun, Boulder, CO, USA) and a Wika S-10 pressure transducer (Wika, Maitland, Cape Town, RSA). Most importantly, the same model of Nonin OEM III and 8000R sensor were used while the aforementioned components are all similar in functionality to that of the second prototype.

Honeywell Pressure Sensor Calibration

Calibration of the pressure sensor was necessary in order to use the sensor for the feedback and monitoring for the cuff control system. The pressure sensor was calibrated using the raw analogue input readings from the Arduino and a TXJ-10 mercury sphygmomanometer. The mercury sphygmomanometer was deemed acceptable for use in calibration as a similar unit would normally be used in the hospital. Calibration was performed by measuring 16 evenly spaced pressures from 0 to 300 mmHg.

Long Term Reliability Tests

Long term reliability tests were performed after any hardware or programme changes. The tests were run for approximately three days after each change. The sensors were left open to ambient light such that there were visible changes in PPG signal and not a constant signal typically generated by covered sensors.

Test Areas for Sensor Response

A single Nonin 8000R sensor was tested on several areas of the author’s body. The areas shown in Figure 26 were selected primarily for testing sensor

functionality on areas commonly used for tissue flaps. For example, forehead, hand, groin, upper thigh and calf area (cross leg flap). The recorded data gave an indication of amplitude variation from the different measurement areas.

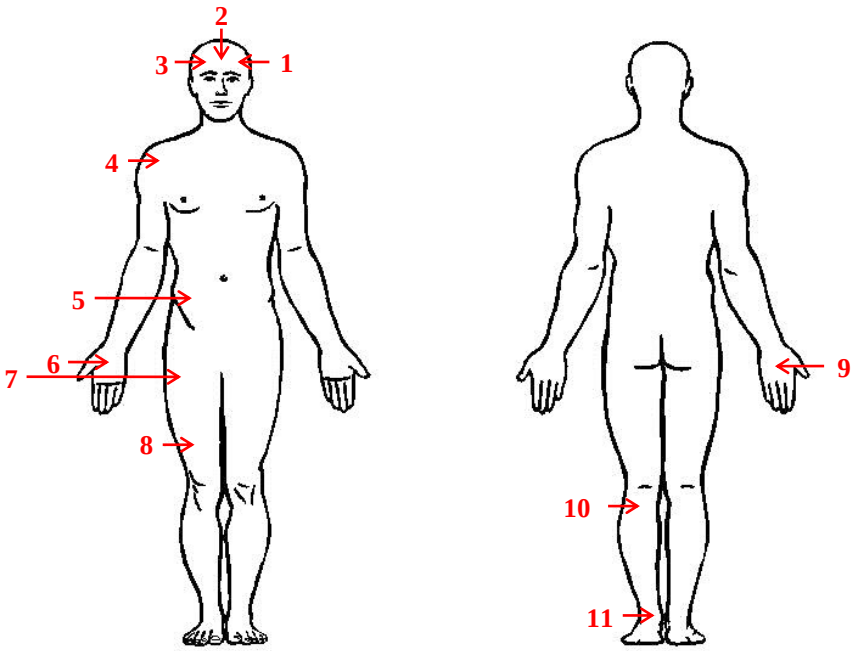

Figure 26: Nonin 8000R sensor locations. 1, Forehead LHS. 2, Forehead centre. 3, Forehead RHS. 4, Anterior shoulder RHS. 5, Pelvis RHS. 6, Palm RHS. 7, Upper thigh RHS. 8, Lower thigh RHS. 9, Dorsum RHS. 10, Upper calf LHS. 11, Ankle LHS. Image adapted from Clip Art Best [S.a.]

Sensor Response to Clamping Event

A sphygmomanometer cuff was applied to the author's right bicep for under 30 seconds at a pressure of 300 mmHg. The inflation of the cuff simulates a brief clamping period where the recipient side receives no flow from the pedicle or its native supply.

PTT Measurements using PPG and ECG

Simultaneous ECG and PPG recordings were conducted on the author to validate the PTT measurement capability of the device. ECG electrodes were placed on the left chest (LA probe), right chest (RA probe) and the right pelvis (RL probe).

Foo *et al.* (2005) showed that the mean PTT in ten healthy adults (mean age of 27 years) increased by 42,7 ms for a vertically raised arm and it decreased by 28,1 ms for a diagonally lowered leg. This type of comparison was conducted as differences in PTT measurements between individuals are not quantifiable due to variations in vascular system compliance (Smith *et al.*, 1999). Despite this

limiting factor, the mean PTT delay between ECG and PPG for the arm measurement was calculated as a rough reference. The mean time was measured at 371,15 ± 7,39 ms.

The data acquisition rate of the developed device is 75 Hz, therefore changes as small as 14 ms are measureable. Although the device will be capable of measuring similar time differences to that acquired by Foo *et al.* (2005), differences larger than 28 ms are preferable.

3.4.2. Analysis

Only tests involving data analysis are mentioned in this section. All other tests were analysed by visual inspection. MATLAB was used for data analysis as well as the display of results for visual inspection (unless otherwise stated).

Honeywell Pressure Sensor Calibration

Microsoft Excel was used to add a linear fit to both measured and calculated results. The graphs were displayed as well as the linear trend equations.

Test Areas for Sensor Response

The mean amplitude and standard deviation of the PPG data was calculated by making use of a peak detection algorithm. Noisy PPG data was filtered using a high order FIR (finite impulse response) Equiripple bandpass filter with a pass band frequency of 0,7 Hz to 4,1 Hz. An FFT (fast Fourier transform) was also performed on the PPG data. Signal to noise ratio (SNR) was calculated for two test positions for comparison. Both signals were filtered and then subtracted from the original signal in order to obtain the noise component. The RMS (root mean square) value of the original signal and the noise was used in equation (4).

$$SNR_{dB} = 20 \log_{10}\left(\frac{A_{signal\,RMS}}{A_{noise\,RMS}}\right) \quad (4)$$

where $A_{signal\,RMS}$ and $A_{noise\,RMS}$ is the RMS amplitude of the signal and noise.

All the aforementioned signals were displayed on a series of figures for visual inspection.

PTT Measurements using PPG and ECG

Simultaneous recordings of PPG and ECG signals were created. A maximum and minimum peak detection algorithm was performed on the PPG data while only maximum peak detection was implemented on the ECG data. The midpoint between each pair of PPG maxima and minima was calculated and the nearest matching point on the PPG curve was marked. A similar strategy was followed for the ECG data where the R peak of the PQRST complex was found and marked as per convention (Smith *et al.*, 1999). The time taken between each ECG R peak to the nearest PPG midpoint was calculated and then averaged to provide an average PTT.

3.4.3. Results and Discussion

The results obtained from each of the tests are discussed in this section.

Honeywell Pressure Sensor Calibration

A linear fit was found to best model the measured data, allowing the linear conversion in Labview from the raw analogue reading to a pressure represented in millimetres mercury. Calculations solely based on the pressure sensor datasheet and ADC resolution were also performed but were found inaccurate when compared to the linear fit. The slope of the calculated data was 0,474 while the measured data was lower at 0,445. The y intercepts were also found to be significantly different with the calculated data being – 48,5 mmHg and the measured data – 19 mmHg. The calibration curve can be found in Appendix D.

Long Term Reliability Tests

Initial long term tests revealed that it was possible for Labview to lose synchronisation with the Arduino serial information. A synchronisation check was implemented and used to reset the device and clear all buffers. Minimal data loss occurred during the long term tests. Less than 20 seconds of data was lost per a resynchronisation event.

Test Areas for Sensor Response

Table 11 shows the mean peak to peak PPG signal amplitude acquired from each measurement site. The PPG measurements are all measured in arbitrary units. Measurements with larger amplitudes indicated higher signal strength, resulting in improved signal quality and SpO_2 calculation. However, large amplitude signals can be obtained from noisy data, specifically when the measurements have been corrupted by movement and light interference. Prior to any calculations, all measurements were inspected for PPG waveform shape similar to that seen in Figure 27. This was done to ensure high data quality. The mean of all the sites was calculated as 818,5 with a standard deviation of 218,1.

Table 11: Mean peak to peak PPG signal amplitude for the chosen measurement sites

Measurement area	Mean peak to peak signal amplitude (raw)	Measurement area	Mean peak to peak signal amplitude (raw)
1	768,5 ± 52,7	7	90,7 ± 19,3
2	1988,8 ± 311,3	8	306,1 ± 103,4
3	3370,4 ± 619,1	9	200,9 ± 64,5
4	268,8 ± 33,5	10	672,2 ± 134,4
5	150,3 ± 43,0	11	522,6 ± 36,3
6	663,8 ± 66,7		

All 11 test areas showed distinct PPG signals similar in shape and frequency to Figure 27. Each area had different PPG amplitudes with upper thigh sensor location being the weakest. The weak PPG signal can be seen in Figure 28. It was noted that low mounting pressure provided unreliable measurements and that small changes in mounting position affect the PPG signal.

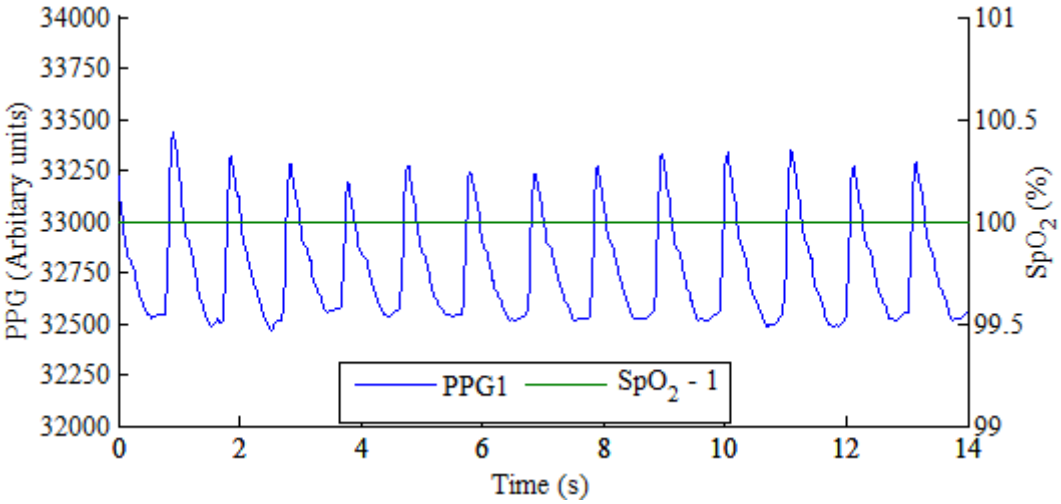

Figure 27: Typical PPG and SpO_2 readings from measurement position 1

Figure 28 shows the noisy low amplitude PPG signal obtained from measurement site 7 (upper thigh). Although the signal is weak and noise levels are high, the distinct PPG waveform is still visibly present. The signal to noise ratio for the waveforms displayed in Figure 27 and Figure 28 were calculated for comparison. Figure 27 had an SNR of 30 dB, while Figure 28 had an SNR of 19,95 dB.

The SpO_2 reading in Figure 29 shows a steady value of 127 % which the OEM III board displays when it is unable to resolve the oxygen saturation. The presence of a PPG waveform is critical for patient monitoring and the subsequent data analysis. The PPG waveform indicates whether the area of interest has pulsating blood flow and also indicates whether the recipient site has supply from the pedicle or from the recipient site itself (while under clamping).

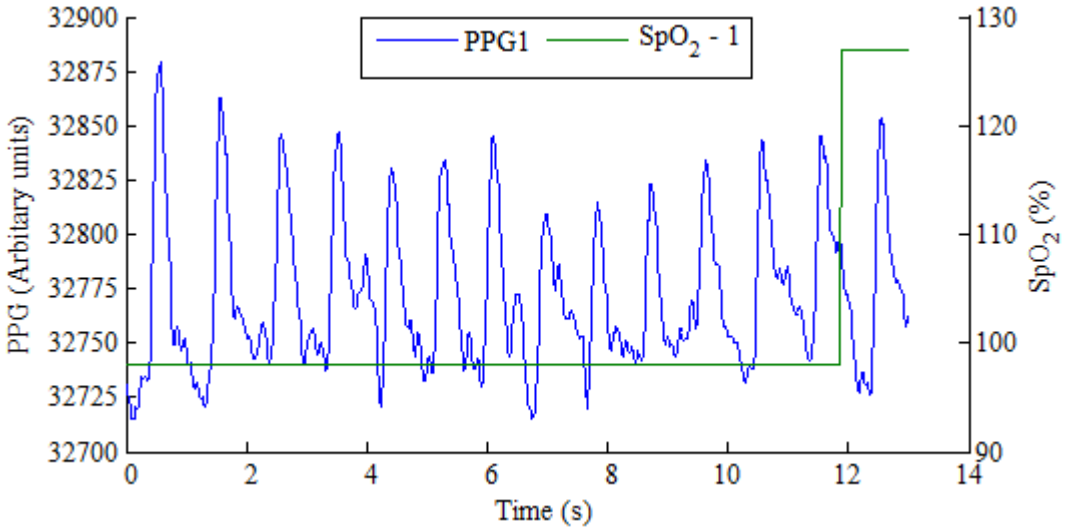

Figure 28: Noisy PPG and SpO_2 readings from measurement position 7

An FFT was performed on the data from each sensor yielding a large signal power at a frequency of approximately 1 Hz. This equates to approximately 60 bpm (beats per minute) which was also reflected in the heart rate measurement from the OEM III module.

PPG data was filtered by a bandpass filter and its performance is demonstrated in Figure 29 and Figure 30.

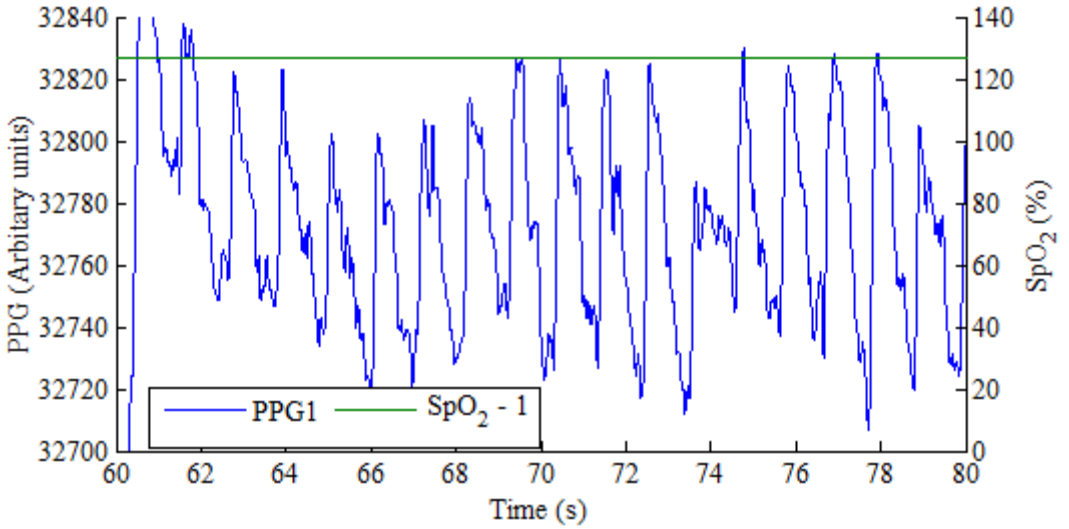

Figure 29: Example of unfiltered data from measurement site 5

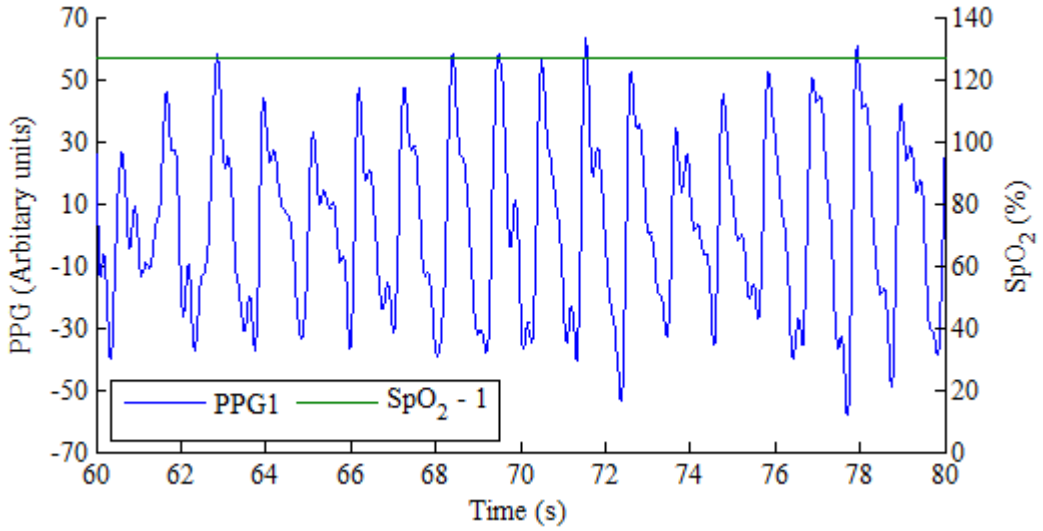

Figure 30: Example of filtered data from measurement site 5

PTT Measurements using PPG and ECG

The signal quality of the PPG and ECG was found to be acceptable through visual inspection. Figure 31 shows the ECG and PPG waveforms with marked peaks and midpoints.

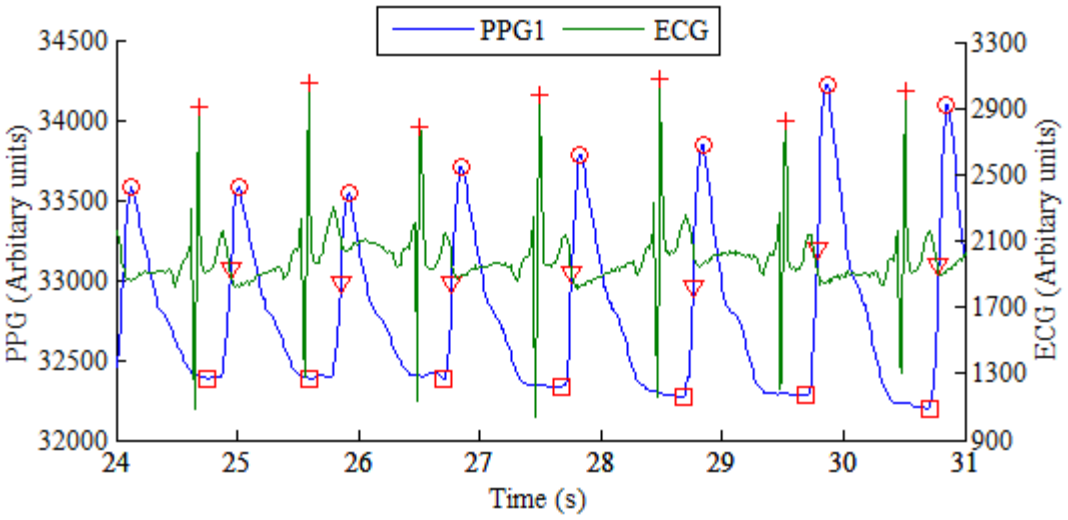

Figure 31: Peak detection performed on ECG and PPG signals

An average PTT of 269 ms was calculated by using the markers created in the peak detection process. Due to the limited sampling rate of the Nonin OEM III modules, a minimum change of 5 % (of the author's PTT) was detectable.

Sensor Response to Clamping Event

The data, as expected, shows high quality signal and strength from the finger. When the cuff is inflated and the pressure approaches and exceeds systolic pressure, the distinct PPG waveform flattens. This is expected as the inflation of the cuff above systolic pressure prevents any arterial pulsations. As the cuff is deflated and approaching the systolic pressure, the PPG waveform reappears at large signal amplitude and stabilises after a few seconds. This is demonstrated in Figure 32.

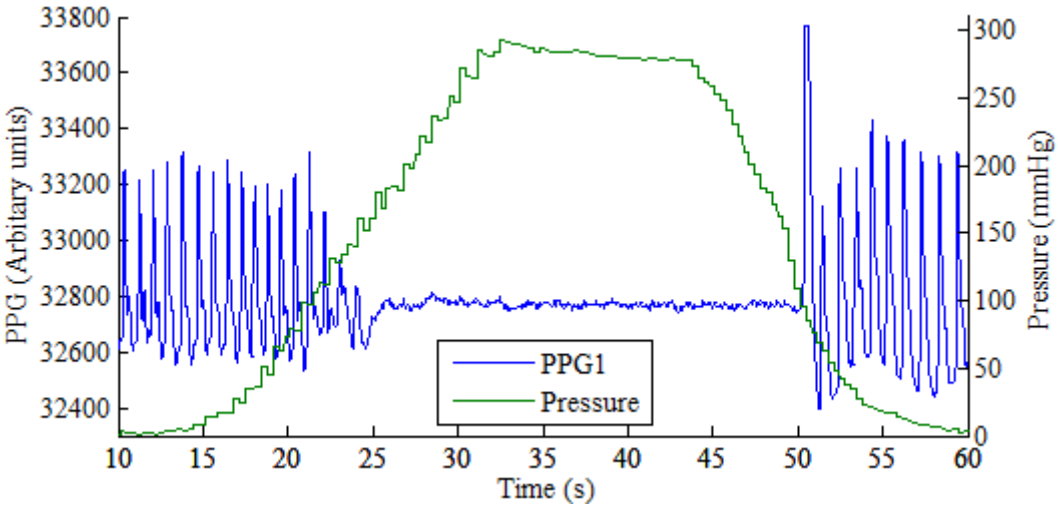

Figure 32: PPG and pressure waveforms during a clamping event

Waveforms similar to this (with lower PPG amplitude) are expected on the distal and proximal part of pedicle for the first few post-operative days during clinical trials. Once supply from the recipient site becomes significant, then a distinct PPG waveform should be displayed even while clamped, indicating that the blood supply is not only from the pedicle.

3.4.4. Conclusion

Device testing prior to clinical trials was necessary. Testing was focused on reliability and functionality. The chosen tests showed that the device is reliable and capable of measuring on multiple sites. The recorded data stored the necessary information required for post-recording analysis.

4. Clinical Testing

Clinical testing was critical in determining device performance and functionality, following the pre-clinical phases. To recap the desired medical outcomes in the clinical setting are as follows:

- Monitor and record photoplethysmogram and SpO_2 values to aid in early flap division.
- Assist in alerting staff to vascular complications.
- Perform automated IP according to chosen protocols.

4.1. Ethical Approval and Considerations

Clinical trials were necessary in order to evaluate the device for functionality and efficiency in the clinical setting. The purpose of the pre-clinical testing was primarily to ensure reliability and to give an indication of areas which yield a strong photoplethysmogram signal. Based on these results, the application areas of the sensors could be determined for the clinical phase.

In order to take part in the study, participants had to give informed consent. Participants were recruited from patients scheduled for pedicled groin flap surgery, which is already frequently performed at the Chris Hani Baragwanath Hospital (Dr. Lahouel's practising hospital). Before the testing could commence, approval was obtained from the Human Research Ethics Committee (medical) of the University of Witwatersrand with application number M141165. The clinical consultant and the author applied well in advance for the approval, however the protocol required one revision and approval took over one year to complete. This large delay reduced the quantity of results available to the author.

4.2. Procedures and Ischemic Preconditioning Protocols

In order to validate and test the device, several procedures and IP protocols were formalised prior to clinical testing. Three testing protocols were chosen for the validation and testing of the device. All IP protocols were preferably applied on the first post-operative day (day 1) to allow time for administration and patient transport between wards (if applicable) and to allow for immediate post-surgery recovery. IP was ideally applied up until the day of division. Reflectance sensors were placed on the flank (sensor 3), proximal area (sensor 2) and distal area (sensor 1) as indicated in Figure 33.

Two IP protocols were chosen from available literature. Protocol 1 was adapted from Furnas *et al.* (1985) by reducing the maximum ischemia time from three hours to two hours due to safety concerns. Dr. Lahouel stated that in clinical practice two hours is the maximum time used when applying a tourniquet to limbs (Lahouel, 2013). Protocol 2 was used as described by Cheng *et al.* (1999).

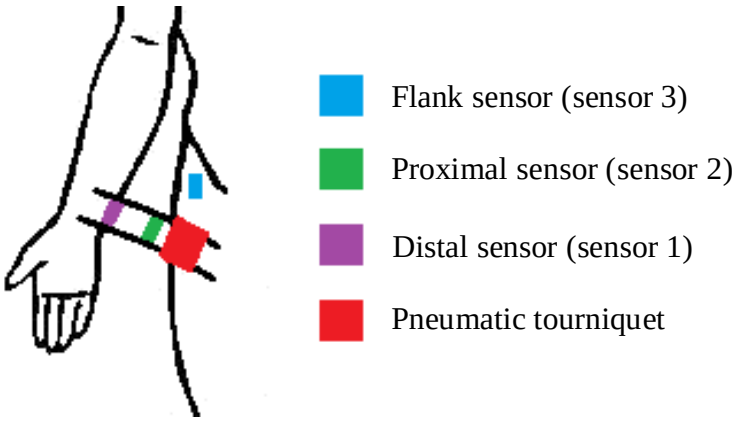

Figure 33: Schematic indicating sensor and pneumatic tourniquet placement. Image adapted from Clip Art Best [S.a.]

A summary of the protocols, which are fully detailed in Table 12, is given below:

Protocol 1:

Day 1 - 0,25 hour clamped, 0,75 hour released

Day 2 - 0,5 hour clamped, 0,5 hour released

Day 3 - 1 hour clamped, 1 hour released

Day 4 - 1,5 hour clamped, 1 hour released

Day 5 onwards - 2 hour clamped, 1 hour released

Protocol 2:

The initial timing used for this protocol is more aggressive than protocol 1 consisting of the following times:

Day 1 - 0,5 hour clamped, 7,5 hour released

Day 2 - 1 hour clamped, 7 hour released

Day 3 onwards - 2 hour clamped, 6 hour released

Protocol 3:

This protocol was set out for the control group where no IP was applied and patients were only monitored by the device. The flap would be divided when the standard clinical tests indicated it was safe to do so. If the device was interfering with the control group in any way, it was removed.

A simple setup and testing procedure was established prior to measurement recording and IP. This procedure allows the operator to perform basic fault finding on the device without the presence of the author before the system was applied to the patient. The flow diagram for this procedure is shown in Figure 34.

Table 12: Clamping protocols

	Protocol 1				**Protocol 2**				**Protocol 3**	
Post-operative day	Clamp ON (hours)	Clamp OFF (hours)	Monitoring method		Clamp ON (hours)	Clamp OFF (hours)	Monitoring method		Monitoring method	
			Needle prick	PPG			Needle prick	PPG	Needle prick	PPG
Day 1	0.25	0.75		Continuous monitoring	0.5	7,5		Continuous monitoring		X
Day 2	0.5	0.5			1	7				
Day 3	1	1			2	6				
Day 4	1.5	1	X		2	6	X			
Day 5	2	1	X		2	6	X			
Day 6	2	1	X		2	6	X			
Day 7	2	1	X		2	6	X			
Day 8	2	1	X		2	6	X			X
Day 9	2	1	X		2	6	X			
Day 10	2	1	X		2	6	X			
Day 11	2	1	X		2	6	X			
Day 12	2	1	X		2	6	X			
Day 13	2	1	X		2	6	X			
Day 14	2	1	X		2	6	X			
Day 15	2	1	X		2	6	X			X
Day 16	2	1	X		2	6	X			
Day 17	2	1	X		2	6	X			
Day 18	2	1	X		2	6	X			
Day 19	2	1	X		2	6	X			
Day 20	2	1	X		2	6	X			
Day 21	2	1	X		2	6	X			
Day 22	2	1	X		2	6	X		X	X

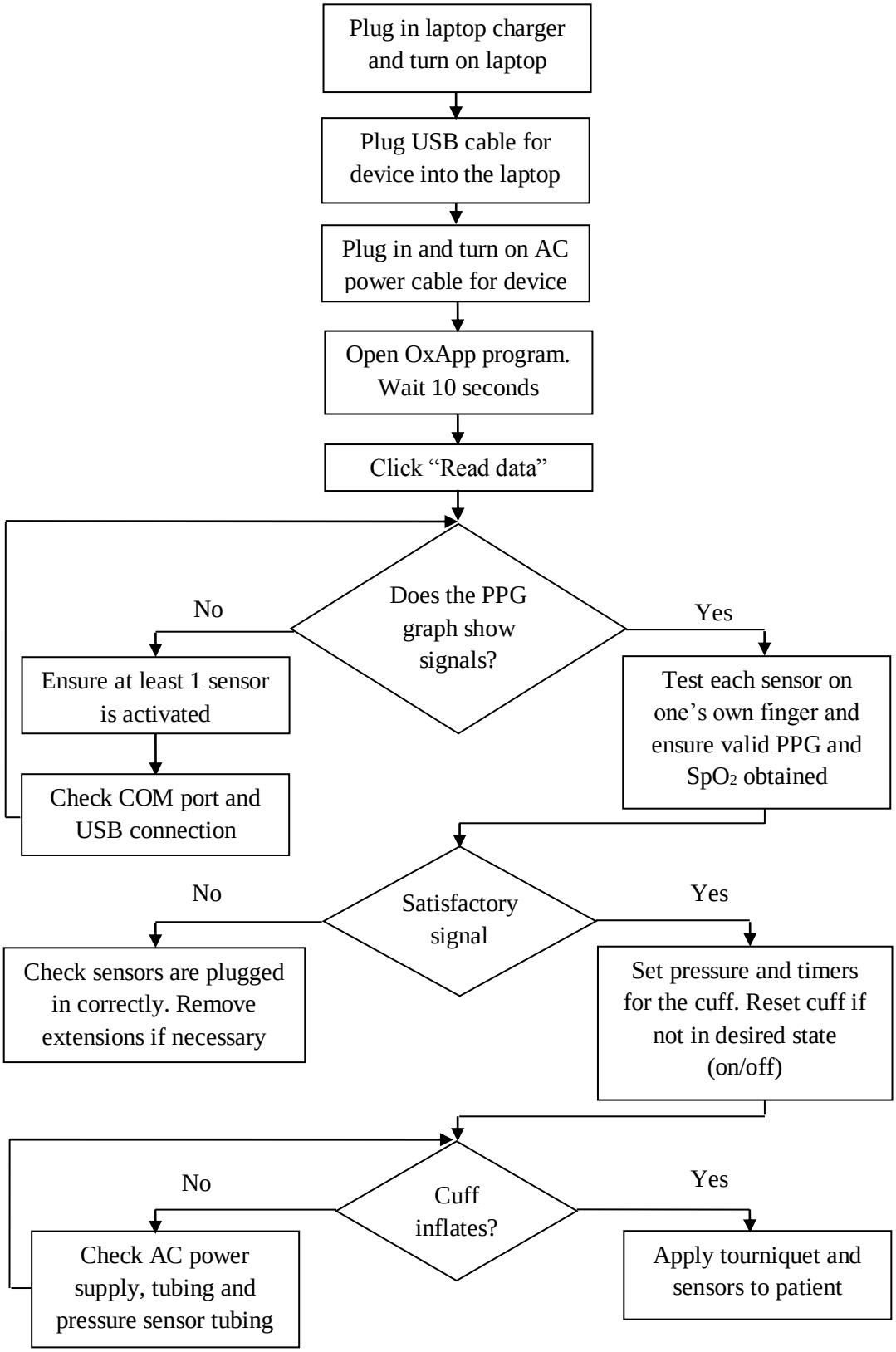

Figure 34: Setup procedure prior to patient application

4.3. Analysis

Primary analysis was performed using MATLAB. Data files of a user-specified time range were read and appended into a single array. An FFT was performed on each sensor's PPG signal. The PPG signals were also filtered using a high order FIR bandpass filter with a pass band of 0,7 Hz to 4,1 Hz. A high filter order was necessary in order to avoid losing data with specifically low frequency components.

Large PPG signal swing caused by external factors (patient motion, wound care and remounting of the sensor) complicated the visual inspection of the data for true PPG signal, as well as the identification of predominant frequencies on the FFT. An example of a signal corrupted by movement can be seen in Figure 35. This movement occasionally caused the signal to saturate at its minimum and maximum values. The saturated PPG data overshadows other frequencies which contain less signal power on the FFT plot. In order to overcome this, the data was limited to a range that was initially determined by observing the average signal amplitude as determined in section 3.4.3 and adjusted as required thereafter.

The data was analysed in approximately 12 hour intervals to reduce computing time and allowing more effective visual inspection. In an effort to identify the healing progress, data was analysed for each *off* and *on* clamping period. The desired result being high quality PPG and SpO_2 signal from sensor 1 and 2 in both *on* and *off* intervals, therefore indicating supply from the recipient side. An algorithm was developed in MATLAB which extracted useful information from these *off* and *on* periods thereby reducing the volume of data which needs to be inspected. This algorithm calculated the mean SpO_2 values as well as the RMS values of the PPG signals for the *on* and *off* intervals. The RMS calculations were performed over five minute sections of each *on* and *off* interval. Five minute sections were created so that an initial inspection could be performed on the variation of the PPG signal during that interval. Standard deviation of the SpO_2 means was calculated, as well as the standard deviation for the mean of the five minute RMS sections. A comparison of mean SpO_2 for the *on* and *off* intervals was graphed together with an associated standard deviation error band. A normalised standard deviation of the PPG RMS sections was also included in the graph. The standard deviation value was normalised with its relevant mean in order to give an indication of the noisiness of the PPG signal, as indicated in equation (5).

$$PPG_{RMS\ NORM} = \frac{\sigma}{\mu_{PPG\ RMS}} 100 \tag{5}$$

where σ is the standard deviation of the PPG signal and $\mu_{PPG\ RMS}$ is the mean.

The PPG, SpO_2, cuff pressure and FFT data were all plotted on figures for visual inspection. A flow diagram of the RMS calculation has been included for clarification in Appendix A.

Lastly, the data was summarised into a macro-automated Microsoft Excel spreadsheet for initial review by the clinical consultant.

4.4. Results and Discussion

This section reports the results and the discussion for the clinical trials. The results and discussion have been separated on a per patient basis, as each patient experienced particular difficulties and differences.

4.4.1. Case 1

Case 1, a 28 year woman, was classified as a "cold case" by the clinical consultant as she had been involved in a motor vehicle accident (MVA) a few weeks prior to being contacted for pedicled groin flap surgery. She had sustained injuries to her scalp, ankle and hand. The scalp injury was treated by means of tissue flaps and the ankle using skin grafts. Part of the hand injury was treated using a skin graft (for two of the fingers) whereas the dorsal aspect of the hand was to receive the pedicled flap. The hand wound had only been cleaned and dressed prior to being moved to Chris Hani Baragwanath Hospital.

The clinical consultant experienced a rare anatomic variation while raising the tissue for the groin flap. The superficial circumflex iliac artery (SCIA), necessary for the construction of the pedicled flap, could not be located. Instead multiple minor pedicles (vessels) were found, of which three smaller vessels were used to continue the surgery.

IP protocol 1 was chosen for this patient and initial measurements were attempted 24 hours post-operatively. When IP had been implemented, all pin prick tests were performed during clamping intervals. The observations during the protocol execution are described below.

Day 1 - Pin prick showed bright red bleeding indicating the presence of venous congestion which signifies a lack of venous drainage. Measurements were attempted on the flank, proximal (near flap base) and distal part of the flap. The flank signal was satisfactory showing good amplitude and waveform, however a very small and unreliable signal was measured proximally. Furthermore, no measurable signal was found on the distal part of the flap. IP was not executed due to the venous congestion and flap tip necrosis.

Day 2 - Pin prick continued to indicate venous congestion. The device was taken off site for testing regarding sensor noise. It was decided to remove the cable extensions for the following days.

Day 3 - No clamping was performed due to the scheduled debridement surgery necessary for the flap tip necrosis. Once again the flank showed a significant signal. A more distinct signal was detected on the distal part of the flap, however no reliable signal was measured proximally. The lack of a pronounced PPG

signal, visual inspection and pin prick methods indicated that debridement of the flap tip was required. Once again no IP was executed.

Day 4 - Debridement was performed and only necrotic tissue excised. The flap was not advanced or moved from the recipient side. No measurements or IP were performed due to the debridement.

Day 5 - No measurements or IP performed due to recovery from debridement surgery.

Day 6 (IP day 1) - Measurements were acquired from the flank and proximal sensor, where Figure 35 shows a noisy but distinct PPG signal and SpO_2 of 99 % (when resolvable) from the latter. IP protocol 1 was implemented. At this stage the flap was already receiving supply from the recipient site as the pin prick revealed venous bleeding.

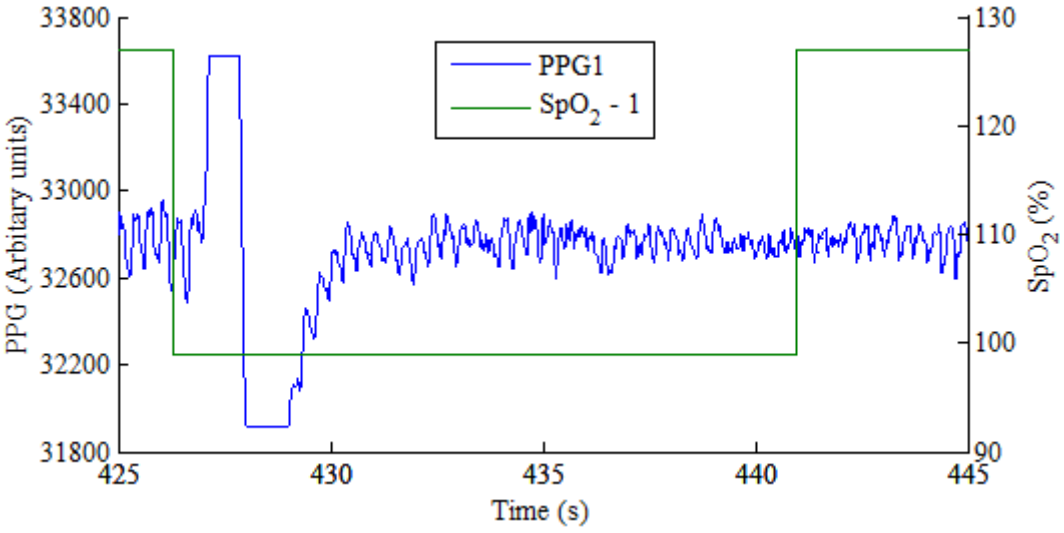

Figure 35: Sensor data from proximal measurement site showing movement noise

Day 7 (IP day 2) - Venous bleeding was noted. Recording was stopped due to poor measurements, however IP was continued.

Day 8 (IP day 3) - Venous bleeding was noted.

Day 9 (IP day 4) - Slow venous bleeding was observed. The tourniquet was found to be leaking and lacking proper fitment. Consequently, it was replaced and applied correctly. At this point the flap was ready for division.

Day 10 - IP was stopped at 10 am and the patient was scheduled for division surgery the same day. This was delayed due to load shedding.

Day 14 - Patient was rescheduled for division surgery, however this was delayed once more, this time due to the lack of linen in the operating theatre.

Day 17 - Successful division of the flap was performed.

Initial inspection of part of the PPG data showed promising signal shape and amplitude, however the FFT analysis revealed a large peak at a frequency of 0,25 Hz. The 0,25 Hz peak found in the third sensor's data is shown in Figure 36, with the remaining sensors displaying similar FFT plots.

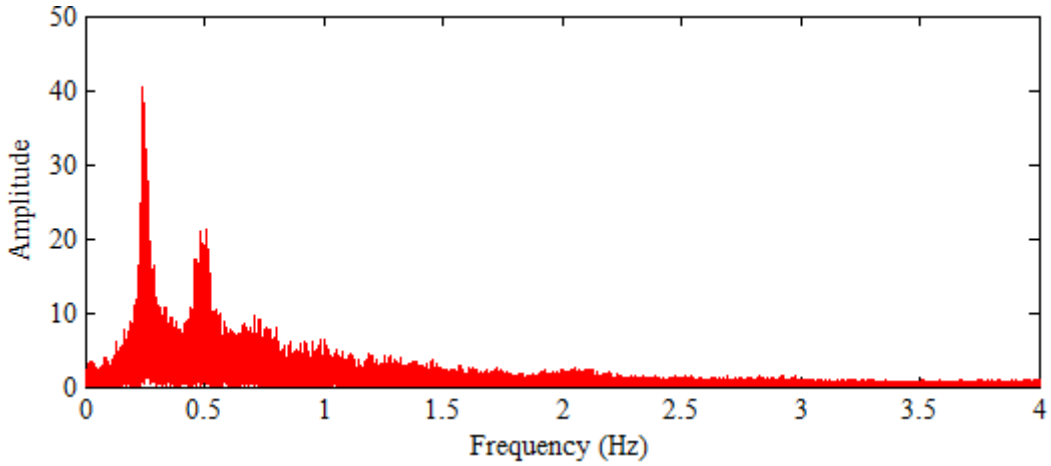

Figure 36: Single-sided amplitude spectrum from sensor three showing large spike at approximately 0,25 Hz

Under normal circumstances the heart rate can be derived from peak detection performed on a PPG signal. A frequency of 0,25 Hz equates to a heart rate of 15 bpm, which is significantly below the patient's heart rate ranging from approximately 100 to 120 bpm. Investigation of the large signal power at 0,25 Hz concluded that the pulsatile signal shown on the PPG and the resultant SpO_2 value were caused by patient respiration (Rosdahl & Kowalski, 2008: 521). The detection of patient respiration on the PPG signal is normal, however the measured signals primarily consisted of the respiration fluctuation (Karlen *et al.*, 2013; Zaman *et al.*, 2011). This was possibly due to movement of the skin relative to the sensor and is an indication that the sensor mounting method was not adequate.

Analysis of *on* and *off* clamping periods was not performed due to a leaking tourniquet and overall poor signal quality which was primarily related to poor sensor mounting. The tourniquet was replaced and IP continued, however data was not recorded after the replacement. Moreover, a lack of detectable PPG

signal, for example as observed on day 3, coincided with the standard clinical checks. Due to patient movement and flap bleeding, the mounting method using medical adhesive tape was ineffective. It was decided to make use of sutures for the next patient case.

4.4.2. Case 2

Case 2, a 39 year old female was involved in an MVA approximately four weeks before receiving pedicled groin flap surgery. There were no complications during the surgery other than that the patient was obese (BMI of 47.8), resulting in a pedicle with a larger fat content and increased diameter.

The patient was discharged from the hand ward to the clinical consultant's plastic surgery ward on the second post-operative day. Figure 37 shows the pneumatic cuff and three sensors applied to the patient. All pin prick tests were performed under clamping, unless otherwise stated.

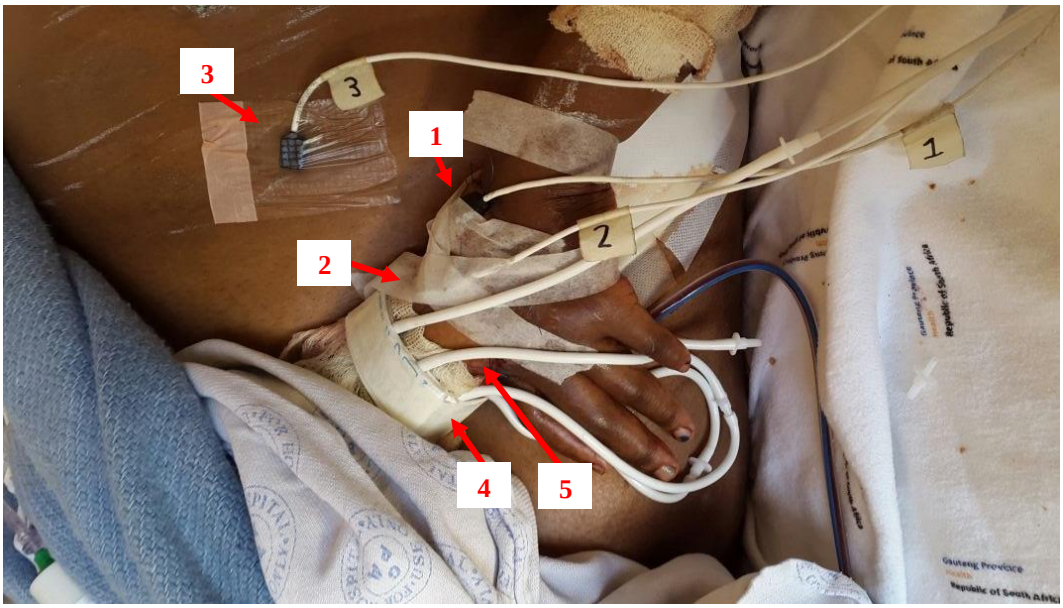

Figure 37: Device applied to patient showing the pneumatic cuff (4) applied to pedicle (5) and all three sensors applied to patient. Sensor 1 (1), distal part of flap. Sensor 2 (2), proximal part of flap. Sensor 3 (3), flank

Day 2 (IP day 1) - Device was applied to patient and the first day of IP protocol 1 was implemented. The flap was bleeding well before clamping. Flank sensor was mounted using a medical adhesive tape and the other two sensors were sutured in place. Acceptable readings were obtained from the proximal and flank sensor while the distal sensor did not register significant measurements.

Day 3 (IP day 2) - Slow venous bleeding was observed. The cuff size was reduced to ensure adequate pressure.

Day 4 (IP day 3) - Red bleeding on distal part, however bluish on the proximal area indicating supply from the recipient side. The bleeding was nonetheless insufficient for proper venous drainage.

Day 5 (IP day 4) - A modified version of IP protocol was implemented with 1,5 hours on and 0,5 hours off. An instance of flap oedema was caused by poor venous drainage. The flap was tied with gauze and the proximal sensor showed good signal and with the flap bleeding well. The device was removed.

Day 6 (IP day 5) - The pedicle was left tied throughout the previous night with a second additional tie with the flap bleeding well.

Day 7 - The flap was divided and bleeding well on all edges. On table, the flap was bleeding so well after division that the clinical consultant decided to defat the raw edges to inset the flap in a single procedure.

Day 8 - The flap turned blue but was still actively bleeding apart from the defatted areas.

It was immediately noticeable that the data obtained from the second case was of higher quality due to secure sensor mounting provided by sutures. This was observed from the FFT plots of the data and from focussing on narrow time intervals of the data set. The flank sensor provided inconsistent measurements as it was still mounted using adhesive tape. It was not practical to use sutures on the flank due to patient discomfort. Figure 38 shows data from the proximal sensor for the first 11 hours of IP. During *on* intervals, the PPG amplitude is reduced and the SpO_2 value typically became 127 % (Nonin OEM III value for unresolvable SpO_2). On the other hand, the PPG amplitude increased and a reasonable SpO_2 value was displayed during *off* intervals.

Figure 39 shows data from the proximal sensor on the second day of IP. Performing the same visual analysis as Figure 38, it is noted that the PPG behaves in a similar fashion whereas the SpO_2 begins to remain well below the 127 % error value indicating that the proximal area is receiving supply from the recipient side. As no IP was performed on post-operative day 1, this improvement in SpO_2 occurs during the course of post-operative day 3.

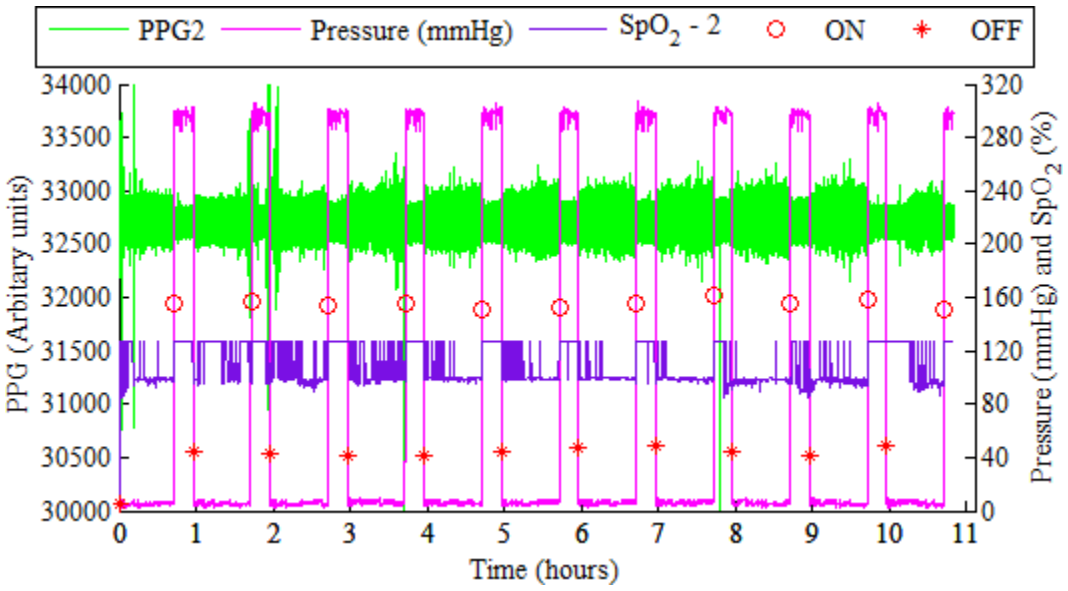

Figure 38: Sensor 2 data from the first 11 hours of IP

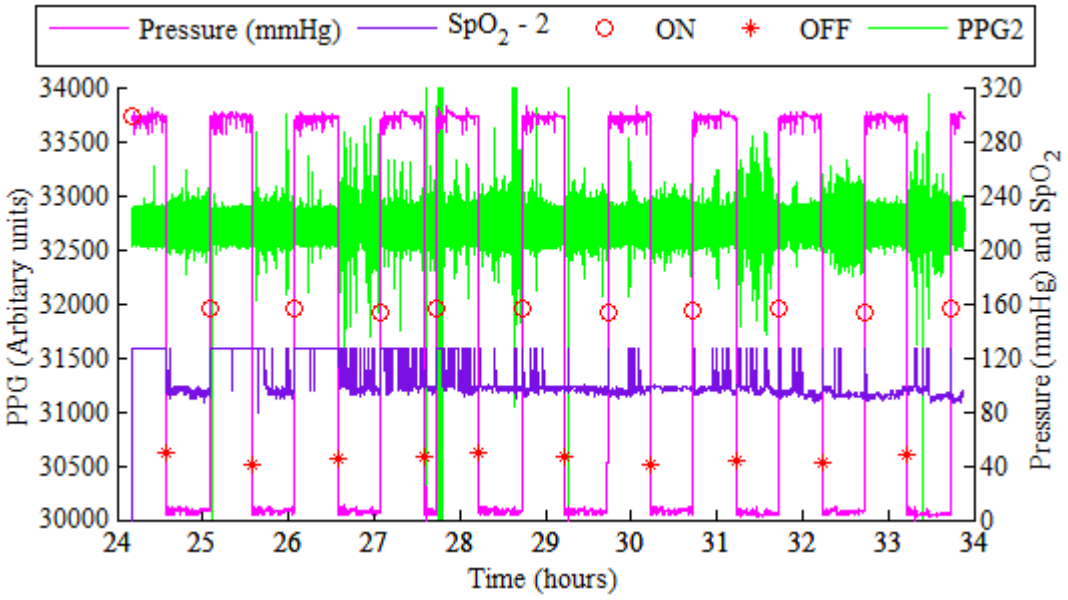

Figure 39: Sensor 2 data from 24 to 34 hours of IP

Figure 40 shows the analysis of the proximal sensor's data. Figure 40a and Figure 40b show the mean SpO_2, including an error band of the standard deviation. It should be noted that pinch points shown in the standard deviation error band occurred whenever the SpO_2 measurement remained constant for that interval. Measurements recorded from the distal area were not as pronounced as the proximal sensor and therefore have been added as Appendix D. The flank sensor (sensor 3) provided inconsistent measurements and had no reaction to IP and was therefore excluded from this analysis. Figure 40a (*on* intervals) shows high PPG noise when a protocol changeover took place. This was likely due to patient checks, wound care, patient movement and possible remounting of sensors. PPG noise remained low from the start until the changeover to the third day of IP. An important change in SpO_2 is seen after the first protocol change (IP day 2). The SpO_2 measurement falls well below the 127 % error value indicating supply from the recipient side, rising again after changeover to the third day of protocol 1. Figure 40b (*off* intervals) shows that the SpO_2 remains within reasonable values up until the third day of IP. Interference similar to that of the *on* interval is seen. Figure 40c shows the SpO_2 of the *on* interval falling with time which is expected in a recovering patient. The standard clinical observations performed on IP day 3 and 4 reflect what is shown in Figure 40. The clinical consultant and the author believe that the aggressive and lengthy clamping times and pressure could be responsible for the interruption of supply from the recipient side after day 2.

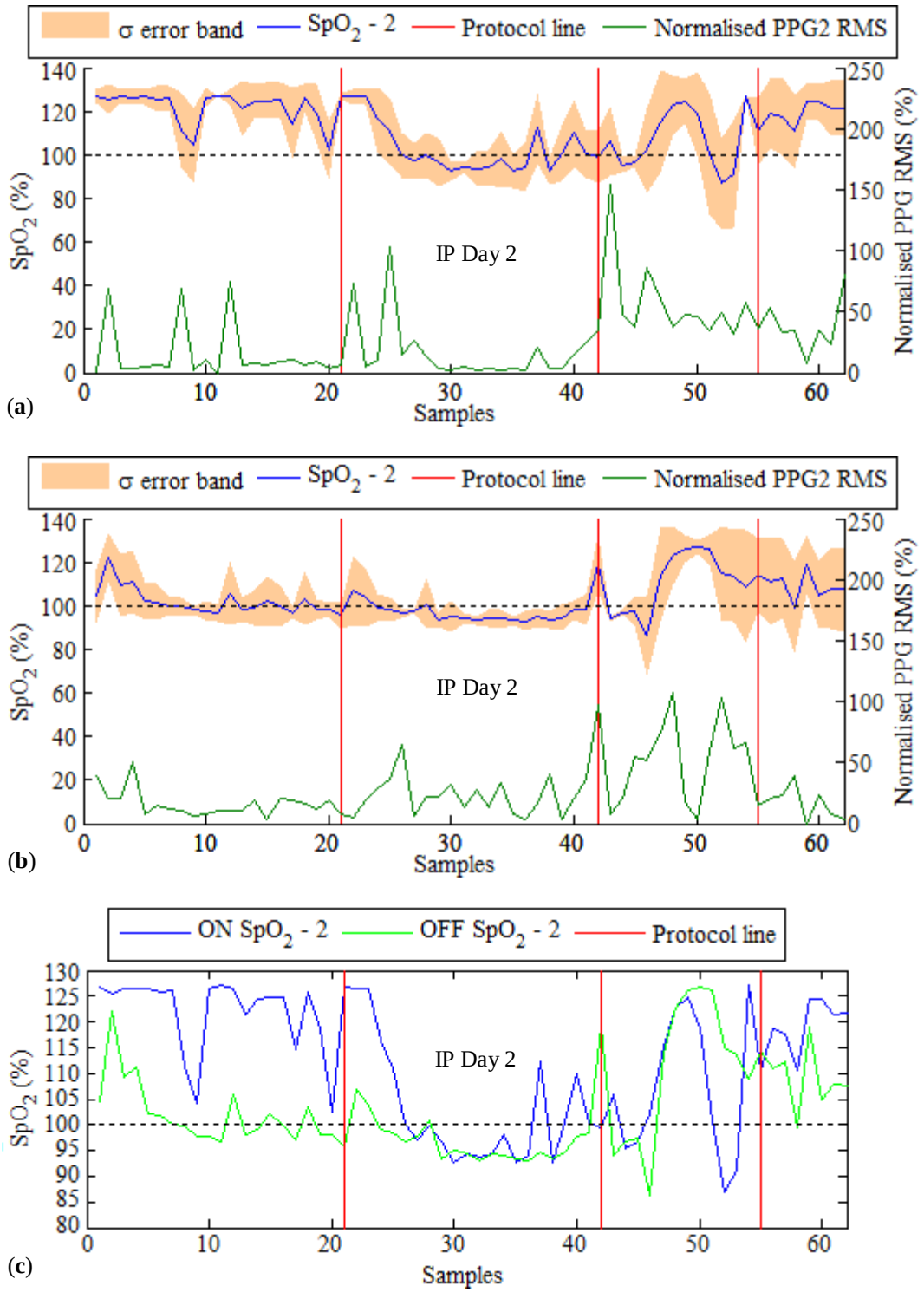

Figure 40: Case 2 data for proximal sensor (sensor 2) for *on* and *off* intervals. SpO_2 values higher than 100 % may be unreliable and are physiologically impossible. 100 % SpO_2 is marked by the dashed black line. Protocol changeover represented by a red vertical line. **a**. Mean SpO_2 and normalised PPG RMS for *on* interval. **b**. Mean SpO_2 and normalised PPG RMS for *off* interval. **c**. *On* versus *off* SpO_2

4.4.3. Case 3

Case 3, a 51 year old female was involved in an MVA approximately four weeks prior to receiving pedicled groin flap surgery. There were no complications during the surgery other than that the patient was obese. It was noted by the clinical consultant that the base of the flap was slightly distant from the usual location of the origin of the SCIA. This is unusual for this type of surgery.

The patient was handed over to the clinical consultant on post-operative day 3.

Day 3 (IP day 3) – The device was applied and day 3 of IP protocol 1 was implemented. Bleeding before IP was red but very slow from both distal and proximal areas. This could indicate that the flap is surviving on minor vessels and not on the SCIA which correlates with the observation that the base is slightly distant from the origin of the SCIA.

Day 4 (IP day 4) - Bluish bleeding on the proximal area and red on distal area was noted.

Day 5 (IP day 5) – IP was continued but measurements were stopped. Slow bleeding occurred when cuff was inflated.

Day 6 (IP day 6) – Following flap congestion, it was decided to stop IP and remove the device from the patient.

Day 7 – Physical appearance of the flap appeared slightly bluish.

Day 10 - Skin loss occurred but flap continued to bleed in the distal region.

Day 13 - Flap necrosis had occurred and flap was consequently dehisced from the recipient site.

Figure 41 shows the analysis of the proximal sensor's data. Figure 41a and Figure 41b show the mean SpO_2, including an error band of the standard deviation. Once again measurements recorded from the distal area were not as pronounced as the proximal sensor and were therefore added as Appendix D. Flank sensor (sensor 3) has no reaction to IP and was therefore excluded from this analysis. Figure 41a (*on* intervals) shows high PPG noise (greater than 18 %) and a SpO_2 value which remains close to the 127 % error value indicating poor or no acceptable PPG signal. Figure 41b (*off* intervals) displays SpO_2 near 100 % with PPG signal noise and SpO_2 rising after the protocol change at the end of IP day 3. Unlike the second case, there was no reduction in SpO_2 during *on* intervals (Figure 41c). This indicates that the recipient site was only receiving supply through the pedicle. The clinical observations coincided with the recorded measurements showing that there was a large amount of congestion within the flap, which eventually led to flap failure. The clinical consultant surmised that the odd location of the vessels within the flap and the decision to begin IP on day 3 of the protocol were the primary reasons for the failure.

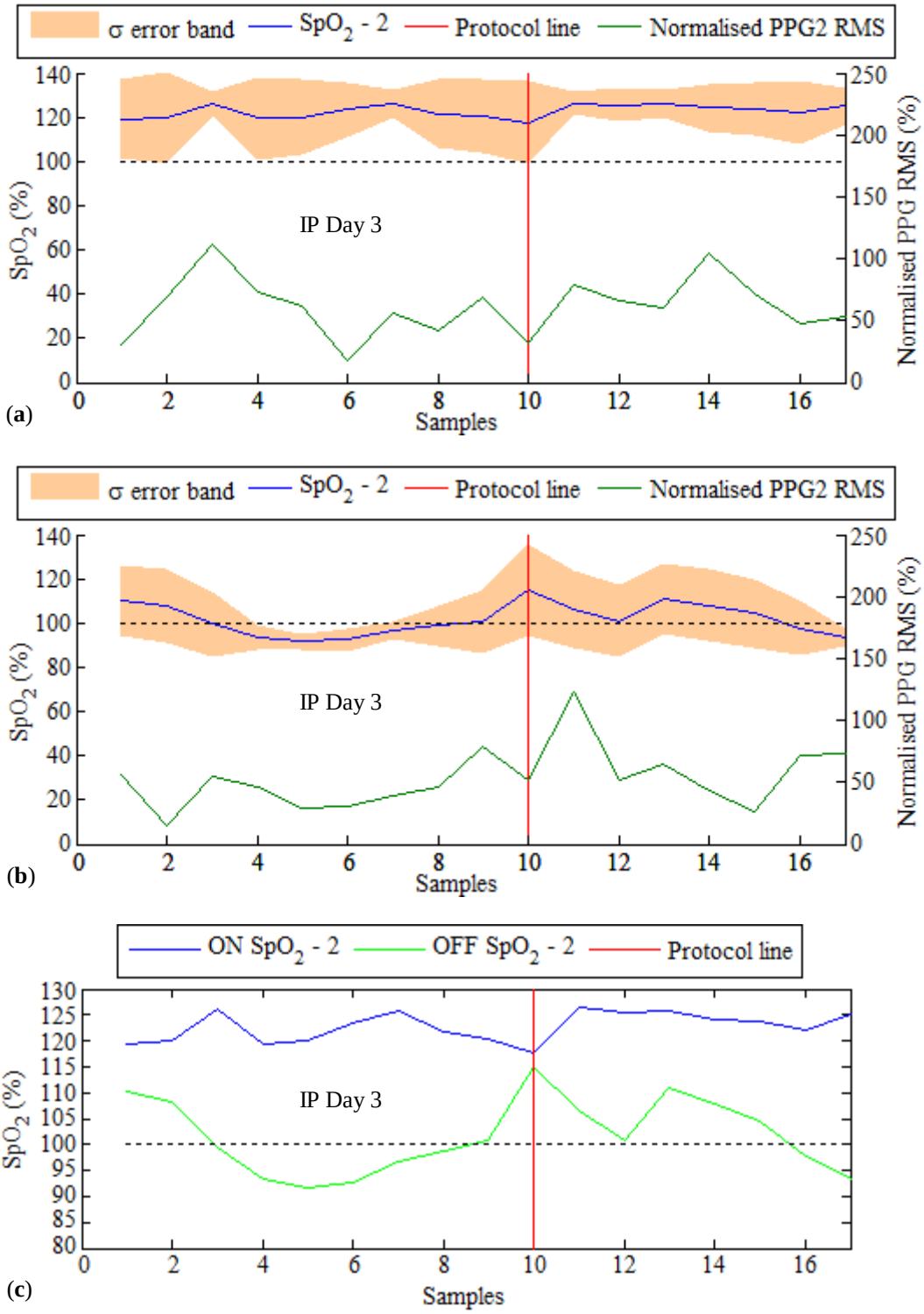

Figure 41: Case 3 data for proximal sensor (sensor 2) for *on* and *off* intervals. SpO_2 values higher than 100 % may be unreliable and are physiologically impossible. 100 % SpO_2 is marked by the dashed black line. Protocol changeover represented by a red vertical line. **a**. Mean SpO_2 and normalised PPG RMS for *on* interval. **b**. Mean SpO_2 and normalised PPG RMS for *off* interval. **c**. *On* versus *off* SpO_2

4.4.4. Case 4

Case 4, the first case of using a control patient. Measurements were taken on post-operative day 7 however the patient did not return for the rest of their weekly appointments. The pneumatic tourniquet was inflated for just over seven minutes to make measurements. The measurements showed good signal quality on the proximal sensor and lower quality on the distal sensor. When the tourniquet was inflated, the proximal sensor indicated no supply from the recipient side. Under inflation the PPG waveform showed no distinct signal with and an average SpO_2 value of approximately 127 %. When the tourniquet was deflated a clear PPG signal was shown and a mean SpO_2 of 95 ± 6 % was measured. The results are similar to those obtained in the pre-clinical testing as seen in Figure 32.

4.5. Error Analysis and Device Modifications

During the early post-operative days of case 1 it was noted that the sensor extension cables added additional noise to the measurements. The additional noise increased the difficulty in distinguishing a PPG signal on the flap. Both Nonin's and the author's extensions caused additional noise despite being constructed of shielded cable. The cables were removed for the remainder of case 1 however reinstalled for cases 2 to 4 for the convenience of increased cable length. The increased length allowed wider patient movement and for the device to be easily placed on a bedside table.

Changes to the software included modification to the PPG graph's auto scale function, modification to the pump control timers, addition of timers for logging and resource optimisations.

One of the reasons for poor signal quality in measurements in case 1 was due to loose sensor mounting that consisted of adhesive medical tape. The author found that tape worked successfully during pre-clinical trials, however in the clinical setting it was not as effective. The sensors were loosened during the course of the day due to patient movement and fluids loosening the adhesive on the tape. The clinical consultant suggested that the sensors be attached using sutures which were to be included during the initial surgery. The sutures performed well in comparison to the tape and this was reflected in the recorded data of case 2 and 3. Despite the sutures fixture over the sensor's rubber casting, the Nonin 8000R sensors still loosened from the patient skin. The surgeon referred to the original housing (Figure 24) which was supplied to him when the device was delivered. He found it not suitable for use in all areas due to its dimensions. A second, smaller sensor housing was then designed and 3D printed. This is shown in Figure 25 and has been designed specifically for use with sutures.

The initial procedure for patient monitoring included hourly checks by the surgeon or nursing staff. During the course of the second case it was realised that these checks were either not possible or not performed. Patient safety is paramount and there was a small possibility that a hardware or software malfunction could go unnoticed. The primary reason that this required attention is

that the clamping cuff could remain inflated for durations longer than those set by the protocol, potentially endangering the success of the surgery. In order to improve the safety of the device a second independent system was designed and developed. The safety device solely monitors the pressure of the system and the duration for which it is applied. In the event of load shedding or any loss of electrical power the device would release the pressure in the system.

The primary components are a pressure transducer, timer, valve and a power supply. The chosen primary components were: Honeywell 24PCC pressure transducer, GIC 1CMDT0 timer, Festo MHE3-MS1H-3/2G-1/8 solenoid valve and Schneider Electric ABL7 RE2403 24VDC power supply. The solenoid valve and power supply were already available as they were used in the first prototype. The pressure transducer's output was amplified by an INA121 instrumentation op-amp and a LM324 op-amp. The gain of the LM324 was fixed while a potentiometer was included for gain adjustment of the INA121. The final output of the LM324 was used to trigger the timer's signal, thereby starting the timer. The Festo solenoid valve was connected to the normally closed contact of the timer and the pneumatics connected in a normally open fashion, thereby requiring power to seal the system and venting the system in case of power loss. A latching circuit was designed using a DPDT (double pole double throw) relay. The relay is activated by the timer's normally open contact which is closed when the timer has timed out. This switches the input signal of the timer from the LM324 output to a fixed 24 V DC, latching the safety device in its venting state. Human intervention is required in order to seal the system again by cycling the power to the device using the provided reset switch. The internal device components are shown in Figure 42 with the circuit schematic displayed in Appendix B. Safety device tests were performed by making use of a desktop sphygmomanometer. The sphygmomanometer's cuff was bypassed and the inflation bubble was placed on the pump input to the device. A mercury manometer was placed on the output of the device which was ordinarily connected to the inflation cuff. The pressure set point potentiometer was adjusted such that the timer was triggered at approximately 35 mmHg. The device was tested specifically for venting functionality. The completed device can be seen in Figure 43.

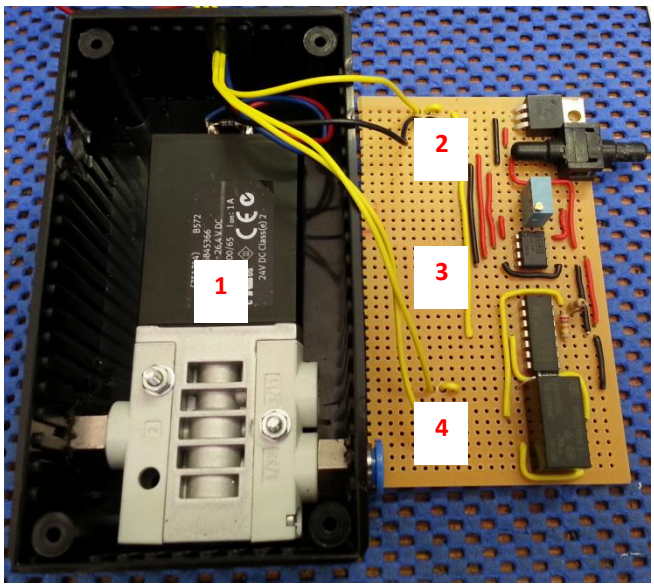

Figure 42: Internal components of the safety device. 1, Festo solenoid valve. 2, Pressure transducer. 3, Pressure set point potentiometer and amplification op-amps. 4, DPDT relay

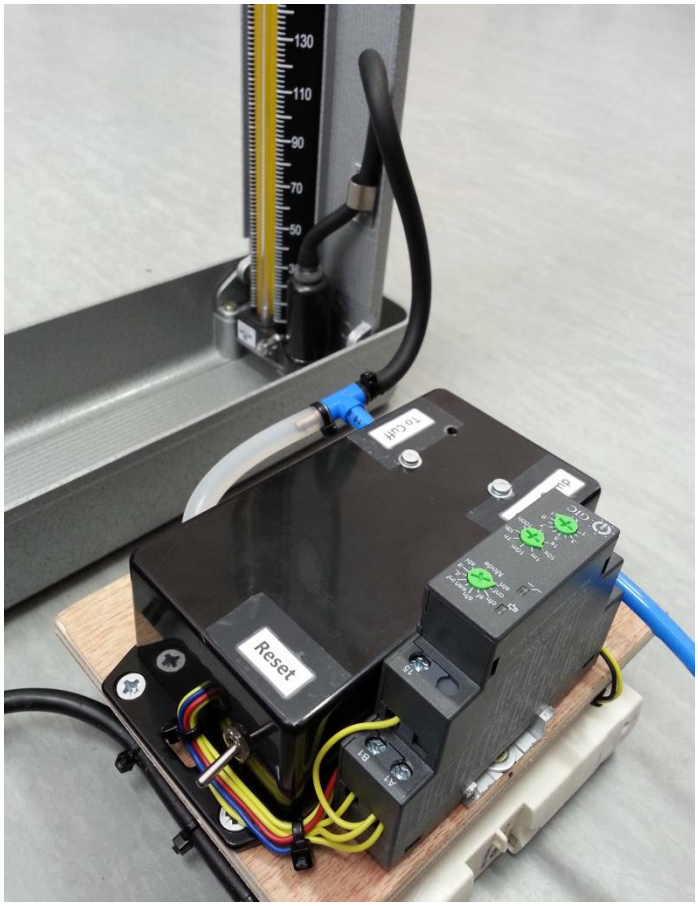

Figure 43: Complete assembly of safety device with the timer shown in the bottom right

5. Conclusions

This chapter summarises the findings made throughout the study. Conclusions are drawn from the findings and recommendations to future work on the device and techniques are also suggested.

5.1. Summary of Findings

A prototype was successfully designed and constructed under budget which was capable of monitoring and recording the SpO_2 and photoplethysmogram from the three incorporated reflectance pulse oximeter probes. The device included a controllable pneumatic system and a two electrode ECG. A GUI was developed through which the device could be monitored and controlled by the user. Prior to clinical trials the device was tested for functionality and reliability. These tests revealed that the probes are capable of measurements on multiple body sites and were primarily tested on areas commonly used for tissue flaps.

Clinical tests were performed on four patients with the second case being the most successful in terms of measurements. The developed device was capable of automated IP and measurements on pedicled groin flaps, however the device is not limited to use on this flap type as indicated by the pre-clinical tests. Two of the three patients who underwent IP benefited from early pedicle division.

Multiple hardware and software improvements were noted after testing was completed on the first patient. Sensor mounting using adhesive medical tape proved to be unreliable and resulted in poor measurements for the majority of the tests. A noticeable pulsatile signal was measured and resolved in a low SpO2 reading. Analysis of the data revealed that a low frequency signal due to respiration was causing this undesired measurement. Zaman *et al.* (2011) and Karlen *et al.* (2013) experienced respiration patterns in their PPG signals. These patterns are normal, however it did not significantly interfere with their measurements. The respiration artefacts seen in the measurements from patient 1 severely overshadowed the desired PPG signal. The first patient was scheduled for flap division on post-operative day 10 but was only divided on day 17 due to external factors.

The second case saw vast improvements in measurements and signal quality. The unreliability of the adhesive tape was solved by suturing the sensors in place. The flank sensor provided inconsistent measurements as it was still fastened using adhesive tape. This sensor was not sutured in place as it was not practical and would cause excessive discomfort to the patient. Results from the proximal sensor showed that on post-operative day 3 (IP day 2) supply was already present from the recipient side. This coincided with the standard clinical observations. Day 4 (IP day 3) saw a negative change in measurements, indicating a loss of supply from the recipient side which also reflected in the clinical observations. The clinical consultant and the author believe that the negative change was likely due to long clamping periods at a high cuff pressure (300 mmHg). The flap was divided on post-operative day 7 fulfilling the objective of monitoring and aiding

in early flap division. The initial condition of the divided flap was good until it was defatted. The clinical consultant speculated that the defatting caused a negative change in flap condition. Despite this degraded condition, the flap was not lost. Division on post-operative day 7 coincided with Cheng *et al.* (1999) who showed that the application of IP to 12 pedicled groin flaps resulted in a mean of 8,4 days until division.

The third patient receiving IP showed measurements of similar quality to that of the second patient. However there was no significant improvement as seen with the second patient. The device measurements showed that supply failed to originate from the recipient side, providing an indication of vascular complications. This correlated with clinical tests in which the clinical consultant noted that the blood vessels included in the flap were in a peculiar position and that the flap was not bleeding well even before IP began. The clinical consultant started IP on the third day of protocol 1 as he received the patient on post-operative day 3. IP was only performed for three days and was stopped due to poor flap condition. The flap was eventually lost on post-operative day 13, however the clinical consultant surmised that the flap was not in acceptable condition from the start as a result of improper surgery.

The fourth case was the first control patient. Measurements on post-operative day 7 showed that there was no supply from the recipient side but ample supply from the pedicle. Unfortunately the patient did not return for the rest of their weekly appointments and no further measurements could be taken.

A potential safety issue arose due to infrequent patient checks. In order to overcome this, an independent safety device was designed and built. This device successfully monitored cuff inflation duration and vented system pressure when necessary. The safety device had not been clinically tested at the time of this thesis, however the tests which were conducted showed its functionality which would remain the same in a clinical setting.

5.2. Conclusions

The reviewed literature showed that IP of pedicled groin flaps can offer improved division times resulting in faster patient recovery. This project investigated the design and development of a monitoring and control device for use with tissue flaps. The focus for this study was the automated IP and monitoring of pedicled groin flaps.

Reflectance pulse oximetry was found to be capable of measurements on pedicled groin flaps and is more affordable than other methods. It is not a perfect monitoring method as it suffers from limitations such as motion and light interference as well the inability to measure when there is no pulsatile flow. However, the cost and availability outweighed these disadvantages for this project.

Having access to recordings of all data allowed for post-testing analysis and experimentation with analysis techniques. With the limited cases available it was

possible to develop an analysis method that assisted in minimising the large quantity of recorded data and in determining healing progress by indication of supply from the recipient side. Additional cases and improved sensor mounting would allow further development and improved accuracy of this method.

The controllable pneumatic system functioned as the automated clamping system required to perform IP on the tested pedicled flaps. The automated system was able to provide consistent pressure and clamping times which can aid in the accurate implementation of IP protocols. This system is beneficial over a manual system which requires frequent human intervention and can be affected by human error and staff availability.

This study showed that reflectance pulse oximetry can be used to monitor pedicled groin flaps and reinforces the use of pulse oximetry to monitor tissue flaps (Edwards & Chapman, 1997; Hallock & Rice, 2003; Pickett *et al.*, 1997; Zaman *et al.*, 2013). Automation of the IP process allowed for accurate IP implementation, which may not always be possible with manual IP. Despite two of the three patients benefitting from early pedicle division, further work is required to prove the effectiveness of the device, primarily in the analysis of IP techniques.

5.3. Recommendations and Future Work

Several recommendations have been made that could improve the device with the desired end result of further assisting patients and surgeons alike.

The reflectance pulse oximetry sensors that were used have only been validated for use on the forehead by the manufacturer. Although the sensors provided valuable data in the form of the PPG waveform and SpO_2 reading, these measurements may be inaccurate. It is recommended that the sensors be validated for multiple tissue types and locations using a CO-oximeter.

The sample size available for this study was small, but sufficient to verify the proof of concept. A larger sample size would further prove the device concept and allow effective analysis of the IP protocols. Having access to more patients would allow improved analysis between patients and not only per patient analysis. As expected with any trial there were problems and shortcomings which were noticed within the first few samples. With additional test subjects, corrective measures could be implemented and further refined, such as the sensor mounting method.

Although automated and continuous measurements are beneficial to patient condition monitoring, it is not completely immune to device failure and still requires human intervention. The author believes that measurements taken three or four times a day by medical staff will be of higher quality and importance than lower quality continuous measurements. The staff member will be available to stand by to ensure correct mounting and signal quality. The staff limitations at a public hospital are noted and for this reason continuous measurements may still be preferable in certain settings.

A custom-made rubber pneumatic tourniquet should be designed and manufactured. This would facilitate even pressure distribution on the pedicle, as well as increased adjustability. A thin transducer should be sourced that can be placed between the tourniquet and skin so that the pressure applied to the pedicle can be measured.

The laptop used with the device had a dated dual core 2 GHz CPU and 2 GB of memory and should be upgraded in order to cope with the computational requirements of the device. A current laptop with dual or quad core CPU and 4 GB of memory would be more than adequate for the device. Any interference with the present laptop could cause processing speed to decrease and result in a device malfunction. Concurrent with the laptop upgrade, the device should be returned with its safety system such that they can be integrated into the same housing and tested as a complete system.

Lastly, should the IP protocols be found to be safe and effective, a simpler, more mobile design is recommended. This design should incorporate a single reflectance sensor, pneumatic tourniquet with relevant pump and timing control as well as a data logging unit, thereby eliminating the need for a laptop. As this device would be more affordable, multiple units could be distributed thereby assisting more patients and increasing the rate at which test data is acquired.

References

Agarwal, R. & Jindal, S.K. 2008. Non-invasive monitoring of oxygenation, in Jindal, S.K. (ed.). *Oxygen therapy.* 2nd ed. New Delhi: Jaypee Brothers Publishers. 313-317.

Agur, A.M.R., Dalley, A.F. & Grant, J.C.B. 2013. *Grant's atlas of anatomy.* 13th ed. Philadelphia: Wolters Kluwer Health/Lippincott Williams & Wilkins.

Akhavani, M.A., Sivakumar, B., Paleolog, E.M. & Kang, N. 2008. Angiogenesis and plastic surgery. *Journal of Plastic, Reconstructive & Aesthetic Surgery,* 61.12: 1425-1437.

Aoyagi,T. 2003. Pulse oximetry: Its invention, theory, and future. *Journal of Anesthesia,* 17.4: 259-266.

Arduino. [S.a.]. *Arduino ADK,* [Online]. Available: http://arduino.cc/en/Main/ArduinoBoardADK [2012, October 29]

Barnette, G., Criner, G. & D'Alonzo, G. (eds.). 2010. Transcutaneous oxygen measurement, in *Critical care study guide: Text and review.* 2nd ed. New York: Springer Science & Business Media. 149-153.

Bequette, B.W. 2003. *Process control: Modeling, design, and simulation.* New Jersey: Prentice Hall PTR.

BIOPAC Systems. [S.a.]. *Advantages of laser doppler flowmetry,* [Online]. Available: https://www.biopac.com/researchApplications.asp?Aid=37&AF=285&Level=3 [2015, September 1]

Buchman, S.J., Eglseder Jr, W.A. & Robertson, B.C. 2002. Pedicled groin flaps for upper-extremity reconstruction in the elderly: A report of 4 cases. *Archives of Physical Medicine and Rehabilitation,* 83.6: 850-854.

Cheng, M., Chen, H., Wei, F., See, L., Lee, H. & Wang, C. 1999. Combined ischemic preconditioning and laser doppler measurement for early division of pedicled groin flap. *Journal of Trauma and Acute Care Surgery,* 47.1: 89-95.

Cheng, M., Chen, H., Wei, F., Su, S., Lian, S. & Brey, E. 2000. Devices for ischemic preconditioning of the pedicled groin flap. *The Journal of Trauma and Acute Care Surgery,* 48.3: 552-557.

Clip Art Best. [S.a.]. *Human body anatomy outline printable for kids,* [Online]. Available: http://www.clipartbest.com/clipart-dT6edzpT9 [2015, October 12]

Cloete, G. 2012. Non-invasive artificial pulse oximetry: Development and testing. Unpublished thesis. Stellenbosch: Stellenbosch University.

Edwards, D. & Chapman, P. 1997. Pulse oximetry as a guide to early division of pedicled flaps. *Journal of the Royal College of Surgeons of Edinburgh,* 42.3: 198-198.

Foo, J.Y., Wilson, S.J., Williams, G.R., Harris, M.A. & Cooper, D.M. 2005. Pulse transit time changes observed with different limb positions. *Physiological Measurement,* 26.6: 1093-1102.

Fredriksson, I., Fors, C. & Johansson, J. 2007. Laser doppler flowmetry - a theoretical framework. Unpublished thesis. Linköping: Linköping University.

Furnas, D.W., Lamb, R.C., Achauer, B.M., Turpin, I.M. & Black, K.S. 1985. A pair of five-day flaps: Early division of distant pedicles after serial cross-clamping and observation with oximetry and fluorometry. *Annals of Plastic Surgery,* 15.3: 262-267.

George, A., Cunha-Gomes, D. & Thatte, R.L. 1996. Early division of pedicled flaps using a simple device: A new technique. *British Journal of Plastic Surgery,* 49.2: 119-122.

Goertz, O. 2012. The effectiveness of pedicled groin flaps in the treatment of hand defects: Results of 49 patients. *The Journal of Hand Surgery,* 37.10: 2088-2094.

Ha, J.F. & Wilson, P. 2009. A modified bowel clamp technique for ischemic preconditioning. *The Ochsner Journal,* 9.2: 63-64.

Haessler, R., Brandl, F., Zeller, M., Briegel, J. & Peter, K. 1992. Continuous intra-arterial oximetry, pulse oximetry, and co-oximetry during cardiac surgery. *Journal of Cardiothoracic and Vascular Anesthesia,* 6.6: 668-673.

Hallock, G.G. & Rice, D.C. 2003. A comparison of pulse oximetry and laser doppler flowmetry in monitoring sequential vascular occlusion in a rabbit ear model. *The Canadian Journal of Plastic Surgery,* 11.1: 11-14.

Hart, M. 2013. *NewSoftSerial,* [Online]. Available: http://arduiniana.org/libraries/newsoftserial/ [2015, November 19]

Hirigoyen, M., Blackwell, K., Zhang, W., Silver, L., Weinbery, H. & Urken, M. 1997. Continuous tissue oxygen tension measurement as a monitor of free-flap viability. *Plastic & Reconstructive Surgery,* 99.3: 763-773.

Hu, C., Lin, Z., Chen, Y., Lin, Y. & Li, M. 2013. Portable laser doppler flowmeter for microcirculation detection. *Biomedical Engineering Letters,* 3.2: 109-114.

Irwin, M.S., Thorniley, M.S., Dore´, C.J. & Green, C.J. 1995. Near infra-red spectroscopy: A non-invasive monitor of perfusion and oxygenation within the microcirculation of limbs and flaps. *British Journal of Plastic Surgery,* 48.1: 14-22.

Jubran, A. 2015. Pulse oximetry. *Critical Care (London, England),* 19: 272-279.

Kanwisher, J. 1959. Polarographic oxygen electrode. *Limnology and Oceanography,* 4.2: 210-217.

Karlen, W., Raman, S., Ansermino, J.M. & Dumont, G.A. 2013. Multiparameter respiratory rate estimation from the photoplethysmogram. *IEEE Transactions on Bio-Medical Engineering,* 60.7: 1946-1953.

Keller, A. 2007. Noninvasive tissue oximetry for flap monitoring: An initial study. *Journal of Reconstructive Microsurgery*, 23.4: 189-197.

Keller, A.M. 2009. A new diagnostic algorithm for early prediction of vascular compromise in 208 microsurgical flaps using tissue oxygen saturation measurements. *Annals of Plastic Surgery,* 62.5: 538-543.

Kenner, C. & Lott, J. (eds.). 2013. Assessment and monitoring, in *Comprehensive neonatal nursing care.* 5th ed. New York: Springer Publishing Company. 147-148.

Lahouel, N. 2013. Personal interview. 4 March, Stellenbosch.

Lindsey, L.A., Watson, J.D. & Quaba, A.A. 1991. Pulse oximetry in postoperative monitoring of free muscle flaps. *British Journal of Plastic Surgery,* 44.1: 27-29.

Mardirossian, G. & Schneider, R. 1992. Limitations of pulse oximetry. *Anesthesia Progress,* 39.6: 194-196.

McGovern, J.P., Sasse, S.A., Stansbury, D.W., Causing, L.A. & Light, R.W. 1996. Comparison of oxygen saturation by pulse oximetry and co-oximetry during exercise testing in patients with COPD. *CHEST Journal*, 109.5: 1151-1155.

McGregor, I.A. & Jackson, I.T. 1972. The groin flap. *British Journal of Plastic Surgery,* 25.0: 3-16.

Mengelkoch, L.J., Martin, D. & Lawler, J. 1994. A review of the principles of pulse oximetry and accuracy of pulse oximeter estimates during exercise. *Physical Therapy,* 74.1: 40-49.

Mittnacht, A.J. 2010. Near infrared spectroscopy in children at high risk of low perfusion. *Current Opinion in Anaesthesiology,* 23.3: 342-347.

Moerman, A. & Wouters, P. 2010. Near-infrared spectroscopy (NIRS) monitoring in contemporary anesthesia and critical care. *Acta Anaesthesiologica Belgica,* 61.4: 185-194.

Moyle, J. 2002. *Pulse oximetry*. 2nd ed. London: BMJ Books.

Nitzan, M., Romem, A. & Koppel, R. 2014. Pulse oximetry: Fundamentals and technology update. *Medical Devices (Auckland, N.Z.),* 7: 231-239.

Nonin Medical Inc. 2008. *PureSAT advantage,* [Online]. Available: http://www.nonin.com/documents/puresat-advantage-brochure.pdf [2012, October 29]

Nonin Medical Inc. 2007. *OEM III module specification and technical information,* [Online]. Available: http://www.nonin.com/documents/OEM%20III%20Module%20Specifications.pdf [2012, October 29]

Nonin Medical Inc. [S.a.]. *Reusable PureLight® sensors for dependable SpO2 readings,* [Online]. Available: http://www.nonin.com/PulseOximetry/Sensors/ReusableSensors [2012, October 29]

Ortega, R., Hansen, C.J., Elterman, K. & Woo, A. 2011. Pulse oximetry. *The New England Journal of Medicine,* 364.16: 33-36.

Patel, K.G. & Sykes, J.M. 2011. Concepts in local flap design and classification. *Operative Techniques in Otolaryngology-Head and Neck Surgery,* 22.1: 13-23.

Pellicer, A. & Bravo, M.d.C. 2011. Near-infrared spectroscopy: A methodology-focused review. *Seminars in Fetal and Neonatal Medicine,* 16.1: 42-49.

Pickett, J., Amoroso, P., Nield, D.V. and Jones, D.P. 1997. Pulse Oximetry and PPG Measurements in Plastic Surgery, in *Engineering in Medicine and Biology Society, 1997. Proceedings of the 19th Annual International Conference of the IEEE,* 5: 2330-2332.

Pololu Corporation. [S.a.]. *Pololu high-power motor driver 18v15,* [Online]. Available: http://www.pololu.com/catalog/product/755 [2012, October 29]

Raul. 2013. *Minimal ECG using an arduino and xoscillo,* [Online]. Available: http://codinglab.blogspot.co.za/2013/07/my-heartbeat.html [2015, October 5]

Repež, A., Oroszy, D. & Arnež, Z.M. 2008. Continuous postoperative monitoring of cutaneous free flaps using near infrared spectroscopy. *Journal of Plastic, Reconstructive & Aesthetic Surgery,* 61.1: 71-77.

Roberts, J.R. (ed.). 2013. Noninvasive oxygenation monitoring: Pulse oximetry, in *Roberts and Hedges' clinical procedures in emergency medicine*. Philadelphia*:* Elsevier. 26-30.

Rosdahl, C.B. & Kowalski, M.T. 2008. *Textbook of basic nursing*. 9th ed. Philadelphia: Lippincott Williams & Wilkins.

Sahni, R. 2012. Noninvasive monitoring by photoplethysmography. *Clinics in Perinatology*, 39.3: 573-583.

Salama, A.R. 2012. Flap classification and principles of flap design for head and neck reconstruction, in *Current therapy in oral and maxillofacial surgery*. Saint Louis: W.B. Saunders. 11-18.

Scheeren, T.W.L., Schober, P. & Schwarte, L.A. 2012. Monitoring tissue oxygenation by near infrared spectroscopy (NIRS): Background and current applications. *Journal of Clinical Monitoring and Computing*, 26.4: 279-287.

Sinex, J.E. 1999. Pulse oximetry: Principles and limitations. *The American Journal of Emergency Medicine,* 17.1: 59-66.

Smith, R.P., Argod, J., Pépin, J. & Lévy, P.A. 1999. Pulse transit time: An appraisal of potential clinical applications. *Thorax,* 54.5: 452-457.

Steele, M.M. 2011. Three-year experience using near infrared spectroscopy tissue oximetry monitoring of free tissue transfers. *Annals of Plastic Surgery,* 66.5: 540-545.

The MathWorks Inc. [S.a.]. *Matlab,* [Online]. Available: http://www.mathworks.com/products/matlab/ [2012, October 29]

Thomason, H., Batki, A. and Nayyar, P. 2010. *Market review: Blood gas analysers*. London: Centre for Evidence-based Purchasing.

Tremper, K.K., Rutter, T.W. & Wahr, J.A. 1993. Monitoring oxygenation. *Current Anaesthesia & Critical Care*, 4.4: 213-222.

Verder International B.V. [S.a.]. *Verderflex EZ OEM pump,* [Online]. Available: http://www.verderflex.com/product-range/peristaltic-oem-pump-heads/verderflex-oem-pump-heads/ez/ [2012, October 29]

Wallace, A.F. 1978. The early development of pedicle flaps. *Journal of the Royal Society of Medicine,* 71.11: 834-838.

Wax, D.B., Rubin, P. & Neustein, S. 2009. A comparison of transmittance and reflectance pulse oximetry during vascular surgery. *Anesthesia & Analgesia,* 109.6: 1847-1849.

Wyka, K., Mathews, P. & Rutkowski, J. 2011. *Foundations of respiratory care.* 2nd ed. New York: Delmar, Cengage Learning.

Zaman, T., Kyriacou, P.A. and Pal, S.K. 2013. Free Flap Pulse Oximetry Utilizing Reflectance Photoplethysmography, in *Engineering in Medicine and Biology Society (EMBC), 2013. Proceedings of the 35th Annual International Conference of the IEEE*. 4046-4049.

Zaman, T., Kyriacou, P.A. and Pal, S.K. 2011. Development of a Reflectance Photoplethysmographic Sensor used for the Assessment of Free Flap Perfusion, in *Engineering in Medicine and Biology Society (EMBC), 2011. Proceedings of the Annual International Conference of the IEEE*. 4006-4009.

Appendix A: Programming code

A-1 Second Prototype Labview Code

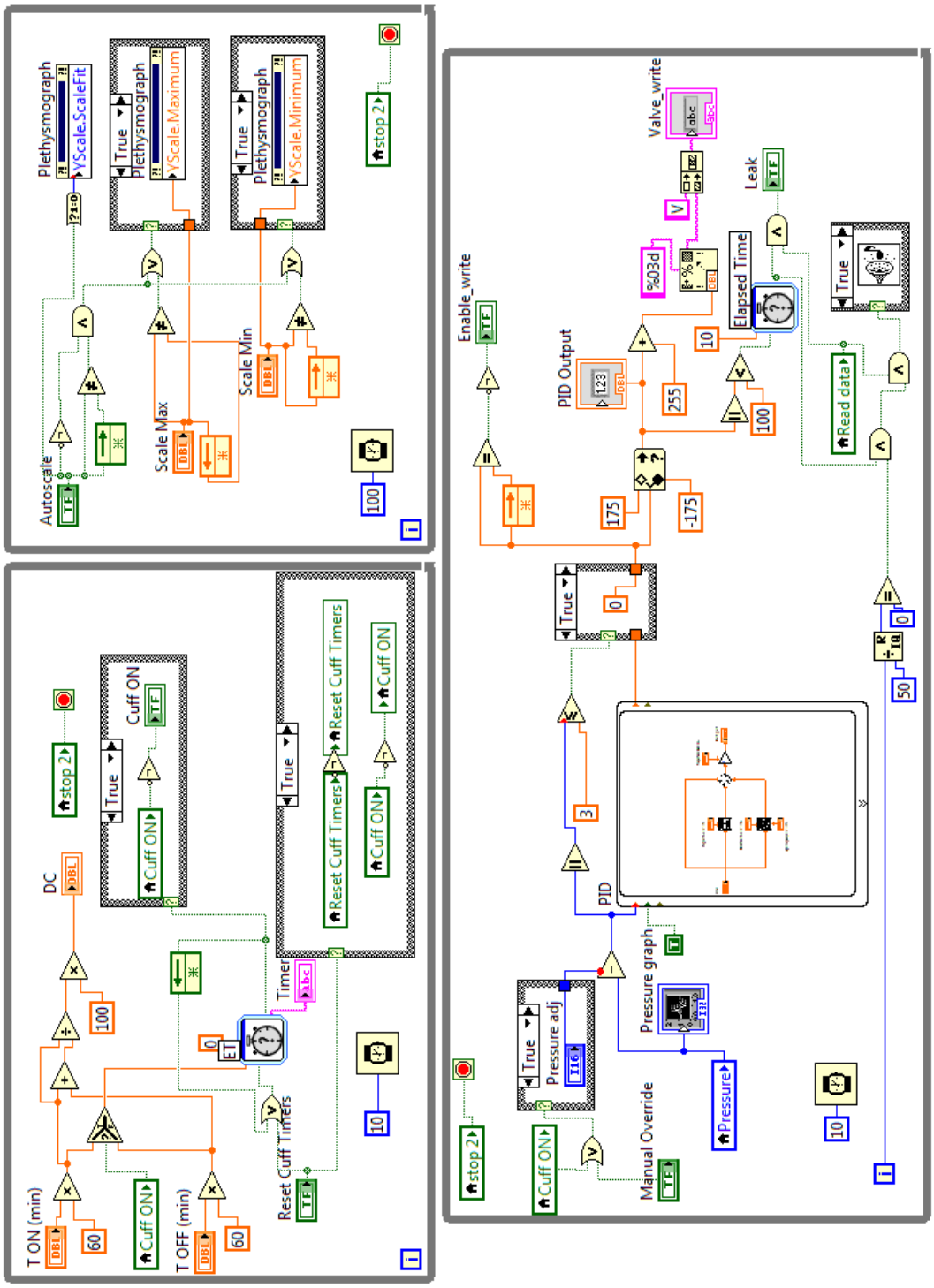

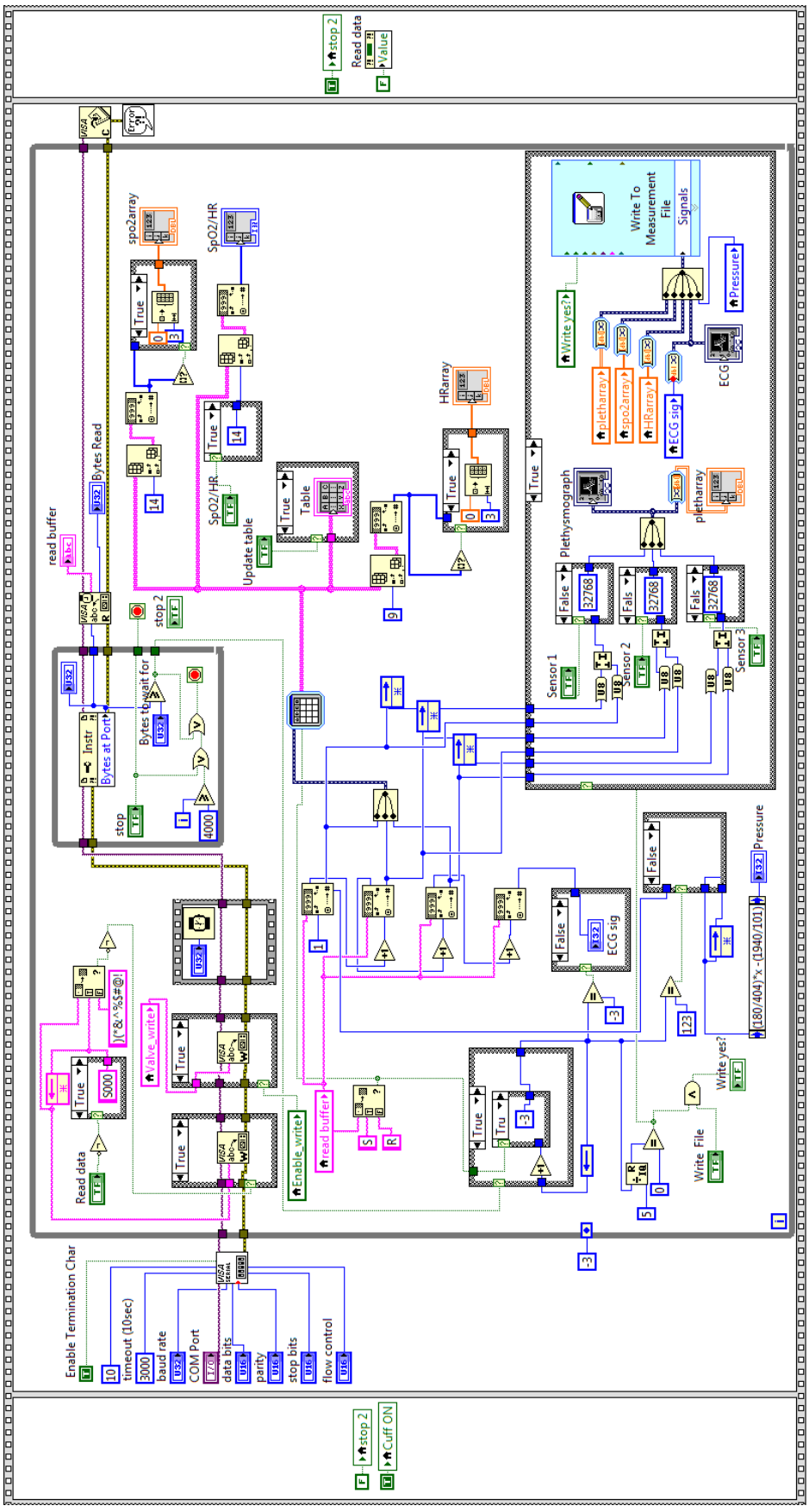

A-2 Flow diagram of MATLAB Analysis Code

Prior to this section, data files are read from a directory (each being 30 000 rows by 9 columns) and appended to an array. *On* and *off* pressure limits are user specified and the data is searched for indices that fall within the range of each *on* and *off* interval. These indices are used in the algorithm below.

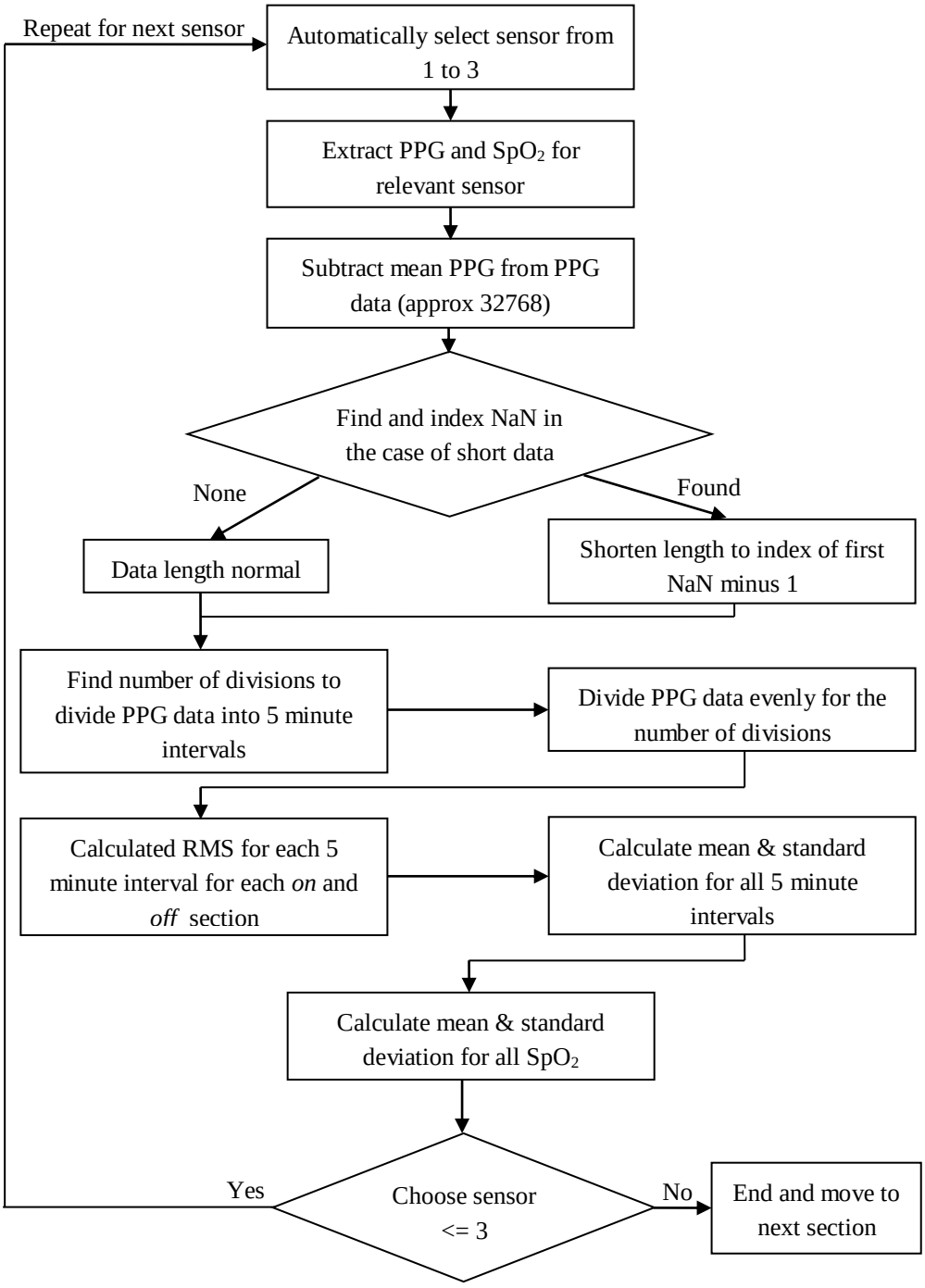

Appendix B: Electrical Schematics

B-1 First Prototype Power Supply Schematic

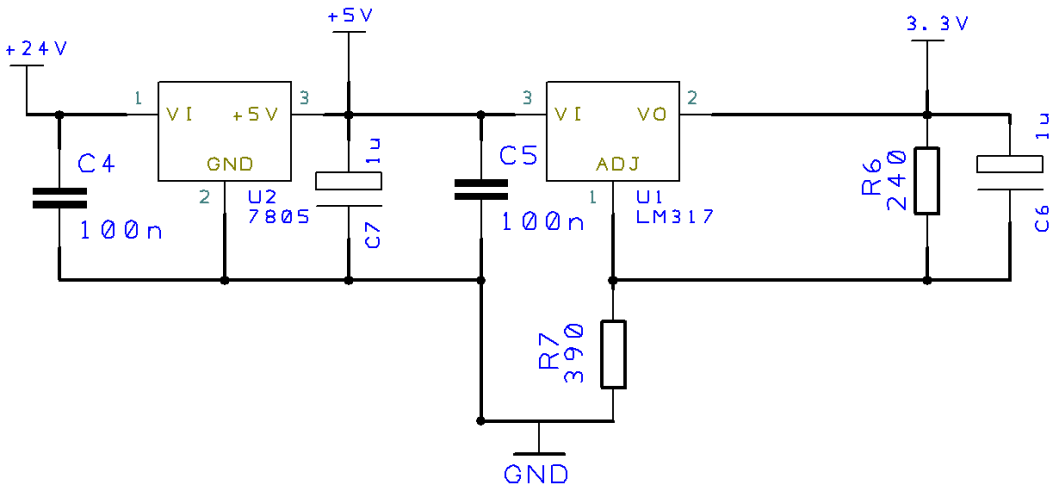

B-2 First Prototype ATmega328 Schematic

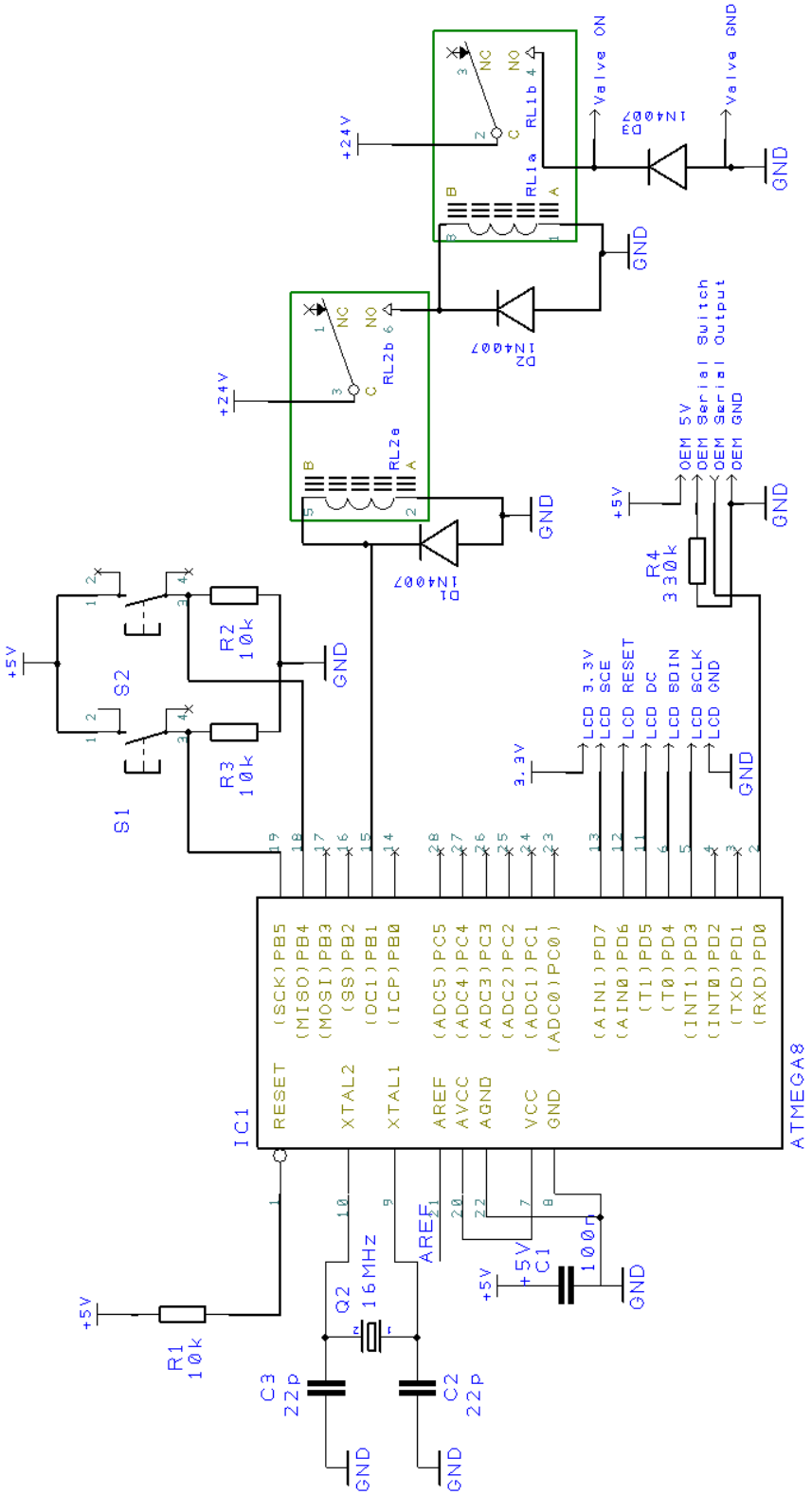

B-3 Second prototype ATmega2560 Schematic

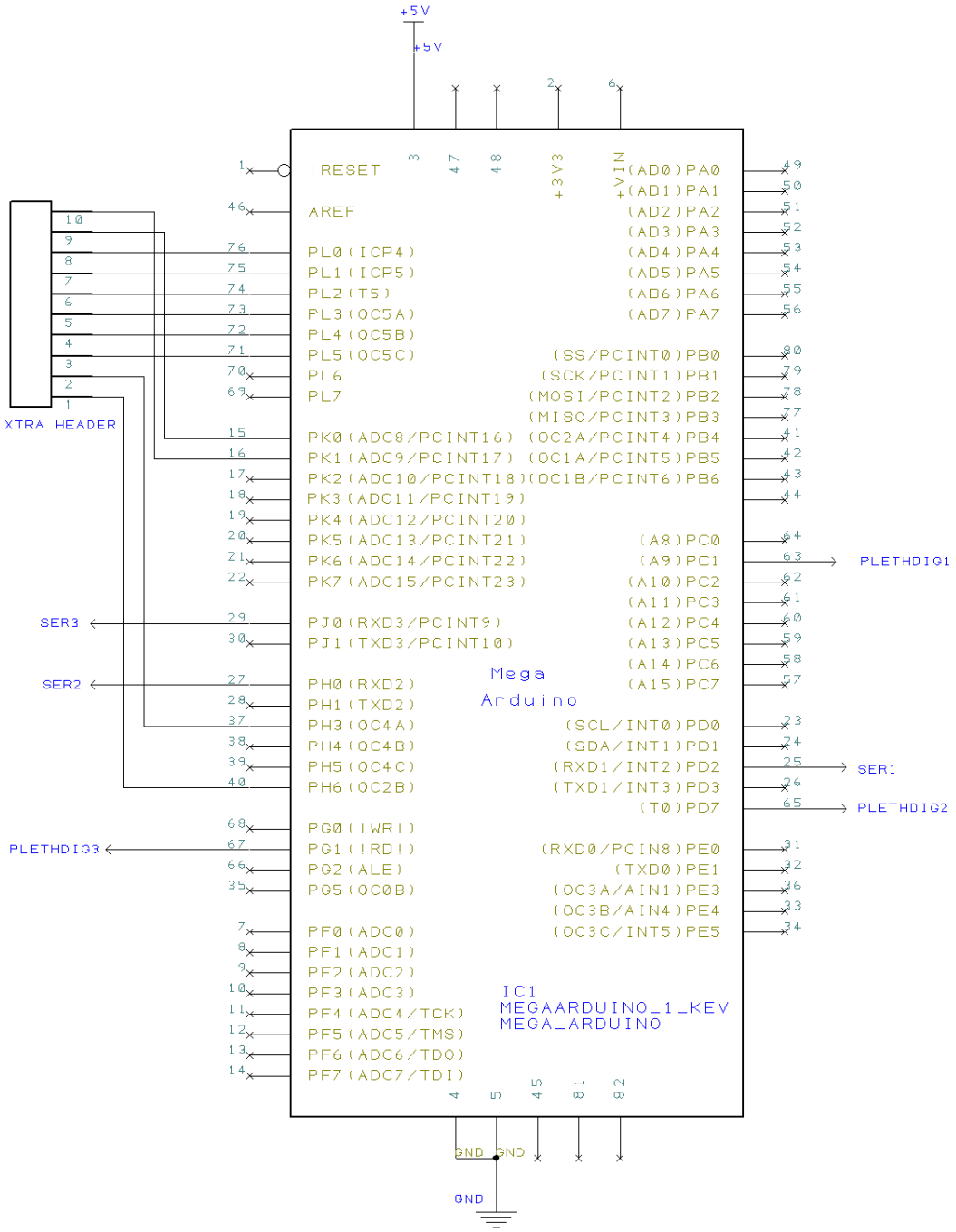

B-4 Second Prototype Sensor Schematic

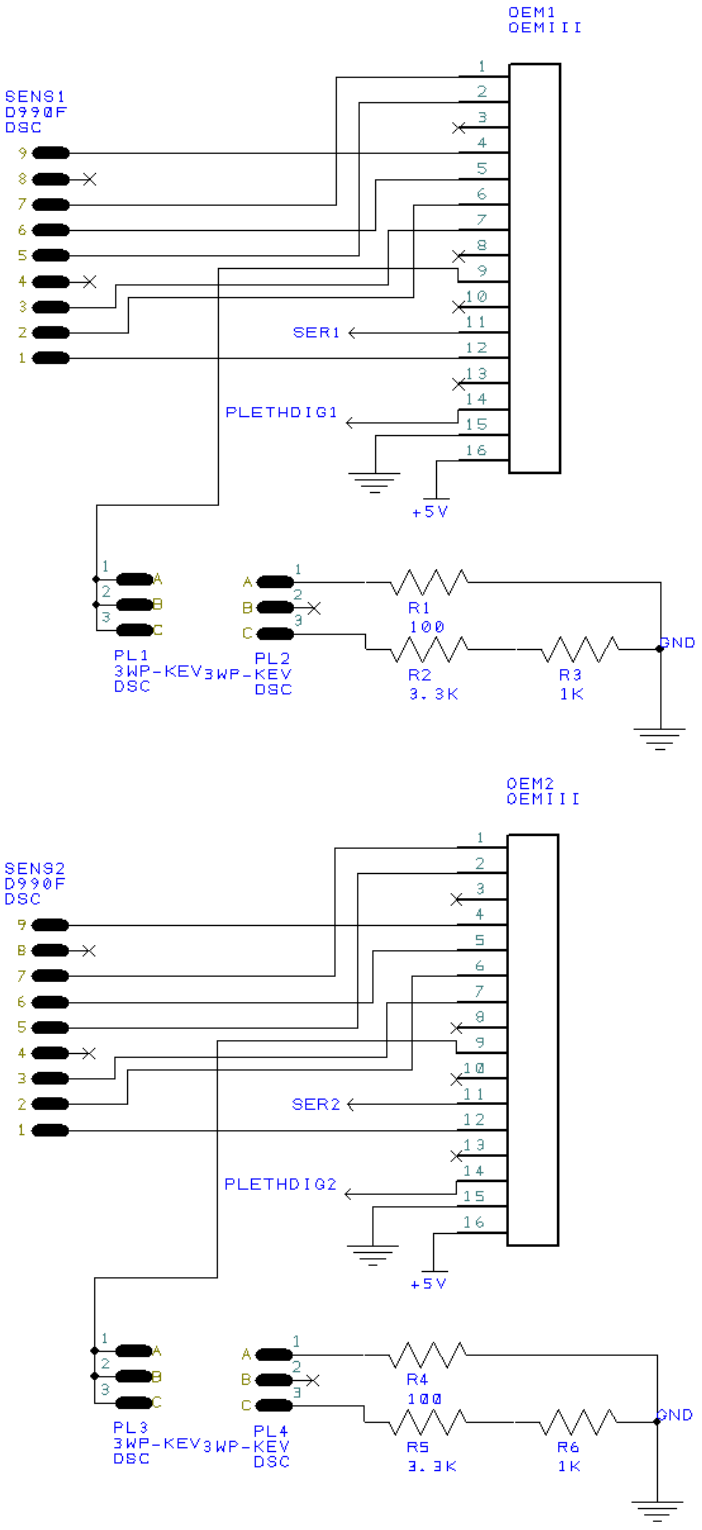

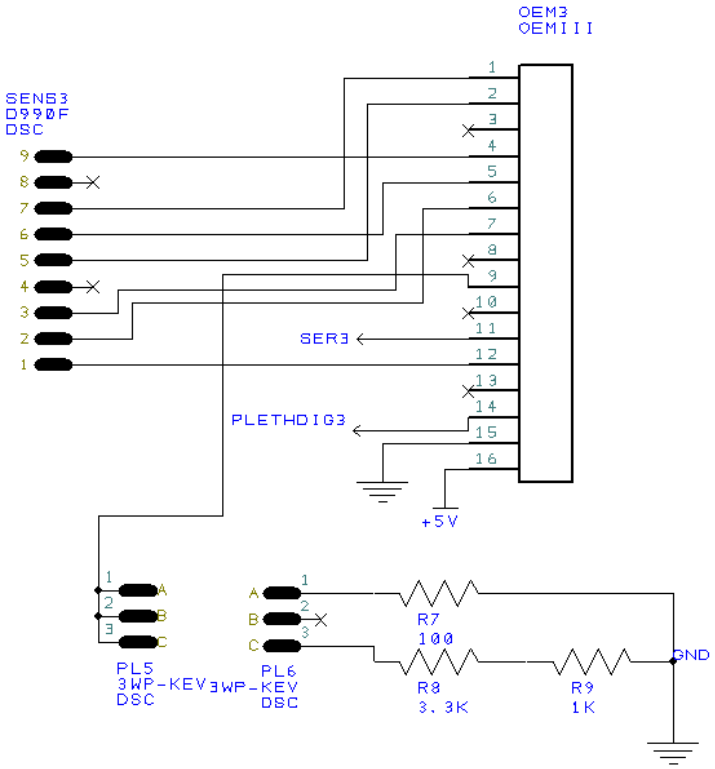

B-5 ECG Schematic

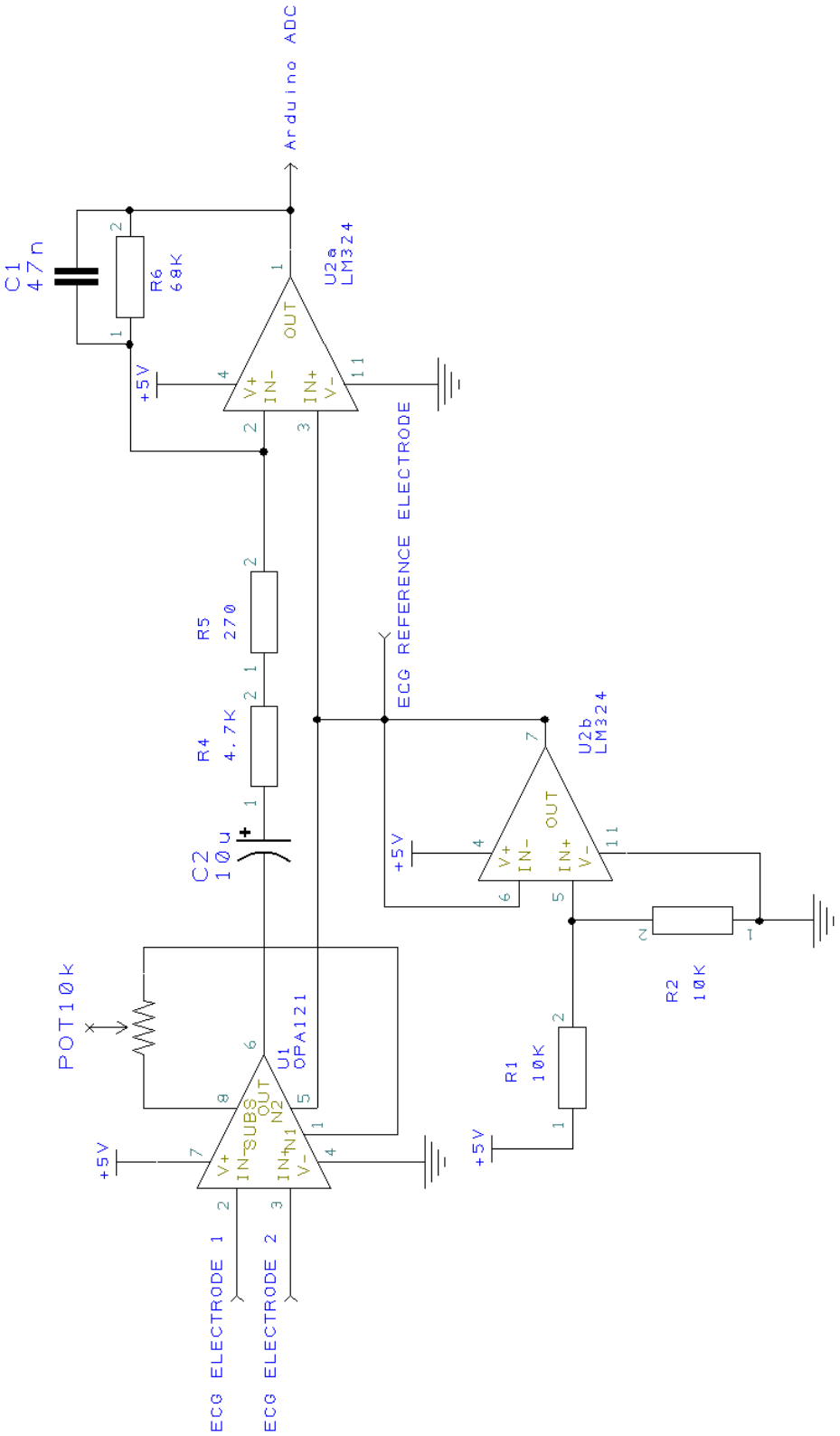

B-6 Safety System Schematic

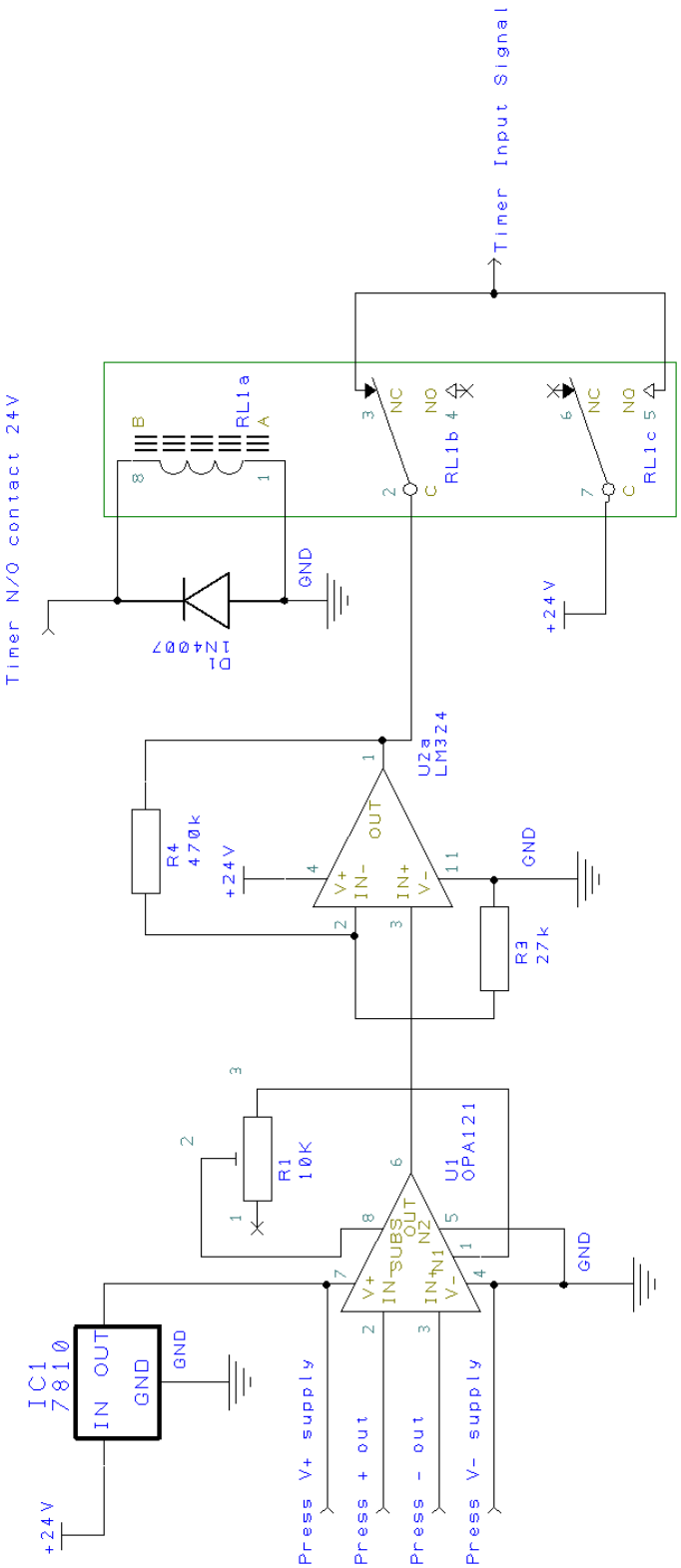

Appendix C: Datasheets

C-1 Nonin OEM III Serial Data #7 Packet Structure

Serial Data Format #7:

Packet Description

A frame consists of 5 bytes; a packet consists of 25 frames. Three packets (75 frames) are transmitted each second.

Frame

Packet

	Byte 1	Byte 2	Byte 3	Byte 4	Byte 5
1	STATUS	PLETH (MSB)	PLETH (LSB)	HR MSB	CHK
2	STATUS	PLETH (MSB)	PLETH (LSB)	HR LSB	CHK
3	STATUS	PLETH (MSB)	PLETH (LSB)	SpO_2	CHK
4	STATUS	PLETH (MSB)	PLETH (LSB)	REV	CHK
5	STATUS	PLETH (MSB)	PLETH (LSB)	reserved	CHK
6	STATUS	PLETH (MSB)	PLETH (LSB)	reserved	CHK
7	STATUS	PLETH (MSB)	PLETH (LSB)	reserved	CHK
8	STATUS	PLETH (MSB)	PLETH (LSB)	reserved	CHK
9	STATUS	PLETH (MSB)	PLETH (LSB)	SpO_2-D	CHK
10	STATUS	PLETH (MSB)	PLETH (LSB)	SpO_2 Fast	CHK
11	STATUS	PLETH (MSB)	PLETH (LSB)	SpO_2 B-B	CHK
12	STATUS	PLETH (MSB)	PLETH (LSB)	reserved	CHK
13	STATUS	PLETH (MSB)	PLETH (LSB)	reserved	CHK
14	STATUS	PLETH (MSB)	PLETH (LSB)	E-HR MSB	CHK
15	STATUS	PLETH (MSB)	PLETH (LSB)	E-HR LSB	CHK
16	STATUS	PLETH (MSB)	PLETH (LSB)	E-SpO_2	CHK
17	STATUS	PLETH (MSB)	PLETH (LSB)	E-SpO_2-D	CHK
18	STATUS	PLETH (MSB)	PLETH (LSB)	reserved	CHK
19	STATUS	PLETH (MSB)	PLETH (LSB)	reserved	CHK
20	STATUS	PLETH (MSB)	PLETH (LSB)	HR-D MSB	CHK
21	STATUS	PLETH (MSB)	PLETH (LSB)	HR-D LSB	CHK
22	STATUS	PLETH (MSB)	PLETH (LSB)	E-HR-D MSB	CHK
23	STATUS	PLETH (MSB)	PLETH (LSB)	E-HR-D LSB	CHK
24	STATUS	PLETH (MSB)	PLETH (LSB)	reserved	CHK
25	STATUS	PLETH (MSB)	PLETH (LSB)	reserved	CHK

Notes:

- Refer to DF#2 for definitions on Status Byte, Byte 4 and Checksum
- PLETH(MSB) and PLETH(LSB) make up a 16-bit pleth (ex. PLETH(MSB)*256 + PLETH(LSB))

C-2 INA121 ECG Application Note

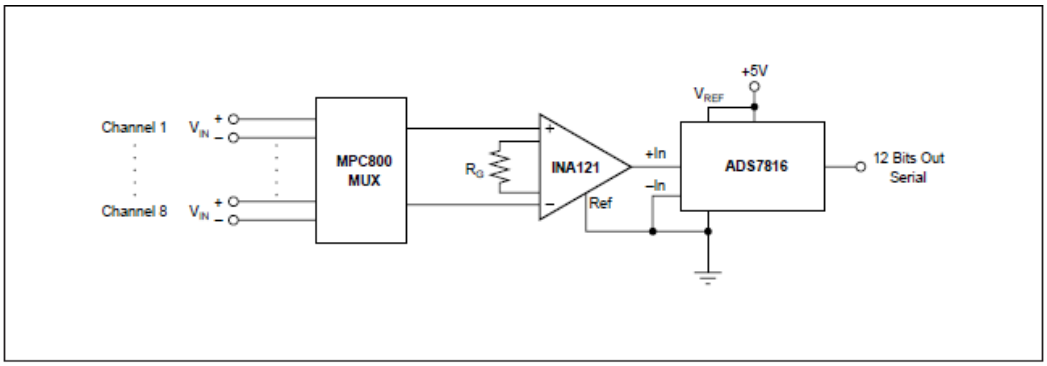

FIGURE 12. Multiplexed-Input Data Acquisition System.

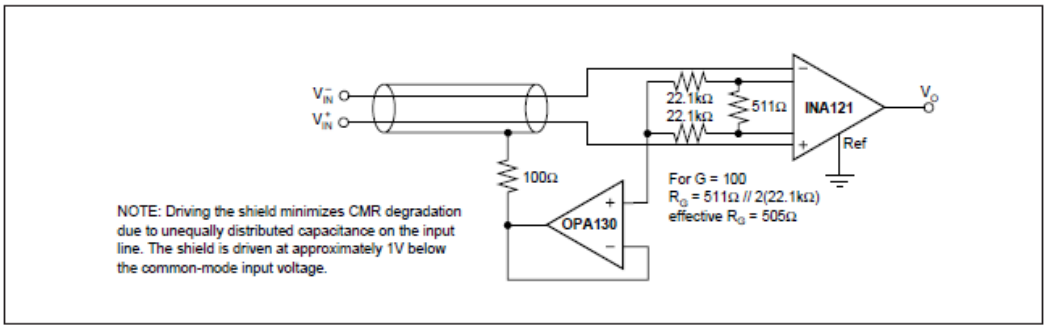

FIGURE 13. Shield Driver Circuit.

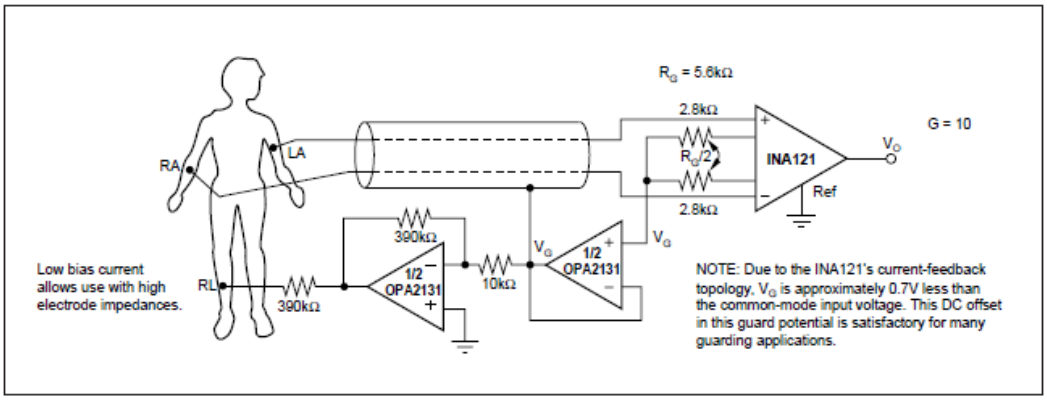

FIGURE 14. ECG Amplifier With Right-Leg Drive.

Appendix D: Measurement and Calibration Data

D-1 Pressure Transducer Calibration Curve

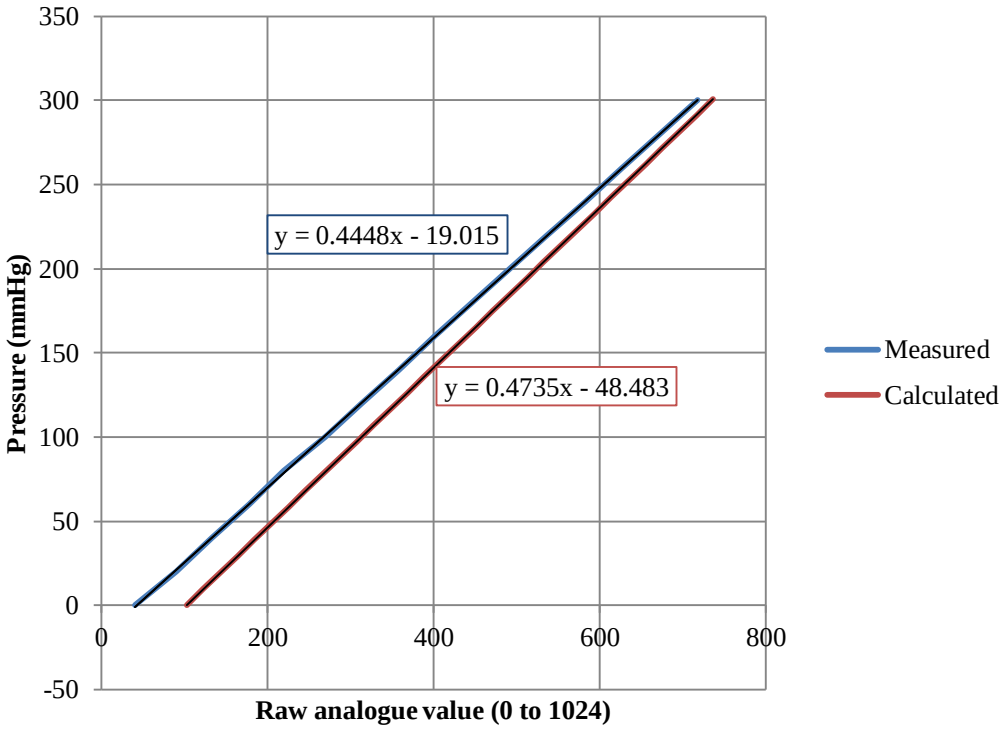

Figure D-1: Calculated and measured calibration curves for Honeywell pressure transducer

D-2 Case 2 Distal Sensor Graphs

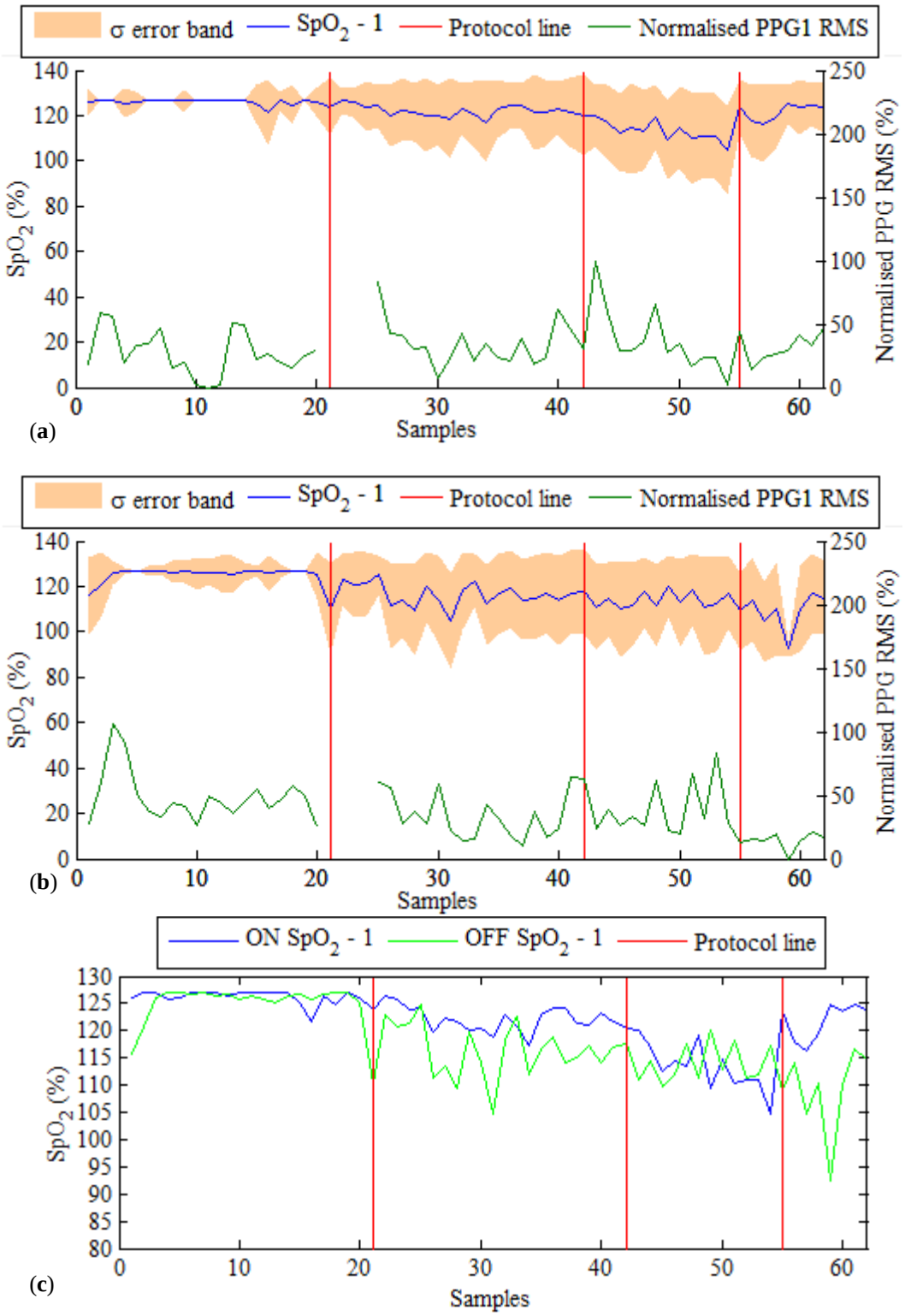

Figure D-2: Case 2 data for distal sensor (sensor 1) for *on* and *off* intervals. Protocol changeover shown by a red vertical line. **a**. Mean SpO_2 and normalised PPG RMS for *on* interval. **b**. Mean SpO_2 and normalised PPG RMS for *off* interval. **c**. *On* versus *off* SpO_2

Table D-1: Data obtained from *on* and *off* analysis for Case 2

	ON PPG						OFF PPG					
Samp	PPG1	PPG2	PPGSTD1	PPGSTD2	STD Perc1	STD Perc2	PPG1	PPG2	PPGSTD1	PPGSTD2	STD Perc1	STD Perc2
1	162.35	43.31	29.76	0.57	18.33	1.32	341.75	97.78	95.20	38.51	27.86	39.39
2	1087.14	113.22	638.07	77.64	58.69	68.57	274.98	73.26	163.99	15.51	59.64	21.18
3	600.26	50.49	334.09	2.00	55.66	3.97	794.13	86.00	839.68	18.07	105.74	21.01
4	403.10	51.17	79.83	1.53	19.80	2.98	1052.18	104.67	964.85	52.54	91.70	50.19
5	349.50	52.32	114.75	2.36	32.83	4.51	506.88	101.71	254.69	8.09	50.25	7.95
6	295.19	55.47	103.37	3.62	35.02	6.52	543.73	101.83	200.74	15.04	36.92	14.76
7	326.71	59.01	150.74	3.25	46.14	5.50	572.42	114.03	193.15	12.98	33.74	11.38
8	347.15	127.15	56.23	87.95	16.20	69.17	543.33	116.78	241.19	12.18	44.39	10.43
9	253.91	66.10	49.86	1.54	19.64	2.34	535.89	121.01	220.38	7.88	41.12	6.51
10	216.52	45.79	4.43	5.05	2.04	11.02	583.47	114.95	156.38	9.65	26.80	8.40
11	264.75	54.89	0.00	0.00	0.00	0.00	532.18	112.82	263.30	12.73	49.48	11.29
12	474.41	116.15	9.42	86.66	1.99	74.61	517.93	108.76	230.19	11.14	44.44	10.25
13	324.56	60.18	162.51	3.93	50.07	6.52	535.26	135.99	190.71	15.40	35.63	11.33
14	318.08	61.28	157.17	5.21	49.41	8.51	504.86	116.71	230.67	22.02	45.69	18.87
15	386.56	58.78	83.95	3.44	21.72	5.85	491.46	144.93	269.09	5.78	54.75	3.99
16	388.97	61.14	102.00	5.62	26.22	9.20	422.48	150.05	167.82	30.98	39.72	20.65
17	681.49	64.27	134.15	6.76	19.68	10.52	437.30	110.14	205.27	21.64	46.94	19.65
18	579.56	58.97	89.72	3.99	15.48	6.76	478.95	104.72	277.73	17.52	57.99	16.73
19	468.89	65.13	115.51	6.04	24.63	9.27	511.02	135.10	250.66	15.76	49.05	11.66
20	305.96	74.67	90.08	2.89	29.44	3.87	334.63	138.79	84.08	25.97	25.13	18.71
21	NaN	57.07	NaN	3.88	NaN	6.79	NaN	83.82	NaN	6.85	NaN	8.17
22	NaN	75.29	NaN	55.52	NaN	73.74	NaN	78.80	NaN	4.46	NaN	5.66

ON PPG							OFF PPG					
Samp	PPG1	PPG2	PPGSTD1	PPGSTD2	STD Perc1	STD Perc2	PPG1	PPG2	PPGSTD1	PPGSTD2	STD Perc1	STD Perc2
23	NaN	53.43	NaN	2.91	NaN	5.44	NaN	107.47	NaN	20.47	NaN	19.04
24	NaN	68.06	NaN	7.28	NaN	10.69	NaN	112.02	NaN	32.95	NaN	29.41
25	60.28	114.88	50.18	118.76	83.25	103.38	176.04	115.75	106.35	41.56	60.41	35.91
26	138.21	64.07	59.49	9.85	43.04	15.38	165.92	128.64	92.47	83.22	55.73	64.70
27	155.49	65.46	63.59	17.35	40.90	26.51	105.73	89.22	29.71	5.69	28.10	6.38
28	144.76	64.05	43.19	8.60	29.84	13.43	233.54	125.70	86.52	27.69	37.05	22.03
29	125.06	60.12	39.54	2.30	31.61	3.83	126.09	141.76	34.28	31.93	27.19	22.52
30	125.07	59.99	8.53	1.09	6.82	1.82	236.74	142.07	137.67	45.67	58.15	32.15
31	208.26	61.43	46.00	2.93	22.09	4.77	197.03	93.41	45.02	12.81	22.85	13.71
32	145.25	58.57	61.86	1.39	42.59	2.38	125.38	131.79	17.41	36.55	13.88	27.73
33	108.93	58.18	22.55	1.95	20.70	3.35	117.95	128.78	18.22	16.53	15.45	12.84
34	97.67	55.04	34.04	0.94	34.85	1.70	132.22	113.38	55.95	38.04	42.32	33.55
35	98.80	57.17	22.72	2.07	22.99	3.62	93.47	78.29	29.25	6.14	31.29	7.84
36	98.49	55.56	20.86	1.27	21.18	2.29	93.47	75.06	17.62	2.17	18.85	2.89
37	171.96	66.79	66.76	13.74	38.82	20.57	109.64	77.11	10.68	12.14	9.74	15.74
38	116.12	62.94	21.52	1.91	18.54	3.03	114.32	94.47	42.37	38.81	37.06	41.08
39	96.64	56.89	23.04	1.67	23.84	2.94	123.44	72.23	20.34	2.55	16.47	3.53
40	131.95	60.38	80.95	9.10	61.35	15.07	185.37	89.41	43.50	18.97	23.47	21.21
41	124.25	66.36	58.18	16.07	46.82	24.22	246.45	103.53	157.74	37.08	64.00	35.82
42	138.75	69.54	42.70	24.53	30.78	35.27	735.23	484.27	457.88	468.14	62.28	96.67
43	427.25	347.04	424.26	535.72	99.30	154.37	168.32	127.45	40.24	10.67	23.91	8.38
44	236.42	144.98	139.72	68.60	59.10	47.31	226.31	129.64	88.11	27.53	38.93	21.23

ON PPG							OFF PPG					
Samp	PPG1	PPG2	PPGSTD1	PPGSTD2	STD Perc1	STD Perc2	PPG1	PPG2	PPGSTD1	PPGSTD2	STD Perc1	STD Perc2
45	166.93	151.16	48.56	56.30	29.09	37.25	288.11	357.57	77.14	194.76	26.77	54.47
46	345.64	705.55	99.38	609.81	28.75	86.43	186.18	1238.71	62.54	641.01	33.59	51.75
47	264.52	540.45	95.28	328.29	36.02	60.74	242.17	1061.07	63.74	791.84	26.32	74.63
48	192.15	331.17	126.92	125.24	66.05	37.82	221.93	473.59	137.96	506.94	62.16	107.04
49	143.24	339.23	39.20	161.01	27.36	47.46	130.98	206.63	28.96	37.51	22.11	18.15
50	165.96	344.59	57.92	158.38	34.90	45.96	136.65	166.72	27.20	6.31	19.91	3.79
51	260.88	975.20	44.46	344.37	17.04	35.31	213.13	236.32	143.23	140.36	67.20	59.39
52	186.06	694.83	45.22	337.85	24.30	48.62	254.11	666.66	79.67	690.27	31.35	103.54
53	123.00	797.96	28.45	252.17	23.13	31.60	221.99	869.85	185.18	531.47	83.42	61.10
54	153.81	346.55	3.28	201.10	2.13	58.03	137.52	485.52	37.56	320.31	27.31	65.97
55	93.77	127.47	41.00	46.08	43.73	36.15	82.02	93.71	10.99	13.36	13.40	14.25
56	130.04	119.17	18.68	63.12	14.37	52.96	115.91	108.33	17.67	22.60	15.24	20.86
57	114.86	100.60	27.22	34.21	23.70	34.01	104.21	117.91	15.36	28.15	14.74	23.87
58	100.09	95.94	25.99	33.43	25.96	34.85	115.44	247.45	22.21	95.78	19.24	38.71
59	83.73	55.75	24.28	4.34	29.00	7.78	78.92	70.56	0.00	0.00	0.00	0.00
60	74.27	59.56	30.74	20.52	41.39	34.44	84.59	71.70	11.59	16.50	13.70	23.01
61	69.59	65.80	22.86	15.65	32.84	23.78	102.23	61.33	20.83	5.18	20.38	8.44
62	78.61	91.54	36.97	73.99	47.03	80.83	97.74	90.42	16.30	3.34	16.68	3.70

D-3 Case 3 Distal Sensor Graphs

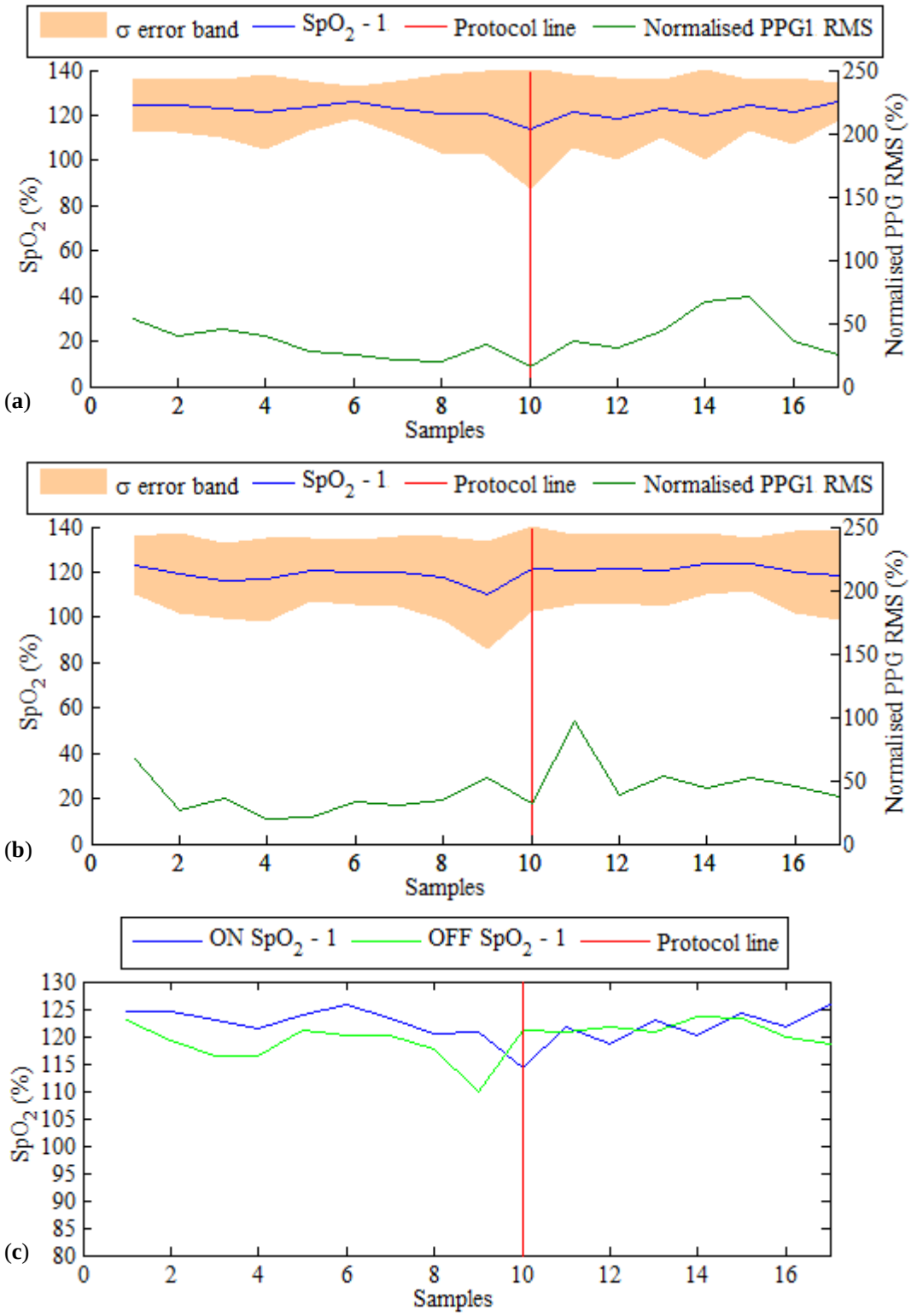

Figure D-3: Case 3 data for distal sensor (sensor 1) for *on* and *off* intervals. Protocol changeover shown by a red vertical line. **a**. Mean SpO_2 and normalised PPG RMS for *on* interval. **b**. Mean SpO_2 and normalised PPG RMS for *off* interval. **c**. *On* versus *off* SpO_2

Table D-2: Data obtained from *on* and *off* analysis for Case 3

	ON PPG						OFF PPG					
Samp	PPG1	PPG2	PPGSTD1	PPGSTD2	STD Perc1	STD Perc2	PPG1	PPG2	PPGSTD1	PPGSTD2	STD Perc1	STD Perc1
1	143.98	153.31	76.43	47.18	53.08	30.77	322.56	140.82	215.57	79.26	66.83	56.29
2	169.17	143.60	67.36	98.72	39.82	68.75	136.71	70.56	35.88	10.75	26.25	15.24
3	142.11	105.89	64.97	118.51	45.72	111.93	218.70	301.34	78.23	166.00	35.77	55.09
4	235.96	289.72	95.63	212.85	40.53	73.47	173.37	146.12	35.03	67.66	20.20	46.31
5	197.73	210.38	56.01	129.13	28.33	61.38	151.27	141.90	30.80	41.82	20.36	29.47
6	127.54	75.21	32.46	13.65	25.45	18.14	135.29	82.99	44.20	25.23	32.67	30.40
7	139.83	76.04	29.60	42.77	21.17	56.25	182.42	103.66	55.75	41.13	30.56	39.68
8	210.85	119.73	40.82	50.34	19.36	42.04	285.27	383.85	98.70	174.55	34.60	45.47
9	226.82	203.84	74.76	139.48	32.96	68.43	338.07	480.67	175.45	379.98	51.90	79.05
10	290.10	284.07	45.58	89.92	15.71	31.65	112.95	119.74	36.12	61.74	31.98	51.57
11	166.08	142.19	59.44	111.29	35.79	78.27	250.84	207.07	241.78	253.71	96.39	122.52
12	167.04	140.76	51.64	93.58	30.91	66.48	160.17	165.30	62.05	84.88	38.74	51.35
13	164.08	171.41	72.67	104.44	44.29	60.93	190.57	192.35	100.78	125.11	52.88	65.05
14	173.80	200.58	117.10	208.24	67.38	103.82	116.88	113.17	51.65	49.56	44.19	43.79
15	132.33	121.41	93.81	86.82	70.89	71.51	118.89	108.72	61.49	28.59	51.72	26.30
16	173.04	165.11	62.89	79.24	36.34	47.99	246.44	231.31	110.51	165.26	44.84	71.45
17	93.67	102.34	23.61	54.39	25.20	53.14	143.74	175.82	52.86	127.71	36.78	72.64